STUDY AND ANALYSIS OF COGNITIVE RADIO FOR WIRELESS NETWORKS

A thesis

submitted towards the partial fulfilment of the requirement for the award of the degree of

DOCTOR OF PHILOSOPHY

in

Department of Electronics and Communication Engineering

by

PAPPU KUMAR VERMA
(2K14/Ph.D/EC/07)

DEPARTMENT OF ELECTRONICS & COMMUNICATION ENGINEERING

DELHI TECHNOLOGICAL UNIVERSITY
(FORMERLY DELHI COLLEGE OF ENGINEERING)
DELHI-110042 INDIA
JANUARY 2019

DELHI TECHNOLOGICAL UNIVERSITY

Established by Govt. Of Delhi vide Act 6 of 2009

(Formerly Delhi College of Engineering)

SHAHBAD DAULATPUR, BAWANA ROAD, DELHI- 110042

CERTIFICATE

This is to certify that the thesis entitled "**Study and Analysis of Cognitive Radio for Wireless Networks**" submitted by Pappu Kumar Verma (2K14/Ph.D/EC/07) for the award of degree of Doctor of Philosophy to the Delhi Technological University is based on the original research work carried out by him under our supervision. He has fulfilled the requirements which to our knowledge have reached the requisite standard for the submission of this thesis. It is further certified that the work embodied in this thesis has neither partially nor fully submitted to any other university or institution for the award of any degree or diploma.

Prof. (Dr.) Sanjay Kumar Soni
(Supervisor)
Professor
Department of ECE
MMMUT, Gorakhpur (UP)

Dr. Priyanka Jain
(Supervisor)
Assistant Professor
Department of ECE
DTU, Delhi, INDIA

CANDIDATE'S DECLARATION

I hereby declare that the research work which is being presented in the thesis entitled, "**Study and Analysis of Cognitive Radio for Wireless Networks**" in fulfilment of requirements of the award of degree of Doctor of Philosophy is an authentic record of my own research work carried under the supervision of Dr. Priyanka Jain and Prof. Sanjay Kumar Soni.

The matter presented in this thesis has not been submitted elsewhere in part or fully to any other University or Institute for award of any degree.

Pappu Kumar Verma
(2K14/Ph.D/EC/07)

ACKNOWLEDGEMENTS

First of all I would like to pay my thanks to Almighty God, faculties and parents who gave me life and power, without which the work would not have seen the light of the day. The paucity of words does not compromise for extending my thanks to all the persons who have directly or indirectly helped me in completing this thesis.

I feel privilege to express my sincere thanks to my endearing my supervisors Dr. Priyanka Jain, Department of Electronics and Communication Engineering (ECED), Delhi Technological University (DTU), Delhi and Prof. Sanjay Kumar Soni, ECED, MMMUT, Gorakhpur, Uttar Pradesh; for the valuable suggestions, special guidance and providing the environment of independent thinking during the course of the thesis. I always availed his priceless supervision, continuous motivation and ever unforgettable humanitarian considerations.

I am deeply thankful to Prof. S. Indu, Head, ECED, DTU, Delhi for providing me all the necessary facilities for completion of my work. I am thankful to all the faculty members of ECED for their time to time advice, support and help. My special thanks to the members of DRC committee Prof. Neeta Pandey, Prof. N. S. Raghava, Prof. R. Pandey, Prof. Asok De and Dr. D. K. Vishwakarma for their criticism and constructive suggestions.

I would also like to express my deep gratitude and thanks to Prof. Rajeevan Chandel, Dr. Rohit Dhiman and Dr. Krishan Kumar, ECED, National Institute of Technology (NIT), Hamirpur, Himachal Pradesh who always helped me and motivated me in numerous ways. I am also thankful to Mr. Anurag Singh Sachan, Indian Ordnance Factory, Jabalpur and Mr. Sanjeev Kumar, Mr. Gainda Lal, AWM, Diesel Locomotive Works, Varanasi, Uttar Pradesh for supporting and motivating me throughput this whole process. I would like to express my sincere thanks to Prof. V. K. Giri (Director), Dr. D. K. Tripathi, Dr. Amod Tiwari, Dr.

Himanshu Katiyar, Dr. S. K. Pandey, Mr. Prashant Pandey, Mr. Ravi Tripathi, Mr. Dharmendra Dixit, Dr. Abhinav Gupta, Mr. Deepak of Rajkiya Engineering College, Sonbhadra, for supporting and motivating me. I am also thankful to Dr. Bhavna Arora for their guidance and support.

More personally, I would to express my sincere thanks to Mr. K. Gurumurthy, Mr. Rahul Bansal, Mr. Vikas, Mr. Amit Kumar, Mr. Manoj Kumar, Research Scholar, ECED, DTU, Delhi, for giving me helpful contribution throughout the work. I would like the thanks Mr. Avnish Mishra, Research Scholar, Indian Institute of Technology (IIT), Madras for boosting my confidence and support like a true friend.

I am also grateful to Prof. Yogesh Singh, Vice-Chancellor, DTU, Delhi for providing the research environment in the institute.

I express my deep sense of respect and gratitude to my father Rajendra Prasad and my mother Jeenat Verma. They were the constant source of motivation and moral support for me. Their scarifies and endless prayers helped me throughout my life. Finally, I would like to thank my wife Astha Singh, Sister Nisha Verma and Brother Vijay Kumar Verma for their understanding and boosting me at every stage of Ph.D. work.

(*Pappu Kumar Verma*)

TABLE OF CONTENTS

LIST OF FIGURES

LIST OF TABLES

LIST OF SYMBOLS

H_0	Null Hypothesis
H_1	Alternate Hypothesis
λ	Threshold
P_r	Received Power
P_t	Transmitted Power
L_0	Path Loss
d_0	Reference Distance
$\Re$	Path Loss Exponent
G_r	Receiver Gain
G_t	Transmitter Gain
f_d	Doppler Shift
v	Speed of Movement
λ	Wavelength
ω	Angle between the Direction of Motion and Wave's Arrival Path
$p(.)$	Probability Density Function
γ	Instantaneous SNR
$\bar{\gamma}$	Average SNR
$I_0(.)$	Modified Bessel Function of the First Kind and Zero-Order
m	Nakagami-m Parameter
α_k	Attenuation Factor of k^{th} Branch
φ	Average Noise Power of Each Diversity Branch
w_i	Branch Gain
P_{DT}	Probability of Detection

P_{FA}	Probability of False Alarm
P_{MD}	Probability if Miss-Detection
$\overline{P_{DT}}$	Average Probability of Detection
$\overline{P_{MD}}$	Average Probability if Miss-Detection
$\overline{A}$	Average Area under the Receiver Operating Characteristic Curve
P_{TE}	Total Probability of Error
$s(t)$	Received Signal
$r(t)$	Unknown Deterministic Signal
g	Channel Gain
$n(t)$	AWGN
T	Time Interval
Δ	Test Statistic
λ	Threshold
2η	Degrees of Freedom
2γ	Non-Centrality Parameter
$\Gamma(.)$	Gamma Function
$Q_{\eta}(a,b)$	η^{th} Order Generalized Marcum Q-function
$\Gamma(a,b)$	Incomplete Gamma Function
$P_{\Delta}(y)$	Cumulative Distribution Function
λ_{opt}	Optimized Threshold
μ	Mean
σ	Standard Deviation
$p_{\gamma}(\gamma\|v)$	Conditional PDF
c , v	Shape Parameter
$H_{r\ s}^{p\,q}\left(.\middle\|\begin{matrix}\cdot\ \cdot\\ \cdot\ \cdot\end{matrix}\right)$	Fox H-Function

$_aF^b\left(x;y;z\right)$	Confluent Hyper-Geometric Function
$\Upsilon\left(a,b\right)$	Lower Incomplete Gamma Function
$G_{c,d}^{a,b}\left[\zeta\middle\vert\begin{matrix}x,y\\w,z\end{matrix}\right]$	Meijer G-Functions
$Q\left(x\right)$	Gaussian Function

LIST OF ABBREVIATIONS

FCC	Federal Communication Commission
CR	Cognitive Radio
PU	Primary User
SU	Secondary User
IEEE	Institute of Electrical and Electronics Engineers
DARPA	Defence Advanced Research Project Agency
IoT	Internet of Thing
5G	Fifth Generation
RF	Radio Frequency
SS	Spectrum Sensing
QoS	Quality of Service
SNR	Signal to Noise Ratio
CRN	Cognitive Radio Networks
RSSI	Received Signal Strength Indicator
MF	Matched Filter
CF	Cyclo-stationary Feature
SCF	Spectral Correlation Function
BPF	Band Pass Filter
PSD	Power Spectral Density
CSS	Cooperative Spectrum Sensing
LOS	Line-of-Sight
NLOS	Non Line-of-Sight
EMF	Electromagnetic Field
SC	Selection Combining
MRC	Maximum Ratio Combining
EGC	Equal Gain Combining
SLC	Square-Law Combining
SSC	Switched and Stay Combining
SLS	Square-Law Selection
MGF	Moment Generating Function

PDF	Probability Density Function
RADAR	Radio Detection and Ranging
ROC	Receiver Operating Characteristic
CROC	Complementary Receiver Operating Characteristic
AUC	Area under the Receiver Operating Characteristic
CAUC	Complementary Area under the Receiver Operating Characteristic
AWGN	Additive White Gaussian Noise
FC	Fusion Centre
SISO	Single Input Single Output
MIMO	Multiple Input Multiple Output
IG	Inverse Gaussian
WCS	Wireless Communication System
TWDP	Two Wave Diffused Power
MG	Mixture Gamma
NL	Nakagami-*m*/Log-normal
EGK	Extended Generalized *K*-Fading
ADT	Adaptive Double Threshold
AF	Amount of Fading
OP	Outage Probability
CC	Channel Capacity
ASEP	Average Symbol Error Probability
TW	Time Bandwidth Product
CDF	Cumulative Distribution Function
RV	Random Variable
MSE	Mean Square Error
WL	Weibull/Log-normal

ABSTRACT

Nowadays, the world is on the cutting edge of the innovative technological revolution in wireless communication networks. The crowding of the device is increasing day by day but the band of spectrum in which devices have to communicate with each other are fixed in nature. So, in the specified band of spectrum, the massive number of device to device connection has to be made in direct or indirect way without interfering with other devices. Cognitive radio is one of the technologies, which is an arrangement of the wireless channel in which transmitter and receiver can logically sense band of spectrum, whether the channels are occupied or not. It can be shift immediately to the available band of the spectrum without interfering the occupied one. By doing so, users can use optimum radio frequency band of spectrum, whereas dropping the interference to primary users. The most important thing to avoid interference is to first sense the particular band of spectrum. Thus, the spectrum sensing is one of the prime function of cognitive radio, which observe the unused band of the spectrum at a given time, space and geographical state. Energy detection is one of the simplest and easiest methods of spectrum sensing due to its simple circuitry and less execution time. The performance of energy detection which is extensively used to accomplish spectrum sensing in cognitive radio over different fading channels. In this study, the average probability of detection and the average AUC curve are derived using the probability density function of the received instantaneous signal to noise ratio. To solve the mathematical complexity, the different mathematical approximation are used as Gaussian-Hermite integration and Holtzman approximation.

The performance analysis of energy detection based spectrum sensing in cognitive radio over multipath and multipath/shadowed fading channels like inverse Gaussian, Nakagami-*m*/shadowed, and Weibull/log-normal have been investigated. The energy detection over inverse Gaussian fading channel with selection combining scheme is presented and the average

probability of detection has been formulated with all three realistic environment conditions such as light, moderate and heavy shadowing. In a similar way, the analytical expressions of average probability of detection and average AUC curves for energy detection over composite Nakagami-*m*/log-normal and Weibull/log-normal fading channels with maximum ratio combining diversity schemes have been studied. The diversity schemes provide better detection of the signal at the receiver's end in comparison to the one without diversity scheme.

Finally, to increase the detection capabilities of the energy detection, threshold should be optimized in comparison to a fixed threshold. So, the optimized threshold can be obtained by minimizing the total probability of error which gives better spectrum sensing even at very low signal to noise ratio. The threshold optimization is applied over inverse Gaussian with selection combining, Nakagami-*m*/log-normal and Weibull/log-normal with maximum ratio combining diversity schemes.

Chapter 1

Introduction

The chapter presents the first background of cognitive radio system mechanism, which includes terminologies of cognitive radio, different functions, various aspects of spectrum sensing, applications and problems involved therein. Thereafter, different types of wireless communication channels and diversity schemes are discussed. At the end of this chapter, the significance of the study and overview of thesis is explained.

1.1 Overview

In wireless communication services, the demand of frequency spectrum is increasing day by day but these spectrums are limited and fixed resources. According to survey of Cisco on Global Mobile Data Traffic, the mobile data traffic will grow 7-fold from 2016-2021, a compound annual growth rate of 47% and monthly use of global mobile data traffic will cross around 15 Exabyte by 2018 due to tremendous use of smartphones, smartphones will reach 67 % of mobile data traffic by 2018 [1]. These facts clearly show that there will be surely spectrum scarcity problem in upcoming years [2]. On the other hand, according to the survey of Federal Communications Commission (FCC)'s Spectrum Policy task force in 2002, [3] showed that there is a very small utilization i.e. from 15% to 85% of the frequency spectrum in time, space and geographical region. This has enthused researchers to explore more on the approaches to resourceful utilization of the available frequency spectrum band. J. Mitola proposed the model of Cognitive radio [4], as an intelligent radio that can sense unused spectrum band and then allocate these bands to secondary users (SUs) for opportunistic usage. SU can utilize these bands of spectrum whenever the primary user (PU) is not using it. If the band is occupied by

the PU, the SU has to immediately vacate that particular band of spectrum without causing any detrimental interference to PU [5].

The fundamental function of Cognitive radio (CR) is to sense the available band of spectrum. A number of surveys have been found that are based on the spectrum sensing methods. The key attention is on spectrum sensing performance using on energy detection technique based spectrum sensing. The motivation of spectrum sensing is to detect spectrum 'holes' so as to maximize the probability of detection and minimize the probability of false alarm [6]. Several ways for spectrum sensing have been stated in literature such as energy detection, matched filter, cyclostationary feature, wavelet transform, covariance mastics, cooperative spectrum sensing and Eigen value based spectrum sensing. Among all of these techniques, energy detection based method has been considered to be the most popular one. According to this technique, there is no need to have prior knowledge of signal [7]. Therefore, this technique becomes more attractive as compared to other techniques, as other techniques, demand prior knowledge of either signal or noise or knowledge of both. The emerging IEEE 802.22 based wireless regional area network will use unoccupied/unused TV channels for CR prototype, as maintained by IEEE [8].

Joseph Mitola at the Defence Advanced Research Project Agency (DARPA) in the US [9] first proposed the idea behind CR as an intelligent radio that can sense unused spectrum bands, and then allocate these bands to unlicensed users or secondary users (SUs) for opportunistic utilization.

1.2 Cognitive Radio

CR is an arrangement of the wireless channel in which transmitter and receiver can logically sense band of spectrum, whether the channels are occupied or not. It can be shifted immediately to the available band of spectrum without interfering the occupied one. By doing so, users can

use optimum radio frequency (RF) band of spectrum, whereas dropping the interference to primary users (PUs) at a given time and geographical region [10]. We use the definition adopted by FCC:

"*Cognitive radio: A radio or system that senses its operational electromagnetic environment and can dynamically and automatically adjust its radio operating parameters to modify the system operation, such as maximize the throughput, mitigate interference, facilitate interpretability, access secondary markets.***"**

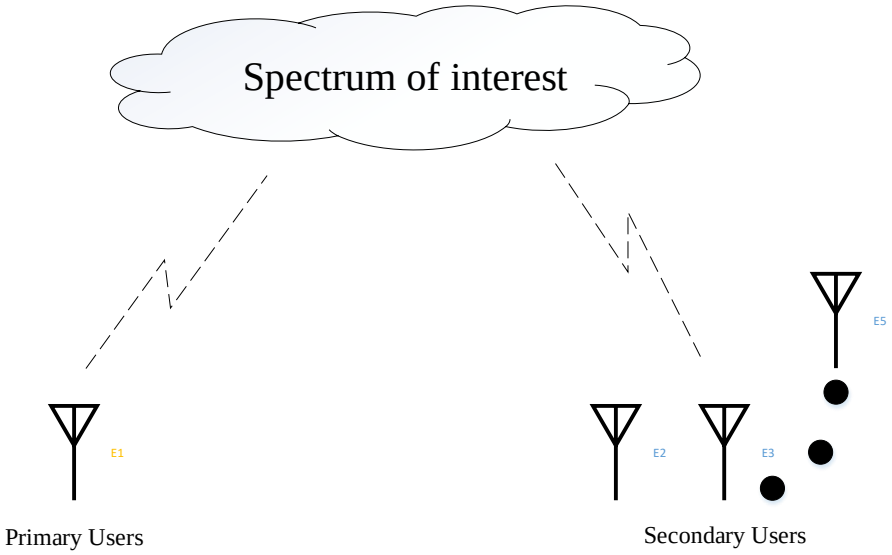

Fig. 1.1 Cognitive radio environments

The major modules of CR theory is the capability to learn, sense, measure and be very much attentive about the constraints associated with radio channel features, power consumed and availability of band of spectrum, channels operating locations, local policies, user requirements and their applications, available infrastructures and their nodes and other operating boundaries. In CR terminologies, *primary users* can be signified as the users who have upper priority or legacy rights on the usage of a definite band of spectrum. On the other hand, *secondary users* (SU) can be defined as the users who have lower priority, exploits this band of spectrum in such a way that they do not cause interference to primary users as shown in Fig.1.1. Therefore,

SUs must have CR abilities, such as recognizing the band of spectrum constantly to check whether it is being used by PUs and to modify the radio constraints to exploit the unused band of the spectrum [11-16].

1.3 Functions of Cognitive Radio

Following are the main functions of cognitive radio [17-18] as shown in Fig. 1.2.

1.3.1 Spectrum Sensing

Spectrum sensing (SS) is the most important function of cognitive radio. The function of SS is to sense the assigned band of spectrum for particular SUs continuously and should have knowledge of all the parameters of the PUs because whenever PU want to connect to the assigned spectrum again, SU has to vacate that band immediately without interfering PU. By doing so, efficiency of the band of spectrum increases.

1.3.2 Spectrum Management

This utility is compulsory for CR to accomplish consumers' needs by catching the best band of spectrum. CR should adopt on the finest band of spectrum and the channels within it to meet the Quality of Service (QoS) supplies overall unused spectrum.

1.3.3 Spectrum Mobility

When the users move from one cell to another cell, their frequency may change depending on the time and location. So, the best part of spectrum mobility is that users can change frequency dynamically by allocating the nodes to operate in the unused band of spectrum.

1.3.4 Spectrum Sharing

The major problem in spectrum usage is to provide resourceful and fair dynamic spectrum allocation to allow the vacant spectrum to PUs.

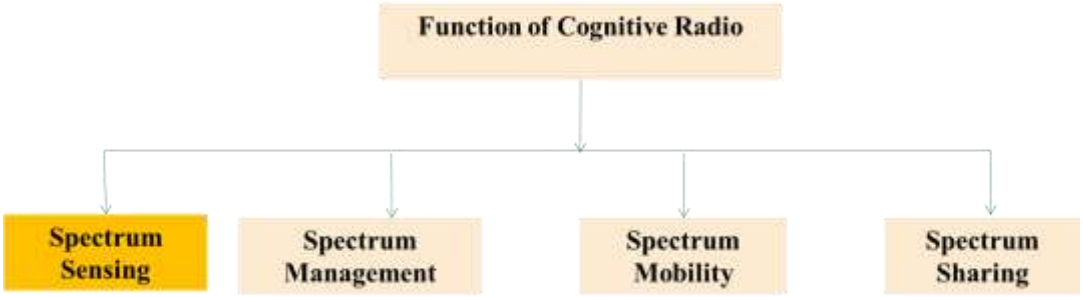

Fig 1.2 Functions of cognitive radio

1.4 Spectrum Sensing

SS is the way to sense or examine the particular band of spectrum whether it is vacant or not. In the process of SS, the SUs investigate all the associated parameters of the band of spectrum for proper communication among users [19]. SS is divided into two sets as shown in Fig. 1.3 and a brief discussion is given below:

1.4.1 Non-cooperative Sensing

The CR users must be so intelligent to decide whether the assigned band of spectrum is free from PU or not. In the non-cooperative, the communication happens between one PU and CR. The non-cooperative spectrum sensing is also known transmitter detection. A brief overview of principles of spectrum sensing based on observation of PU signal is given below:

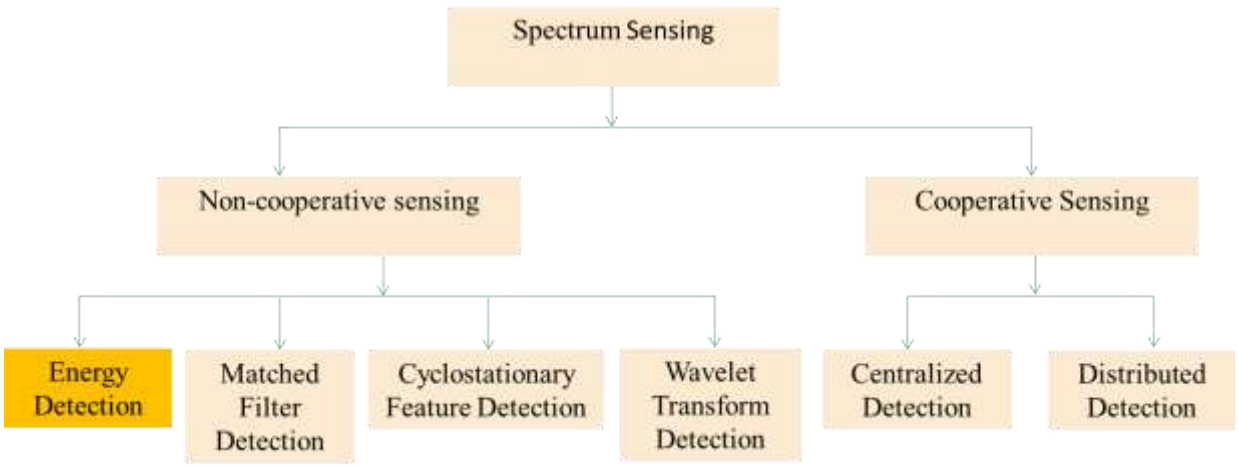

Fig. 1.3 Classifications of spectrum sensing

1.4.1.1 Energy Detection

Energy detection (ED) is especially suitable for wideband SS when CR cannot gather sufficient information about the PU signal. In the detection of signal, either signal is absent or signal is present and it is characterized by the two hypothesis, first one is known as a null hypothesis H_0, and the second one is known as an alternate hypothesis H_1, respectively as shown in Fig. 1.4, which shows the probability density function of received signal with and without active PU. In the ED, first filter the signal, square it and integrate over the time interval (T). The output of the integrator, Δ acts as test statistic that decides whether the received signal energy corresponds to noise energy or energy of both. At the end of ED, Δ compares with the threshold (λ) and if $\Delta < \lambda$, the signal is absent otherwise present [20-24].

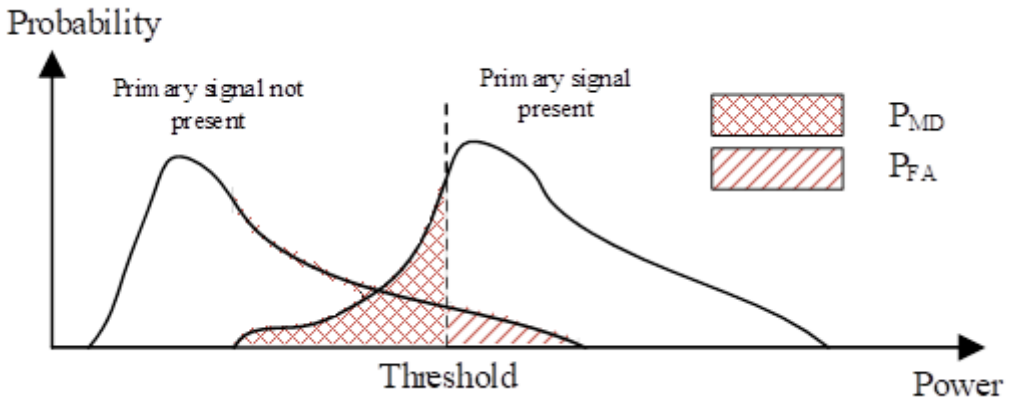

Fig. 1.4 Threshold setting in ED

If the selected threshold is too low, the probability of false alarm increases which results in low spectrum utilization. On the other hand, if the threshold kept unnecessarily high, the probability of miss-detection is increased which may result in interference with an active PU. Hence, the careful trade-off is considered while setting the threshold for ED. In practice, if a certain spectrum reuse probability of unused spectrum is targeted, the probability of false alarm is fixed to a small value (e.g. less than 5%) and the probability of detection is maximized. If the probability of miss-detection is set at a minimum value (e.g. greater than 95%) and the probability of false alarm minimized. Recently, a weighted combination of the probability of

miss-detection and probability of false alarm is proposed to define the spectrum sensing error which is minimized to get the optimum threshold. The optimum threshold value adapts to change in the radio operating environment and is suitable in dynamic scenarios.

Hence, above are the brief discussion about the ED based SS but each and every method have its own advantages and disadvantages which is given in Table 1.1 From the table, it is obvious that ED based SS is very simple and popular from the circuit point of view. On the basis of a survey of the different techniques of the spectrum sensing are summarized some advantages and disadvantages [25-38].

Table 1.1: Advantages and Disadvantages of SS Techniques

Spectrum sensing techniques	**Advantages**	**Disadvantages**
Energy Detection	• Low computation cost • Does not need any prior information	• Cannot work in low SNR • Cannot distinguish Users • Sharing the same channel
Matched Filter	• Optimal detection performance • Low computational cost	• Requires prior knowledge of primary Users
Cyclostationary Detection	• Robust in low SNR • Robust to interference	• Requires partial information of primary users • High computational cost
Wavelet Detection	• Effective for wideband signal	• High computational cost • Does not work for Spread spectrum signals

1.4.2 Cooperative Spectrum Sensing

SS may be directed nearby by one CR user; the concept after cooperative spectrum sensing (CSS) is that statistics can be a clubbed from different CR users. There are many complications that can be handled by CSS, such as multipath fading and shadowing noise uncertainty as

shown in Fig. 1.5; it decreases sensing time and resolves the problem of hidden PUs [39-42]. These problems are summarized as below:

- Shadowing uncertainty detection problem
- Cooperative PUs faded by composite fading
- Sensing time

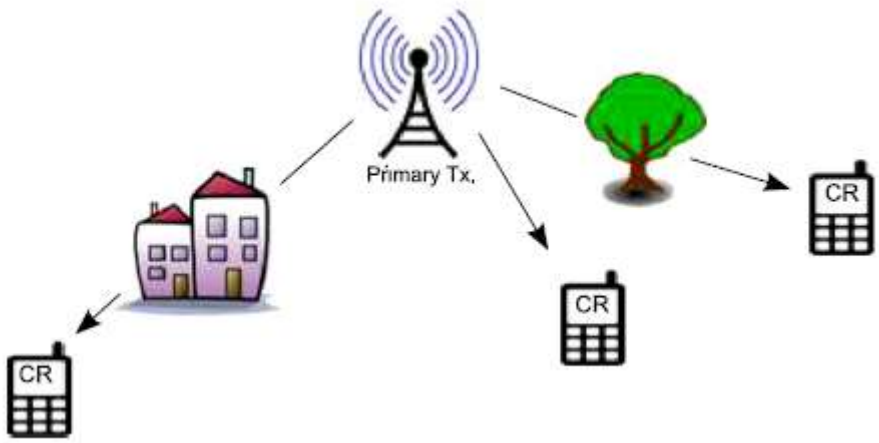

Fig. 1.5 CSS in a shadowed environment [16]

There are some advantages and disadvantages in both type of spectrum sensing, Table 1.2 provides the same about non-cooperative and cooperative spectrum sensing.

Table 1.2 Non-cooperative versus Cooperative detection

Sensing technique	Advantages	Disadvantages
Non-cooperative Detection	• Simplicity of implementation	• Hidden nodes problem
Cooperative Detection	• High accuracy • Reduced sensing time • No problem with hiding and shadowing	• Higher complexity of system collaboration and of sensor • Overhead traffic

Cooperative spectrum detection can be implemented either centralized or distributed [43-46].

In the centralized cooperative spectrum sensing, the access point (AP), such as the master node or base station collects sensing information from the CR users and takes a decision whether the primary signal is present or not and delivers this information to other CR users. On the other hand, in the distributed method, CR users make their own decision, adding to the information shared between each CR user.

1.5 Wireless Fading Channel

In wireless communication, the signal is transmitted from transmitter to receiver through the air along with the dedicated transmission path. This path can be obstructed not only by object or obstacle in the line of sight (LOS) between the transceiver but also cause a drastic change in the strength of the electromagnetic field (EMF) at the receiver end. The signals of wireless channel are random in nature and can be modeled statistically. The rapid fluctuation caused by small variation in the spatial distance of the receiver is called small scale fading. On the contrary, the large scale fading shows the signal attenuation on an average basis [47] as shown in Fig. 1.6. A brief introduction of classifications of fading channels is given below:

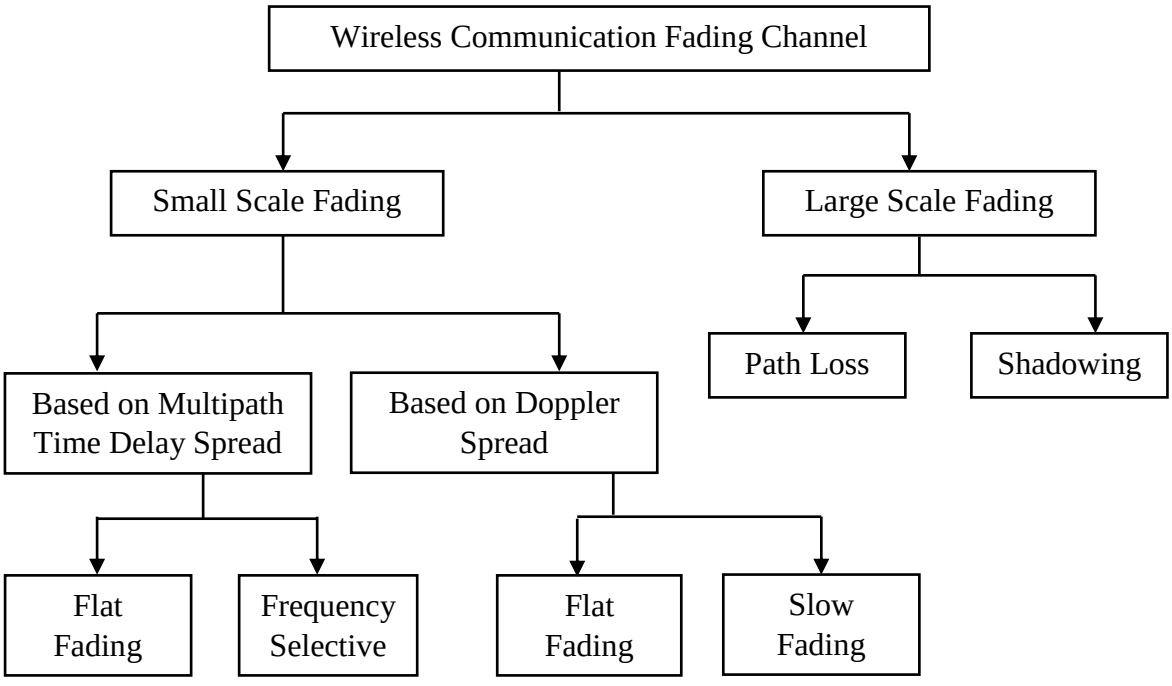

Fig. 1.6 Classifications of wireless communication fading channel

1.5.1 Large Scale Propagation

Large scale propagation model can be classified into two models; first is path loss and the second one is shadowing as shown in Fig. 1.7. These models are used to predict the average received signal strength at large transmitter receiver distance [48]. The large-scale fading describes how the signal at the receiver's end changes on an average sense as it moves with respect to the transmitter. This information is very useful in network planning and deployment of base station in some urban area. There are various path loss models available which describe the signal attenuation on an average basis. These are Hata Model, Okumura model and some other theoretical models. These models predict the signal on an average basis.

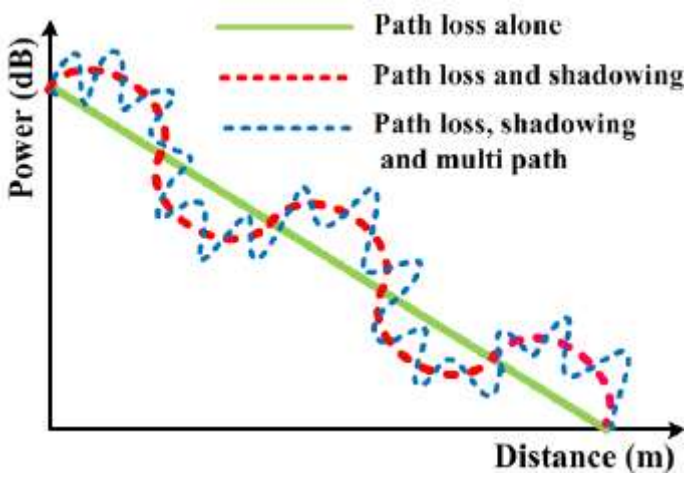

Fig. 1.7 Characterization of fading channels [48]

1.5.1.1 Path Loss

Path loss is used to model the attenuation of the signal which travels from the transmitter to the receiver. If the signal further travels at long distance, the received signal experiences more attenuation. Therefore, path loss increases exponentially with the increase in distance.

The propagation model for the path loss at distance x is given by

$$\frac{P_r}{P_t} = \frac{L_o}{x^{\Re}} \tag{1.1}$$

where $\Re$ is path loss exponent which is different and dependent on the propagation environment, for instance, it is 2 for free-space propagation and 4 to 6 under shadowed urban cellular radio. P_r and P_t are the received and transmitted power respectively. L_0 is the path loss at a reference distance d_0, which is given as

$$L_0 = \frac{\left(4\pi d_0\right)^2}{\lambda^2 G_t G_r} \tag{1.2}$$

$$L_0\left(dB\right) = 10log_{10}\left(\frac{\left(4\pi d_0\right)^2}{\lambda^2 G_t G_r}\right) \tag{1.3}$$

where λ is the wavelength, G_r and G_t are the antenna gains for the transmitter and receiver respectively.

1.5.1.2 Shadowing

Shadowing is an effect of the variation in terrain and presence of obstacles. This affects the received power at different locations with a fixed distance x and is modeled as log-normal (LN) distribution. The effect of shadowing [49] can be expressed as

$$L\left(dB\right) = L_0\left(dB\right) + 10\Re log_{10}\left(\frac{x}{d_0}\right) + X_\sigma \tag{1.4}$$

where the summation for the first two terms (L_0 and the log_{10} terms) are the path loss at distance d and X_σ, which is a zero-mean Gaussian distributed random variable in log-scale, represents the log-normal shadowing effect. Gamma and Inverse Gaussian distribution are used as an alternate of the log-normal distribution.

1.5.2 Small Scale Propagation

Small scale fading describes the instantaneous fluctuation of the received signal as the receiver moves with respect to the transmitter. In this case, the rapid fluctuation is caused by the

coherent addition of the multipath components arriving at the receiver with different phase and varying attenuation. The ray-based models give the field prediction on small scale as it traces each individual paths. There are two types of small-scale fading. One is based on multipath time delay spread, while the other is based on Doppler spread.

1.5.2.1 Multipath Fading

Multipath fading happens when the signal reaches at the receiver over different paths, as an outcome of reflection, diffraction or scattering as shown in Fig. 1.7. This creates many replicas of the transmitted signal as each path can reach with diverse gains, phases, and delays.

1.5.2.2 Doppler Shift

Doppler shift is the change in the received signal frequency due to the relative motion of transmitter and receiver. This shift can influence small-scale fading and it depends on the velocity and direction of motion of the mobile. The Doppler shift f_d can be expressed as

$$f_d = \frac{v}{\lambda} cos\omega \tag{1.5}$$

where, v, λ and ω is the speed of movement, the wavelength and the angle between the direction of motion and the wave's arrival path.

1.6 Some Channel Model

In this section, some common channel models are presented; AWGN channel, Rayleigh, Rician, Nakagami-*m*, Weibull, Inverse Gaussian and log-normal fading channel [50] as

1.6.1 AWGN Channel

The Additive White Gaussian Noise (AWGN) channel model is an ideal channel model as it merely adds the white Gaussian noise linearly into the signal. Being the nonfading channel

model, the spectacle of fading is not reserved into account for this channel type, where the channel gain is always 1.

1.6.2 Rayleigh Fading Channel

In Rayleigh distribution is used to model communication systems when independent scatters are very large. In this distribution, there is no LOS component of the signal present at the receiver and the envelope is the sum of two quadrature Gaussian signals. The instantaneous SNR follows the probability density function (PDF) given by

$$p(\gamma) = \begin{cases} \frac{1}{\bar{\gamma}} exp\left(\frac{\gamma}{\bar{\gamma}}\right) & ,\gamma \geq 0 \\ 0 & ,otherwise \end{cases} \tag{1.6}$$

where γ and $\bar{\gamma}$ is respectively the instantaneous and average SNR.

1.6.3 Rician Fading Channel

The rician channel is used to model propagation paths between the transmitter and the receiver when there is a dominant LOS path and many weaker multipaths. Rician is distributed as follows

$$p(\gamma) = \begin{cases} \frac{\gamma}{\sigma^2} exp\left(-\frac{\gamma^2 + A^2}{2\sigma^2}\right) I_0\left(\frac{A\gamma}{\sigma^2}\right) & ,A \geq 0,\ \gamma \geq 0 \\ 0 & ,otherwise \end{cases} \tag{1.7}$$

where A denotes the peak amplitude of the dominant signal and $I_0(.)$ is the modified Bessel function of the first kind and zero-order.

1.6.4 Nakagami-*m* Fading Channel

The Nakagami-*m* fading channel is used to model ionosphere radio and indoor mobile propagation radio links, the instantaneous SNR follows the PDF given by

$$p(\gamma) = \frac{m^m \gamma^{m-1}}{\bar{\gamma}^m \Gamma(m)} exp\left(-\frac{m\gamma}{\bar{\gamma}}\right) \ , \gamma \geq 0 \tag{1.8}$$

where *m* is the Nakagami-*m* parameter. For *m*=1, the PDF of Nakagami-*m* distribution can be simplified to Rayleigh distribution.

1.6.5 Weibull Fading Channel

The Weibull channel is the another calculated explanation of the likelihood model for the describing amplitude fading in the multipath environments, particularly that related to mobile radio systems operating in 800/900 MHz range. The Weibull PDF is given as

$$p(\gamma) = c\left(\frac{\Gamma\left(1+\frac{2}{c}\right)}{\bar{\gamma}}\right)^{c/2} \bar{\gamma}^{c-1} exp\left[-\left(\frac{\gamma^2}{\bar{\gamma}}\Gamma\left(1+\frac{2}{c}\right)\right)^{c/2}\right] , \gamma \geq 0 \tag{1.9}$$

where *c* is a parameter that is chosen to yield the best fit to quantify results and as such gives the shape litheness of the Nakagami distributions. For c = 2, the above PDF becomes Rayleigh distribution.

1.6.6 Inverse Gaussian

The IG distribution is used to model turbulence affected free space optical (FSO) communication. The closeness of the PDF of IG distribution to the LN model has been verified using Kullback Leibler divergence. The PDF of IG is given by

$$p_{\Delta}(y) = y^{-3/2}\sqrt{\frac{\lambda}{2\pi}} exp\left(\frac{\lambda}{\theta}\right) exp\left(-\lambda\left(\frac{y}{2\theta^2}+\frac{1}{2y}\right)\right) \tag{1.10}$$

where,

$$\theta = \exp\left(\frac{\mu}{\xi}+\frac{\sigma^2}{2\xi^2}\right); \quad \lambda = \frac{\theta}{\left(exp\left(\frac{\sigma^2}{\xi^2}\right)-1\right)} \text{ and } \xi = \frac{10}{ln(10)}$$

1.6.7 Log-normal Shadowing

The shadowing can be modeled by a log-normal distribution for various outdoor and indoor environments, So, the PDF is given as

$$p(\gamma) = \frac{\xi}{\sqrt{2\pi}\sigma\gamma} exp\left[-\frac{\left(10log_{10}\gamma - \mu\right)^2}{2\sigma^2} \right] \tag{1.11}$$

Where, μ (dB) and σ (dB) are the mean and the standard deviation of $10\log_{10}\gamma$, respectively. Gamma distribution is the most suitable approximation of log-normal distribution and is widely used in literature to model shadowing effects. Inverse Gaussian is another distribution, which is used to model log-normal distribution.

1.7 Diversity Schemes

The key motivation of diversity is to club the independent fading paths so that the effects of fading are mitigated. There are different combining techniques available in the literature. These techniques entail various trade-off between performance and complexity [47-48]. The combining techniques are:

- Selection combining (SC)
- Maximal ratio combining (MRC)
- Equal-gain combining (EGC)

Further, our objective shall be to come up with the optimum combining techniques for the propagation channel under consideration.

1.7.1 Selection Combining

In this, consider N as independent channels whose outputs are $r_i, i = 1,2,..,N$ as shown in Fig. 1.8. The receiver, monitors the SNR at each receiver input and chooses the maximum SNR channel as its output. Here, each channel is called the diversity branch. Let us assume that each

channel average SNR is constant and denoted as $\bar{y}_c$. The instantaneous SNR of k^{th} channel is y_k and it is given as:

$$y_k = \frac{E_b}{N_0}\alpha_k^2 \tag{1.12}$$

where α_k is the attenuation factor of kth branch. Since α_k is Rayleigh distributed random variable, y_k will also be a random variable with Chi-square distribution and it is given as

$$p(y_k) = \frac{1}{\bar{y}_c} exp(-\frac{y_k}{\bar{y}_c}) \qquad y_k \geq 0 \tag{1.13}$$

$$\bar{y}_C = E[Y_k] = \frac{E_b}{N_0}\bar{\alpha}_k^2 \tag{1.14}$$

Suppose we use only one receiving antenna, then, there is probability that the instantaneous received SNR is less than some threshold SNR y is

$$P_r[y_k \leq y] = \int_0^y p(y_k)dy_k = \int_0^y \frac{1}{\bar{y}_c} exp(-\frac{y_k}{\bar{y}_c})dy_k = 1 - exp(-\frac{y}{\bar{y}_c}) \tag{1.15}$$

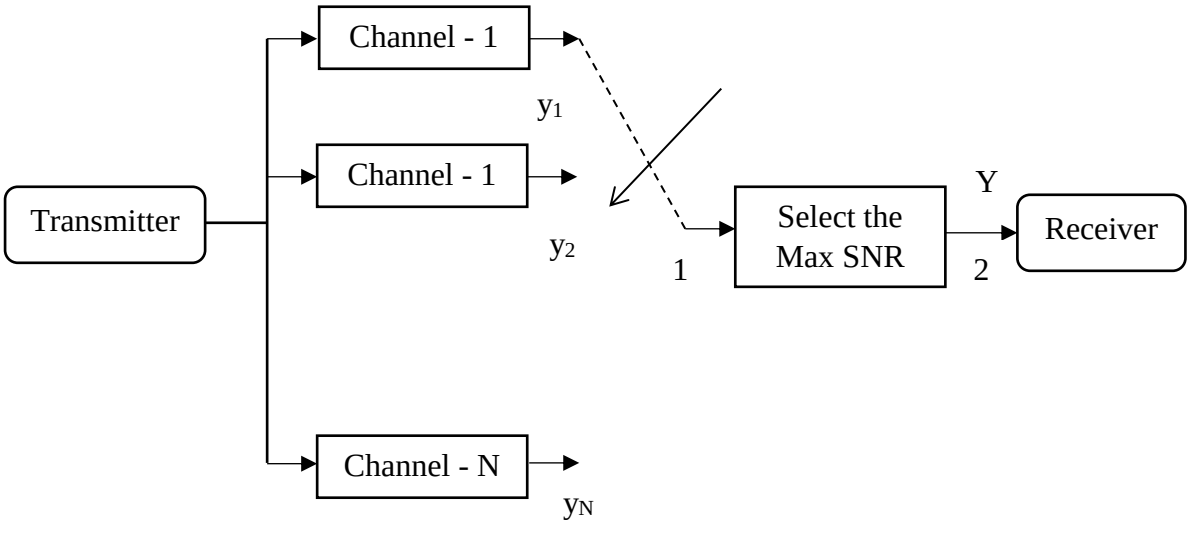

Fig. 1.8 Selection Combining Technique

Here, note that Y is the random variable at the output of selector point 2 and the value it can have is y. If we introduce N independent diversity branches, then, introduce the diversity of

order N. Therefore, the probability that random variable Y is less than some value y is equal to the probability, output of each of the channel is less than y. It is because of the fact that in selection combiner, Y can have a value less than y only when all the channel output will have value less than y. Hence the probability that Y is less than some value y is given as

$$P(Y \le y) = F_Y(y) = P_r[y_1, y_2, ...y_N \le y] = \left[1 - \exp(-\frac{y}{\overline{y}_c})\right]^N \tag{1.16}$$

Therefore, the probability that at least one of the channel output SNR exceeds the certain threshold is given as

$$P_r[y_k > y] = 1 - \left[1 - \exp(-\frac{y}{\overline{y}_c})\right]^N \tag{1.17}$$

So this is the probability of successful transmission.

1.7.2 Maximal Ratio Combining

Let $r_i, i = 1,2,..N$ be the output of antenna of ith diversity branch. Each branch has a gain of w_i as shown in Fig. 1.9, then, the total signal at the output of the combiner is given as

$$s = \sum_{k=1}^{N} w_k r_k \tag{1.18}$$

Similarly, if φ be the average noise power of each diversity branch, then, total noise power at the output of the combiner is

$$\varphi_T = \varphi \sum_{k=1}^{N} w_k^2 \tag{1.19}$$

SNR at combiner output is given as

$$Y = \frac{(s/\sqrt{2})^2}{\eta_T} = \frac{s^2}{2\eta_T} = \frac{\left[\sum_{k=1}^{N} w_k r_k\right]^2}{2\eta \sum_{k=1}^{N} w_k^2} \tag{1.20}$$

The above ratio is maximized when

$$w_k = \frac{r_k}{\eta} \tag{1.21}$$

The result in (1.21) implies that the tap coefficient is proportional to the channel output. Thus, if the channel is more reliable, the output will be larger and hence, this will be multiplied with the greater value of the tap coefficient. This is something similar to the water-fall algorithm where the more reliable channel is used to send more transmitted power in order to obtain the optimum result. Let us expand the above result for N=2. For this value of gain factor, Equation (1.21) can be rewritten as

$$Y = \frac{\sum_{k=1}^{N}(r_k^2)}{2\eta} = \sum_{k=1}^{N}(\frac{r_k^2}{2\eta}) = \sum_{k=1}^{N} y_k \tag{1.22}$$

where, $y_k = (\frac{r_k^2}{2\eta})$ is the instantaneous SNR of kth channel. The average of Y is given as

$$E[Y] = E\left[\sum_{k=1}^{N} y_k\right] = \sum_{k=1}^{N} E[y_k] = \sum_{k=1}^{N} \bar{y}_k \tag{1.23}$$

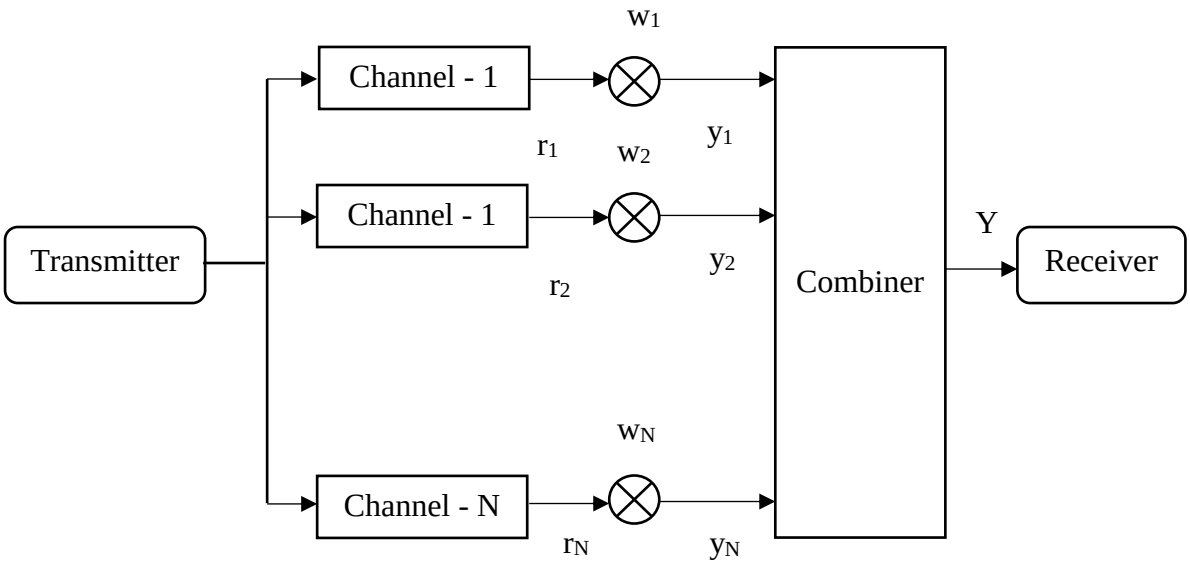

Fig. 1.9 Maximal Ratio Combining Technique

Thus, SNR at the output of the combiner is the sum of SNR at each receiving input. Note that SNR at each channel output (before tap) is equal to SNR at combiner input because signal and noise voltage at channel output is equally multiplied by weight coefficient so in taking the ratio of signal and noise SNR, the tap coefficient will get cancelled.

1.7.3 Equal Gain Combining

In certain cases, if it is not possible to provide variable gain as per the requirement of individual diversity branch, then, we can set all the gain to be one. In this way, it produces SNR at the combiner output lower than that of maximal ratio combiner. Yet, it includes the same advantage of maximal ratio technique of considering SNR of all diversity branches. It also has the advantage of producing acceptable output SNR even when none of the individual branches SNR is acceptable [50].

1.8 Motivation

Cognitive radio is one of the emerging techniques by which secondary users can use the underutilized band or sub-band of spectrum in a very efficient manner without interfering with the primary users or licensed users. The applications of cognitive radio are also involved in the fifth generation mobile communication and internet of thing. When the primary users are busy in their idle band of spectrum, CR has to scan continuously to sense the band of spectrum whether the particular spectrum is available or not. If the spectrum is available, CR immediately connects through that spectrum and communicates to their receiver. However, if PUs retransmit again, CR users should stop their transmission immediately to avoid interference to PUs. Hence, spectrum sensing is the fundamental function of CR. The better CR know about the existence of the PUs, the better it communicates and utilizes the underutilized spectrum. There are several ways to sense the spectrum for CR such as, energy detection, matched filter detection, cyclo-stationary detection. But energy detection is one of

the best techniques of spectrum sensing due to its simplicity, low computational and implementational cost. Energy detection also does not require any prior knowledge of primary users signal.

1.9 Organization of Thesis

In this thesis work, performance analysis of energy detection based on spectrum sensing over multipath and composite fading channels with and without different diversity schemes is carried out. The major contributions of the research work are summarized into different chapters and a brief description of each chapter is as follows:

Chapter 2: Literature Survey: A comprehensive and in-depth literature survey is presented for the various approaches and techniques used in the spectrum sensing in cognitive radio over different fading channels. The performance evaluation of energy detection based spectrum sensing employed in the literature is also discussed with and without different diversity schemes. Based on the literature survey, research gaps are identified, and research objectives of the thesis are formulated.

Chapter 3: Performance Evaluation of IG Channel with SC Reception: The analytical expression of the average probability of detection is derived over IG fading channel with SC reception. Additionally, the threshold is optimized by minimizing the total probability of error that improves the detection probability even at a very low signal to noise ratio.

Chapter 4: Performance Evaluation of Nakagami-*m*/Shadowed Channel with MRC Reception: This chapter presents the analytical expression of different performance analysis parameters. The average probability of detection and average AUC is derived and evaluated. Furthermore, the threshold is optimized by minimizing the total probability of error.

Chapter 5: Performance Evaluation of Weibull/Shadowed Channel with MRC Reception: The analytical expression of average probability of detection and area under the

receiver operating characteristic curve are derived over Weibull/Shadowed with MRC reception. Additionally, the threshold is optimized by minimizing the total probability of error.

Chapter 6: Performance Evaluation of Nakagami-m/Log-normal Fading Channels: It presents the analytical expressions of the amount of fading, outage probability, average channel capacity, and average symbol error rate. Moreover, the analytical expression of the average probability of detection is derived over NL fading channels.

Chapter 7: Conclusion and Future Scope: Conclusions of proposed methods and algorithms are presented in this chapter. A detailed discussion of possible avenues of future scope in regards to this research work is presented.

Chapter 2

Literature Survey

This chapter covers the details of earlier analysis carried out over different fading channels either multipath or composite fading channels i.e. the combination of both multipath and shadowing. To mitigate the detection problem in low signal to noise ratio, several diversity schemes are also incorporated in the literature. Furthermore, to get the high probability of detection, the threshold is optimized which gives better performance in comparison to convention threshold.

2.1 Introduction

Today the world is on the edge of the innovative technological revolution in wireless communication networks. Internet of thing (IoT) is the challenging technique and is likely to be an obligatory portion of the fifth generation (5G). The IoT contains direct device-to-device and massive machine communication that create interference with other devices. Therefore, the signal of PU is not probable to sense, without any appropriate SS technique. SS is the utility of CR, which monitor the unused spectrum at the given time, space and geographical area. Hence, CR has seemed like a capable resolution to the insufficiency band of the spectrum because bands of spectrum are fixed. There are several ways for SS has been quantified in the literature such as wavelet transform, energy detection, cyclostationary feature, matched filter, covariance matrix, and eigenvalue. Among these SS methods, ED is the most simple and popular methods as addressed in the literature [51-52].

In most of the wireless communication systems (WCS), simultaneous effect of both kinds of fading is encountered very frequently in a realistic environment, that is, shadowing and multipath fading. Combination of these two fading effects is called composite fading [53].

2.2 SS based on Multipath Fading

Rician, Rayleigh, Weibull, and Nakagami fading channels [54-55] capture the multipath. The multipath fading is also modelled by generalized alpha-mu, kappa-mu, eta-mu, alpha-eta-mu, alpha-lambda-mu, and alpha-eta-kappa-mu fading channels. The alpha-eta-mu is a generic fading distribution, which is wont to characterize multipath fading. It includes special cases such as alpha-mu, eta-mu, Weibull, Nakagami-m, Rayleigh, Nakagami-q, Exponential, Hoyt and one-sided Gaussian distributions [56-62].

ED is one of the fundamental technique of SS due to its simplicity, low computational and implementational cost as compared to other available SS techniques [63]. The problem of detection of the deterministic signal by the ED method over the white Gaussian noise has been considered by Urkowitz. When the signal or absent and present, the decision statistics have to central chi-square distribution and non-central chi-square distribution. For the number of the time-bandwidth product, the receiver operating characteristics (ROC) curves are presented [64]. The explicit expressions of the P_{DT} and P_{FA} are derived for number of channels such as Rayleigh, Rice, Nakagami, and others in the presence of band-limited Gaussian noise by Kostylev [65] and after few years, considered quasi-deterministic signals over multipath fading channels [66].

Many studies have been presented to the performance analysis of the ED based SS for various communications channels and fading environments. The mathematical closed-form expressions are formulated for the average probability of detection ($\overline{P_{DT}}$) over several fading channels as Nakagami-m, Rice and Rayleigh fading channels for single and multi-channel environments [67]. In a similar way, for Nakagami-m fading channel, the performance of ED has been studied along with equal gain combining (EGC) diversity reception [68] while the analysis of ED in CSS and in-relay based CRNs was examined in [69-74].

A novel tactic is used to calculate the P_{DT} and P_{FA} named semi-analytical computation for correlated Rayleigh and Rician fading channels. The ED used dual square-law combining (SLC) diversity reception which is presented to be low complexity diversity scheme for the analysis [75]. The comprehensive analysis of ED over different fading channels has been discussed with different diversity reception. The expressions of P_{DT} are derived using moment generating function (MGF) and probability density function (PDF) over Nakagami-m and Rician fading channels with MRC reception. Due to some mathematical problem, Marcum-Q function is used to avoid mathematical analysis. Both diversity reception EGC and SC are incorporated over Nakagami-m fading channels for the number of diversity branches 1, 2, 3, and 4. A comparison on the performance of ED has also presented for both methods i.e. MGF and PDF based analysis. For truncating the infinite series error, series truncation error bounds is applied by Herath *et. al.* [76]. ED is most leading technique and used for reliable detection of the signal by due to its non-coherent arrangement and low complication. The main problem in ED analysis is the involvement of generalized Marcum-Q function but Begheri and Shahzadi overcome this hurdle by introducing incomplete Toronto function. The analytical expression of $\overline{P_{DT}}$ is formulated over non-faded and faded channel i.e. Gaussian noise and Nakagami-m fading channel respectively using both MGF and PDF based approaches. The two diversity schemes such as MRC and switched and stay combining (SSC) also incorporated for both fading channels and Monte Carlo simulation also integrated with the exact analysis [77]. The ED based SS is also used in radio detection and ranging (RADAR) systems. The novel analytical and numerical expression of $\overline{P_{DT}}$ has been derived over Weibull fading channels. This channel is very flexible and practical and provides the perfect characterization of multipath fading which is typically used in mobile communications at 800/900 MHz [78]. The performance of ED based analysis is investigated in terms of ROC curves over N*Rayleigh

channels. The novel analytical expression is derived that is the combination of several mathematical functions such as product of Meijer G-function, Marcum Q-function, and arbitrary power terms. The obtained outcomes also extended for SLS diversity reception [79]. The complementary ROC (CROC) presented for different situations over Rayleigh channels for independent and identically distributed (i.i.d) and correlated channel. The expression of $\overline{P_{DT}}$ is derived with SLC and square-law selection (SLS) diversity reception [80]. In [81], an alternative analytical expression of the average probability of missing detection ($\overline{P_{MD}}$) is examined under Nakagami-m fading channel with and without diversity schemes. The authors have also proposed the new parameter called sensing gain. The closed-form expressions of P_{MD} and P_{FA} is discussed for non-fading channel i.e. AWGN and faded channels such as Rayleigh, Nakagami, log-normal and Weibull fading channels [82].

Another performance parameter of ED is the average area under the receiver operating characteristics (AUC) ($\overline{A}$) curves which is nothing but the area under the ROC curves. The closed-form analytical expression is derived for both the performance parameters such as $\overline{P_{DT}}$ and $\overline{A}$ curves over eta-mu fading channel using PDF. Eta-mu is the generalization of generalized multipath fading for non-line-of-sight (NLOS) wireless communication environments. Again performance of ED is investigated over eta-mu fading channel and closed-form expression of $\overline{P_{DT}}$ is derived for the unknown received signal. Further, the analysis is extended over two diversity schemes namely MRC and SLC reception [83]. A very accurate characterization of ED based analysis has been examined over kappa-mu and kappa-mu extreme fading channels. A novel mathematical closed-form analytical expression of $\overline{P_{DT}}$ has been derived for the single user and SLS diversity reception. The performance of ED is highly reliant on the severity of the fading since the small deviation in the fading environments

affects significantly the value of $\overline{P_{DT}}$ but as the number of branches increases, the conditions recovers for moderate and high shadowing. The kappa-mu extreme fading model is skilful of accounting for fading deviations even at very low SNR values [84]. In [85], ED is such a scheme that does not need any prior knowledge of the received signal. The analytical expression of $\overline{A}$ curves is derived over the generalized fading conditions characterized by kappa-mu and eta-mu fading distributions.

The performance of ED in terms of average AUC is discussed using MGF based approach over generalized fading channels. The analytical expression is the presentation of several functions as the generalized Marcum Q-function, contour integral. The derived expression is also extended to SLC diversity reception [86]. Based on MGF, ROC and $\overline{A}$ curves have been presented under kappa-mu and eta-mu fading channels with diversity schemes [87]. A novel MGF based method to combine the performance of ED for sensing unknown deterministic signals over eta-mu, kappa-mu, alpha-mu, *K*, *G*, and K_G generalized fading channels with MRC and SLS receptions. The authors have also presented the impact of signal strength, fading parameters, time-bandwidth product, diversity orders and single combining techniques on the ROC curves [88]. The PDF based approach is used to derive an analytical expression for $\overline{P_{DT}}$ of ED at the FC for centralized cooperative multiple input multiple output (MIMO) CR networks over i.i.d. eta-mu fading channels [89]. The PDF of alpha-kappa-mu has been derived to formulate ED for sensing. The detection probability has been investigated in terms of Marcum Q-function. The analytical closed-form of $\overline{P_{DT}}$ and $\overline{A}$ curves are derived and these result further extended to MRC, SLC, and SLS diversity receptions [90]. The performance of ED is discussed in terms of CROC and average AUC curves and analytical expressions are formulated in Fox-H function over a generalized fading channel, alpha-eta-mu. The obtained

results are generic that can be used for further analysis of eta-mu and alpha-mu fading channels as special cases. This analysis is also involved with CSS and SLS reception [91].

2.3 SS based on Composite Fading

Shadowing is captured by log-normal distribution addressed on the indoor and outdoor scenario. Gamma and inverse Gaussian (IG) distribution are used as an alternate of the log-normal distribution [92-95]. In most of the WCS, simultaneous effect of both kinds of fading is encountered very frequently in a realistic environment, that is, shadowing and multipath fading. Combination of these two fading effects is called composite fading. The number of alternatives for composite fading has been suggested in literature survey like Rayleigh/log-normal, Nakagami/Gamma, Weibull/Gamma, Nakagami-inverse Gamma, Weibull/log-normal, Hoyt/log-normal, Hoyt/Gamma and two waves diffused power (TWDP) with mixture Gamma etc. [96-99]. The performance evaluation of ED in Hoyt/Gamma fading with MRC reception has been considered for $\overline{P_{DT}}$ and $\overline{A}$ curves. The simulation results are also incorporated with the exact one for accuracy purpose [100]. The mixture Gamma (MG) distribution is used for analysing the Hoyt/log-normal with MRC reception. The performance is studied in terms of CROC, ROC and average AUC curves [101]. In [102], the analysis of ED in composite fading channels is considered. For mitigating the effect of fading components, diversity techniques are superimposed such as MRC, SLS, and SLC. As compared to G-distribution, which presents Suzuki and Nakagami/log-normal is more accurate than K and K_G distribution, which is nothing but a Nakagami/log-normal distribution. The performance of detection does not reduce expressively at the light and moderate shadowing conditions because that is greatly reduced by diversity order. The Performance of MRC reception is better than the SLC and SLS receptions. The combined effect of slow and fast fading is considered and the output of detection is derived in closed-form expression [103]. The following diversity schemes

well known as SC, MRC and EGC are involved while calculating the mathematical expressions of $\overline{P_{DT}}$ and $\overline{A}$ over Shadowed Rician Gamma channels. The performance matrices are obtained in terms of $\overline{A}$ and CROC curves [104]. The alternate way to approximate log-normal is Gamma distribution of the shadowing which provides similar and better response and very close to real time scenario. The *K* distribution, a combination of Rayleigh and Gamma distribution, is used to approximate the Rayleigh/log-normal distribution in a real scenario, represented as *K*-channel. In K_G distribution, a mixture of Nakagami and Gamma distribution is presented to approximate Nakagami/log-normal channel in real-time environments, designated to as K_G channel. The K_G channel includes special cases, such as the *K* channel, and can also approximate the Nakagami-m, Rayleigh/log-normal, and Suzuki channel. A closed-form expression is derived for $\overline{P_{DT}}$ without diversity and with diversity as MRC and SC reception and results are verified by simulation results [105]. The closed-form analytical expression is derived for P_{MD} over Rayleigh/shadowing, where shadowing is estimated by log-normal distribution [106]. The analysis of ED based SS in the vehicle to vehicle and vehicle to roadside infrastructure in vehicular networks is very much practical, nowadays. The analytical expression of $\overline{P_{DT}}$ and amount of fading (AF) is investigated over Nakagami-m/Gamma fading channel [107]. The performance of ED over Gamma shadowed Rice fading channels, namely Rice fading channels with fluctuating LOS components following the Gamma distribution. For accurate characterization of channel performance, firstly an analytical expression of $\overline{P_{DT}}$ is derived using PDF or MGF based. Another performance metric, average AUC is also derived with infinite series and presented performance of detection in the shadowed environment [108]. In a similar way, the performance of ED over Rician/shadowed fading channel is discussed without and with MRC and EGC diversity reception and both the performance parameter is also derived i.e. $\overline{P_{DT}}$ and $\overline{A}$ curves and infinite series is also convergent [109]. In [110], new

composite fading channel is derived which involved with an exponential integral representation for the generalized Marcum Q-function based on MGF approach. ED without and with SLC and SLS is demonstrated in terms of ROC curves for different *m*-fading parameters, shadowing mean and shadowing variance. A novel tractable expression for $\overline{P_{DT}}$ in SS CR system is investigated over extended generalized K-fading (EGK) channels. The following distributions like Weibull, Rayleigh, log-normal, Nakagami-m, generalized distribution and some other distributions are the special or limiting cases for EGK distributions [111]. The novel analytical expression of the average probability of detection for single channel scenario and SLC and SLS reception is derived over composite MG fading channels [112]. By considering both types of fading environments i.e. small scale and large scale which are generally encountered in real time scenario. In [113], composite fading is modelled by Nakagami-m/shadowed fading channel. The P_{DT} and P_{FA} is derived for composite fading channels in CSS environments. The performance analysis detection is also compared with the Rayleigh/Gamma channel. Yoo *et. al.* has proposed the Fisher-Snedecor *F*-distribution to model composite fading channels in which RMS power of a Nakagami-*m* signal is assumed to be subject to variations induced by inverse Nakagami-*m* random variable. The *F*-distribution provides a good and in most cases better fit to real-world fading channels as compared to K_G distribution. Computationally tractable analytical expressions for $\overline{P_{DT}}$ and $\overline{A}$ curves are derived in CSS scenario and the derived expression are extended for SLS diversity receptions. Along with these, performance matrices, a closed-form expression of Shannon entropy and cross entropy over composite *F*-distribution is investigated for different channel conditions [114]. The CSS based detection over Suzuki fading channel is investigated and presented soft decision is better than the hard decision for detection of the unknown deterministic signal with EGC diversity reception. The performance is done based on PDF and MGF using Gaussian-Hermite integration

approximation [115]. The ED based SS over generalized K_G distribution is analysed using AUC curves. The derived expressions are used to extend the diversity receptions for MRC, SLC, and SC [116].

The performance of ED based SS over different generalized composite fading channels such as alpha-mu/IG, kappa-mu/IG, and eta-mu/IG has been investigated in terms of $\overline{P_{DT}}$ and $\overline{A}$ curves. Firstly, a unified PDF is derived for all three generalized fading channels based on Gauss-Laguerre integration. Furthermore, the obtained expressions to utilize for CSS under all three channel conditions such as light, moderate and heavy shadowing [117]. Shadowing is also modelled by Gamma distribution. So, unified analytical expressions for $\overline{P_{DT}}$ and average AUC curves are formulated using Gauss-Laguerre integration approximation over generalized composite fading for alpha-eta-mu/Gamma, alpha-kappa-mu/Gamma. The produced results are very much generic that can be also stretched for alpha-eta-mu, alpha-kappa-mu, kappa-mu, eta-mu/Gamma, alpha-mu/Gamma and kappa-mu/Gamma [118]. The diversity receptions MRC and SLC has been incorporated in kappa-mu/shadowed and kappa-mu extreme/shadowed fading channels for the performance of ED. The analytical expression of $\overline{A}$ curves is derived for both the composite fading channels [119]. The mathematically tractable and unified analytical expression of $\overline{P_{DT}}$ and average AUC curves are derived over composite generalized fading channels, kappa-mu/Gamma, eta-mu/Gamma, and alpha-mu/Gamma [120]. The physical fading model is resembled to eta-mu/inverse Gaussian fading channel. The eta-mu distribution is nothing but a generalized small scale fading channel which effectively for NLOS scenarios and includes special cases like Hoyt, Rayleigh, Rice, Nakagami-m, and one-sided Gaussian distribution. In a similar fashion, the inverse Gaussian (IG) is a more convenient model recently for characterizing the shadowing effect than the Gamma distribution. The novel analytical expression is derived for the power and envelope PDF of eta-mu/IG. The derived

expressions can be utilized for various field of study like radio communications, ultrasound imaging and free space optical communications and others [121]. The analytically and numerically, $\overline{P_{DT}}$ is derived over a composite generalized fading channel, kappa-mu/inverse Gamma. The effectiveness and soundness of this fading channel are validated by means of modelling the fading effects faced in body-centric communication channel, which is known to be vulnerable to the shadowing effects [123].

2.4 Threshold Optimization

To enhanced spectrum utilization, the threshold should be optimized and that can be optimized if and only if by minimizing the total probability of error (P_{TE}). In convention threshold method, the threshold is static a specific point so when the received power of the signal swing SU. It is not possible to identify the signal along with it also does not work at very SNR, adaptive or optimized threshold is wont to overwhelm the problem of low SNR. The threshold is varied by the variation of the received signal is called an optimized threshold. While comparing the fixed one with an optimized threshold, the optimized threshold provides better results [123].

The problem of optimizing threshold by reducing the probability of error for CSS has been measured for Rayleigh, hyper-Rayleigh and myriad fading channels [124-126]. For minimizing the probability of miss-detection and the probability of false alarm, optimum threshold process has been conferred [127-128]. Adaptive double threshold (ADT) overwhelms the delinquent of identifying failure for CSS. ADT is enhanced methods in contrast to the local threshold, which offers improved spectrum detecting even at very low SNR through multiple EDs [129]. A global threshold is achieved by minimizing the total probability of error through enriched ED and each detector are incorporated by SC [130-131]. In open literature, MG fading channel is considered for CSS with multiple antenna nodes. The exact closed-form expression of P_{DT}

is achieved with a generic infinite series representation and finite upper bound for the involved truncation error. The derived $\overline{P_{DT}}$ also incorporated with diversity schemes, MRC, SLC, and SLS. Furthermore, the P_{TE} is also minimized by applying optimum fusion rule [132]. The analytical expressions of $\overline{P_{DT}}$ and average AUC curves over Hoyt/Gamma fading channels with MRC reception are derived and investigated. In addition, the optimized threshold has been incorporated to overcome the problem of SS at low SNR [133]. The three main factors of CRN comprises wireless channel between PUs and CRs nodes, sensing time and detection threshold. The closed-form expression of $\overline{P_{DT}}$ over TWDP fading channel is derived and it is also known as a Hyper-Rayleigh fading channel. Further, this expression is used to optimize the threshold by minimizing the total probability of error [134].

2.5 Research Gaps

The literature survey presented on the energy detection based spectrum sensing over different fading channels without and with reception schemes exploits to use the spectrum efficiently. Therefore, the key concern of this thesis is to propose the frameworks which can exploits the spectrum sensing efficiently over fading channels. The study and analysis of inverse Gaussian, Nakagami-*m*/log-normal and Weibull/log-normal channel with diversity reception has not been considered. Hence, from the literature survey following research gaps of energy detection based spectrum sensing in cognitive radio are identified:

- Energy detection and threshold optimization over Inverse Gaussian fading channel with selection combining have not been explored in the literature.
- Performance analysis of energy detection based spectrum sensing in cognitive radio over Nakagami-*m*/shadowed fading channel with maximum ratio combining has not been considered in the literature.

- Spectrum sensing based on energy detection over Shadowed Weibull fading environments with maximum ratio combining is not investigated in the literature.
- Performance matrices and energy detection over Nakagami-*m*/log-normal fading environments have not been explored in the literature.

2.6 Research Objectives

The objective of this thesis is to sense the white space spectrum in cognitive radio based on energy detection technique over different fading channels such as multipath, shadowed or composite multipath/shadowed fading with or without different diversity techniques such as maximum ratio combining and selection combining has identified based on the research gaps. Furthermore, the optimized threshold has been incorporated to overcome the problem of spectrum sensing even at low signal to noise ratio. The objectives of this thesis are includes:

- To derive the closed-form expression of the average probability of detection for energy detection based spectrum sensing over Inverse Gaussian fading channel with section combining diversity. The performance is analysed in terms of CROC and ROC curves.
- To analyse the behaviour of energy detection based spectrum sensing and threshold optimization over Nakagami-*m*/shadowed fading channel with maximum ratio combining reception using a Gaussian-Hermite approximation in terms of CROC and AUC curves.
- To study energy detection and threshold optimization based spectrum sensing in cognitive radio over Shadowed Weibull fading environments for maximum ratio combining diversity with the arbitrary number of branches.
- To analysis performance matrices and energy detection over Nakagami-*m*/log-normal fading channel in terms of the amount of fading, outage probability, channel capacity, average symbol error probability.

Chapter 3

Performance Evaluation of IG Channel with SC Reception

Shadowed fading channel is modelled by a log-normal distribution. However, when the channel severity increases, it may be modelled by other distributions keeping the behaviour of distribution remain same. Therefore, IG distribution is one of another option to replace log-normal distribution. The IG distribution is used to model turbulence affected free space optical (FSO) communication. In this chapter, the performance evaluation of SS based ED technique in CRNs over Inverse Gaussian (IG) channel for SC diversity technique has been analysed. The analytical expressions for $\overline{P_{DT}}$ under different detection scenarios such as SISO and with diversity reception are studied. In addition, the optimized threshold is achieved by minimizing the P_{TE} over several diversity branches. The impact of shadowing parameters of ED is considered in terms of CROC curves.

3.1 System Model

In ED technique, SUs detects whether the PU is present or not. By considering a narrow band signal, which is identified as a received signal $s(t)$. The $s(t)$ can be consist of either noise only or both signal and noise only. It can be represented as

$$s(t)=\begin{cases} n(t) & ;H_0 \quad (Signal\ is\ absent) \\ g\,r(t)+n(t) & ;H_1 \quad (Signal\ is\ present) \end{cases} \tag{3.1}$$

where, $r(t)$ represents the unknown deterministic signal, g is the channel gain, and $n(t)$ is an AWGN.

Furthermore, in the detection of the signal, either signal is absent or signal is present and it is characterized by the two hypothesis, first one is known as a null hypothesis H_0, and the second one is known as an alternate hypothesis H_1, respectively. The ED, first filter the signal, square it and integrate over the time interval T as shown in Fig. 3.1. The output of the integrator Δ acts as test statistic that decides whether the received signal energy corresponds to noise energy $n(t)$ or energy of both $r(t)$ and $n(t)$. At the end of ED, Δ compares with the threshold (λ) and if $\Delta < \lambda$, the signal is absent otherwise present [135].

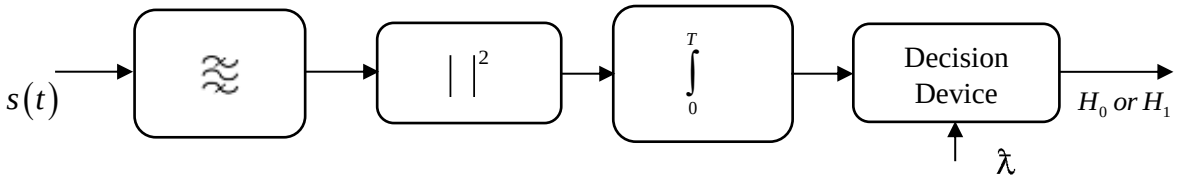

Fig. 3.1 Block diagram of ED

The output of ED can be denoted as $\Delta = \left(\frac{2}{N_0}\right)\int_0^T y^2(t)dt$. So, the analogous to the null hypothesis H_0, the Δ can be represented as

$$\Delta = \left(\frac{2}{N_0}\right)\int_0^T n^2(t)dt = \sum_{k=1}^{2n}\left(\frac{n_k}{\sqrt{(N_0 W)}}\right)^2 : H_0 \tag{3.2}$$

$$\Delta \sim \chi^2_{2n} \tag{3.3}$$

Note that since $n_k \sim N(0, N_0 W)$, Δ under H_0, is the square sum of 2η Gaussian random variable with mean 0 and variance 1. Thus, chi-square distribution (central, 2η degrees of freedom) with the PDF is given as

$$p_\Delta(y) = y^{\eta-1}\left(\frac{exp\left(-\frac{y}{2}\right)}{2^\eta \Gamma(\eta)}\right) : H_0 \tag{3.4}$$

Here, $\eta = TW$ (time-bandwidth product). Similarly, under the alternate hypothesis H_1, the decision statistic is chi-square distribution (non-central, 2η degrees of freedom and 2γ non-centrality parameter), the decision statistic [64] can be denoted as

$$\Delta = \left(\frac{2}{N_0}\right)\int_0^T \left(gr(t)+n(t)\right)^2 dt = \sum_{k=1}^{2\eta}\left(\frac{\left(gr_k+n_k\right)}{\sqrt{\left(N_0W\right)}}\right)^2 \qquad : H_1 \tag{3.5}$$

$$\Delta \sim {\chi_{2\eta}}^2\left(2\gamma\right) \tag{3.6}$$

Note that mean of Δ under H_1, is $\frac{gr_k}{\sqrt{\left(N_0W\right)}}$. Thus, the chi-square distribution (non-central) with $(\sigma^2 = 1)$ PDF is given as

$$p_\Delta(y) = \left(\frac{1}{2}\right)\left(\frac{y}{r^2}\right)^{(\eta-1)/2} exp\left(-\frac{\left(r^2+y\right)}{2}\right) I_{\eta-1}(y,r) \qquad : H_1 \tag{3.7}$$

where, $r^2 = \sum_{k=1}^{2\eta}\left(\frac{gr_k}{\sqrt{N_0W}}\right)^2 = \frac{g^2}{N_0W}\sum_{k=1}^{2\eta} r_k^2 = \frac{2g^2S}{N_0W} = 2\gamma, \gamma = \frac{g^2S}{N_0}$ *and* $S_r = \frac{\left(\frac{r_k}{\sqrt{2}}\right)^2}{W} = r_{k,rms}T$ and

$\Gamma(.)$ is the gamma function[136].

Thus, knowing the PDF of decision statistic Δ, one can easily estimate the probability of Δ being less than a certain threshold (λ) which is nothing but the outage probability of Δ so, P_{FA} P_{DT} are given as

$$P_{FA} = Prob\left(\Delta > \frac{\lambda}{H_0}\right) = 1 - \int_0^\lambda p_{\gamma,H_0}(y)\,dy = \frac{\Gamma(\eta,\lambda/2)}{\Gamma(\eta)} \tag{3.8}$$

$$P_{DT} = Prob\left(\Delta > \frac{\lambda}{H_1}\right) = 1 - \int_0^\lambda p_{\gamma,H1}(y)\,dy = Q_\eta\left(\sqrt{2\gamma},\sqrt{\lambda}\right) \tag{3.9}$$

where, $P_{MD} = 1 - P_{DT}$ and $Q_\eta(a,b)$ is the η^{th} order generalized Marcum Q-function and $\Gamma(a,b)$ is the incomplete Gamma function. Generalized Marcum Q-function [136] is denoted as

$$Q_p(\alpha,\psi) = \frac{1}{\alpha^{p-1}} \int_{\psi}^{\infty} \tau^p \exp\left(-\frac{(\alpha^2+\tau^2)}{2}\right) I_{p-1}(\alpha,\tau)\, d\tau \tag{3.10}$$

Marcum Q-function can be represented as also in [50] equally

$$Q_\eta\left(\sqrt{2\gamma},\sqrt{\lambda}\right) = \sum_{h=0}^{\infty} exp(-\gamma)\left(\frac{\gamma^h}{h!}\right) \sum_{l=0}^{h+\eta-1} \left(exp\left(-\frac{\lambda}{2}\right)\right) \left(\frac{\left(\frac{\lambda}{2}\right)^l}{l!}\right) \tag{3.11}$$

Equation (3.11) can be given in [136] as

$$Q_\eta\left(\sqrt{2\gamma},\sqrt{\lambda}\right) = \sum_{h=0}^{\infty} exp(-\gamma)\frac{\gamma^h}{h!}\frac{\Gamma\left(h+\eta,\frac{\lambda}{2}\right)}{\Gamma(h+\eta)} = exp(-\gamma)\sum_{h=0}^{\infty}\frac{\gamma^h}{h!}\frac{\Gamma\left(h+\eta,\frac{\lambda}{2}\right)}{\Gamma(h+\eta)} \tag{3.12}$$

So, from equations (3.9) and (3.12) as

$$P_{DT} = Q_\eta\left(\sqrt{2\gamma},\sqrt{\lambda}\right) \approx exp(-\gamma s)\sum_{h=0}^{\infty}\left(\frac{(\gamma s)^h}{h!}\right)\frac{\Gamma\left(h+\eta,\frac{\lambda}{2}\right)}{\Gamma(h+\eta)} \tag{3.13}$$

It is marked from (3.8) that the P_{FA} is same over any fading channel as it does not depend on the fading parameter. It only depends on the number of samples and the threshold parameter. The expression in the equations (3.8) and (3.9) are achieved by considering the channel as non-fading and thus channel parameter or gain g in (3.7) is assumed constant.

3.2 Channel Model

If the channel is characterized by IG distribution, then P_{DT} in (3.9) becomes a statistical parameter and hence its average with respect to the given distribution needs to be found.

Considering SC diversity with each branch as i.i.d., the PDF of output SNR of SC [137] is defined as

$$p_{SC}(y) = B\left(P_{\Delta}(y)\right)^{B-1} \times p_{\Delta}(y) \tag{3.14}$$

where, $P_{\Delta}(y)$ and $p_{\Delta}(y)$ are the cumulative distribution function (CDF) and PDF of a random variable (RV) Δ, B is the number of diversity branches of SC. The CDF and PDF for IG distribution [53] are given as

$$P_{\Delta}(y) = Q\left[\sqrt{\frac{\lambda}{y}}\left(\frac{1-y}{\theta}\right)\right] + exp\left(\frac{2\lambda}{\theta}\right)Q\left(\sqrt{\frac{\lambda}{y}}\left(\frac{1+y}{\theta}\right)\right) \tag{3.15}$$

$$p_{\Delta}(y) = y^{-3/2}\sqrt{\frac{\lambda}{2\pi}}exp\left(\frac{\lambda}{\theta}\right)exp\left(-\lambda\left(\frac{y}{2\theta^2}+\frac{1}{2y}\right)\right) \tag{3.16}$$

Equation (3.14) can be written again by the property of Q-function $Q(-x) = 1-Q(x)$ given in equation (3.17).

The Q-function reduces analytical complexity while solving the integral using equation (3.17) along with other function. The difficulty is overcome by using 2nd order exponential estimation of Q-function [136]. Putting CDF and PDF in (3.14) and restoring to the 2nd order exponential approximation of Q-function, the PDF of IG distribution for SC is given in equation (3.18).

$$p_{SC}(\gamma) = \begin{cases} B\left[Q\left(\sqrt{\frac{\lambda}{y}}\left(\frac{1-y}{\theta}\right)\right) + exp\left(\frac{2\lambda}{\theta}\right)Q\left(\sqrt{\frac{\lambda}{y}}\left(\frac{1+y}{\theta}\right)\right)\right]^{B-1} & \gamma < \theta \\ \times\left(\frac{\lambda}{2\mu y^3}\right)^{1/2} exp\left(-\frac{\lambda(y-\theta)^2}{2\theta^2 y}\right) & \\ B\left[\left(1-Q\left(\sqrt{\frac{\lambda}{y}}\left(\frac{1-y}{\theta}\right)\right)\right) + exp\left(\frac{2\lambda}{\theta}\right)Q\left(\sqrt{\frac{\lambda}{y}}\left(\frac{1+y}{\theta}\right)\right)\right]^{B-1} & \gamma > \theta \\ \times\left(\frac{\lambda}{2\mu y^3}\right)^{1/2} exp\left(-\frac{\lambda(y-\theta)^2}{2\theta^2 y}\right) & \end{cases} \tag{3.17}$$

$$p_{SC}(\gamma)=\begin{cases}\sum_{k=0}^{B-1}\sum_{n=0}^{K}\sum_{j=0}^{M}B\sqrt{\frac{\lambda}{2\pi}}\binom{B-1}{k}\binom{K}{n}\binom{M}{j}\left(\frac{a_1}{2}\right)^{B-n-j-1}\left(\frac{a_2}{2}\right)^{n+j}\times & \gamma<\theta\\ exp\left(\left(\frac{\lambda}{\theta}\right)\left\{-b\left(M+j-k-n\right)+2M+1\right\}\right)\left(\gamma^{-3/2}\right)exp\left(-\left\{\frac{\xi_1}{\gamma}+\xi_2\gamma\right\}\right) & \\ \sum_{k=0}^{L-1}\sum_{i=0}^{K}\sum_{n=0}^{I}\sum_{j=0}^{M}B\sqrt{\frac{\lambda}{2\pi}}\binom{B-1}{k}\binom{K}{i}\binom{I}{n}\binom{M}{j}\left(\frac{a_1}{2}\right)^{B-n-j-1}\left(\frac{a_2}{2}\right)^{n+j} & \gamma>\theta\\ \times exp\left(\left(\frac{\lambda}{\theta}\right)\left\{-b\left(M+j-i-n\right)+2M+1\right\}\right)\left(\gamma^{-3/2}\right)exp\left(-\left\{\frac{\xi_3}{\gamma}+\xi_4\gamma\right\}\right) & \end{cases} \tag{3.18}$$

where, $M=B-K-1$; $\xi_1=\frac{\lambda}{2}\left[b\left(B+n+j-1\right)+1\right]$; $\xi_2=\frac{\lambda}{2\theta^2}\left[b\left(B+n+j-1\right)+1\right]$

$$\xi_3=\frac{\lambda}{2}\left[b\left(B-K+n+i+j-1\right)+1\right];\quad \xi_4=\frac{\lambda}{2\theta^2}\left[b\left(B-K+n+i+j-1\right)+1\right]$$

$$J_1=B\sqrt{\frac{\lambda}{2\pi}}\binom{N-1}{k}\binom{K}{n}\binom{M}{j}\left(\frac{a_1}{2}\right)^{N-n-j-1}\left(\frac{a_2}{2}\right)^{n+j}$$

$$J_2=B\sqrt{\frac{\lambda}{2\pi}}\binom{B-1}{k}\binom{K}{i}\binom{I}{n}\binom{M}{j}\left(\frac{a_1}{2}\right)^{B-n-j-1}\left(\frac{a_2}{2}\right)^{n+j}$$

$$x_1=-b\left(M+j-k-n\right)+2M+1;\qquad x_2=-b\left(M+j-i-n\right)+2M+1$$

$$\theta=\exp\left(\frac{\mu}{\xi}+\frac{\sigma^2}{2\xi^2}\right);\qquad \lambda=\frac{\theta}{\left(exp\left(\frac{\sigma^2}{\xi^2}\right)-1\right)}\text{ and }\xi=\frac{10}{ln(10)}$$

Proof: See Appendix A

Now, using the above notations, the equation (3.18) can concisely be expressed as

$$p_{SC}(\gamma)=\begin{cases}J_1\gamma^{-3/2}exp\left(\left(\frac{\lambda}{\theta}\right)r_1\right)exp\left(-\frac{\xi_1}{\gamma}-\xi_2\gamma\right) & \gamma<\theta\\ J_2\gamma^{-3/2}exp\left(\left(\frac{\lambda}{\theta}\right)r_2\right)exp\left(-\frac{\xi_3}{\gamma}-\xi_4\gamma\right) & \gamma>\theta\end{cases} \tag{3.19}$$

here, $\mu > 0$ is the mean, θ is the mean of fluctuations and $\lambda > 0$ is the shape parameter. As λ inclines to infinity, the IG becomes more likely to a Gaussian distribution. The above obtained closed-form expression provides the low computational cost.

3.3 Average Probability of Detection

When experiencing a fading channel, P_{FA} in equation (3.8) will remain, be the same, since it does not dependent on the SNR. But, when g varies the $\overline{P_{DT}}$ can be easily evaluated by averaging P_{DT} in equation (3.9) over the SNR distribution [135] as

$$\overline{P_{DT}} = \int_0^\infty P_{DT}(\gamma, \tilde{\lambda}) p(\gamma) d\gamma = \int_0^\infty Q_\eta\left(\sqrt{2\gamma}, \sqrt{\tilde{\lambda}}\right) p_{SC}(\gamma) d\gamma \tag{3.20}$$

The output of the combiner picks that branch which is having the highest SNR among all diversity branches. The instantaneous SNR at the output of the SC is $\gamma_{SC} = \max\{\gamma_1, \gamma_2 ....., \gamma_B\}$, where γ_B is the SNR in the B^{th} branch.

The P_{FA} will remain the same as given in equation (3.8). $\overline{P_{DT}}$ with SC diversity is derived by substituting equations (3.13) and (3.19) into equation (3.20) as

$$\overline{P_{DT}} = \left\{ \begin{array}{l} J_1 exp\left(\frac{\lambda}{\theta} r_1\right) \int_0^\theta \gamma^{-3/2} exp\left(-\frac{\xi_1}{\gamma} - \xi_2 \gamma\right) exp(-\gamma s) \sum_{h=0}^\infty \frac{(\gamma s)^h}{h!} \frac{\Gamma\left(h+\eta, \frac{\tilde{\lambda}}{2}\right)}{\Gamma(h+\eta)} d\gamma + \\ J_2 exp\left(\frac{\lambda}{\theta} r_2\right) \int_\theta^\infty \gamma^{-3/2} exp\left(-\frac{\xi_3}{\gamma} - \xi_4 \gamma\right) exp(-\gamma s) \sum_{h=0}^\infty \frac{(\gamma s)^h}{h!} \frac{\Gamma\left(h+\eta, \frac{\tilde{\lambda}}{2}\right)}{\Gamma(h+\eta)} d\gamma \end{array} \right\} \tag{3.21}$$

Using the relation $\int_0^\infty r^{v-1} exp\left(-\beta r^p - \frac{\gamma}{r^p}\right) dx = \frac{2}{p}\left(\frac{\gamma}{\beta}\right)^{\frac{\gamma}{2p}} K_{v/p}\left(2\sqrt{\beta\gamma}\right); \beta > 0, \mathrm{Re}\,\gamma > 0$ and $\Gamma(t, r, b) = \int_r^\infty t^{r-1} e^{-t-(b/t)} dt$; $r > 0, \mathrm{Re}\, b > 0$ [136] in (3.21), we get the expression for the $\overline{P_{DT}}$ in equation (3.22).

In Table 3.1, the truncation error incurred in approximating the series of (3.22) to the term $h=3$ and $h=5$ for several SNR (dB) values has been analysed for all the three realistic scenarios such as light shadowing, moderate shadowing and heavy shadowing [138].

Table 3.1 Mean square error (MSE) for convergence of the $\overline{P_{DT}}$ for various value of SNR (dB) and time-bandwidth product (η) =10 for various realistic scenarios

SNR (dB)	Light Shadowing		Moderate Shadowing		Heavy Shadowing	
	$h=3$	$h=5$	$h=3$	$h=5$	$h=3$	$h=5$
-10	8.752×10^{-8}	5.424×10^{-31}	7.467×10^{-8}	4.293×10^{-28}	1.380×10^{-9}	3.571×10^{-22}
-5	9.431×10^{-7}	2.541×10^{-28}	1.279×10^{-7}	8.249×10^{-25}	6.128×10^{-8}	5.407×10^{-20}
0	4.901×10^{-6}	3.807×10^{-26}	6.478×10^{-6}	9.780×10^{-23}	4.257×10^{-7}	6.245×10^{-18}
5	9.027×10^{-5}	8.568×10^{-23}	9.472×10^{-5}	6.241×10^{-21}	9.021×10^{-6}	9.042×10^{-16}
10	1.021×10^{-4}	3.781×10^{-20}	6.498×10^{-5}	5.152×10^{-18}	7.421×10^{-5}	4.654×10^{-14}

$$\overline{P_{DT}} \approx \left[\left(J_1 exp\left(\frac{\lambda}{\theta}r_1\right)\right)\sum_{h=0}^{\infty}\frac{s^h}{h!}\frac{\Gamma\left(h+\eta,\frac{\hat{\lambda}}{2}\right)}{\Gamma\left(h+\eta\right)}\left\{2\left(\frac{\xi_1}{s+\xi_2}\right)^{h-1/2}K_{h-1/2}\left(2\sqrt{\left(s+\xi_1\right)\xi_1}\right)-\left(\frac{1}{\left(s+\xi_2\right)^{h-1/2}}\right)\Gamma\left(\frac{h-1}{2},T_0,\xi_1\left(s+\xi_2\right)\right)\right\}\right] + \left[\left(J_2 exp\left(\frac{\lambda}{\theta}r_2\right)\right)\sum_{h=0}^{\infty}\frac{s^h}{h!}\frac{\Gamma\left(h+\eta,\frac{\hat{\lambda}}{2}\right)}{\Gamma\left(h+\eta\right)}\left(\frac{1}{\left(s+\xi_4\right)^{h-1/2}}\right)\Gamma\left(\frac{h-1}{2},y_0,\xi_3\left(s+\xi_4\right)\right)\right] \quad (3.22)$$

where, $K_{h-1/2}(\varepsilon)$ designates the modified Bessel Function of the 2nd kind with order ($h-\frac{1}{2}$).

3.4 Optimization of Threshold

Deciding the detection threshold parameter is crucial for accurate estimation of the available spectrum. If the threshold is too low, it will it will give an overestimate of the presence of the

signal and thus false alarm will be high resulting in loss of scarce primary spectrum. If the threshold level is too high, then, the primary signal present could also be treated as noise and probability of detection will decrease. This will result in PU being less protected. There are various approaches to improve the performance of CR performance. The sensing time is optimized to enhance the throughput. The work in [124] has analysed the problem of optimizing threshold parameter by minimizing the error probability for cooperative sensing has been considered for Rayleigh channel. To optimize the threshold can be achieved by minimizing the probability of error for IG distributed channel with diversity scheme. The P_{TE} [123,124,139] can be characterized as

$$P_{TE} = P(H_0)P_{FA} + P(H_1)P_{MD} \tag{3.23}$$

Substituting the value of P_{FA} and P_{MD} for SISO and for SC diversity, one can formulate the expression of the probability of error for no diversity and with diversity respectively. The optimum threshold can be acquired by differentiating P_{TE} and equating it to zero, $\frac{\partial(P_{TE})}{\partial(\lambda)} = 0$

It is evident that the P_{TE} given by (3.23) has a global minimum w.r.t. λ. So, the optimized threshold is presented in [124] as

$$\lambda_{opt} = arg\,min_{\lambda}\,(P_{TE}) \tag{3.24}$$

It can be solved by $\frac{\partial(P_{TE})}{\partial(\lambda)} = 0$. Thus considering apriori probability of both the hypothesis to be same, we have

$$\frac{\partial P_{FA}}{\partial\lambda} + \frac{\partial P_{MD}}{\partial\lambda} = 0 \tag{3.25}$$

The first term $\frac{\partial P_{FA}}{\partial \hat{\lambda}}$ is obtained by resorting to the identity $\frac{\partial\left[\Gamma(a,z)\right]}{\partial z} = -z^{a-1}exp(-z)$ [64]. So using this relation, $\frac{\partial P_{FA}}{\partial \hat{\lambda}}$ can be expressed as

$$\frac{\partial P_{FA}}{\partial \hat{\lambda}} = -\frac{\hat{\lambda}^{\eta-1}exp\left(-\frac{\hbar}{2}\right)}{2^{\eta}\Gamma(\eta)} \tag{3.26}$$

The second term $\frac{\partial P_{MD}}{\partial \hat{\lambda}} = \frac{\partial \overline{P_{MD}}}{\partial \hat{\lambda}}$ is obtained as

$$\frac{\partial \overline{P_{MD}}}{\partial \hat{\lambda}} = \frac{\partial\left(1-\overline{P_{DT}}\right)}{\partial \hat{\lambda}} = -\frac{\partial \overline{P_{DT}}}{\partial \hat{\lambda}} \tag{3.27}$$

Substituting (3.22) into (3.27), we get $-\frac{\partial \overline{P_{DT}}}{\partial \hat{\lambda}}$. Now, adding (3.26) and (3.27) then we have

$$\begin{aligned}
&J_1\left(\frac{\theta}{r_1}\right)\left\{exp\left(\frac{r_1\lambda}{\theta}\right)\sum_{h=0}^{\infty}\Gamma\frac{\left(h+\eta,\frac{\hat{\lambda}}{2}\right)}{\Gamma(h+\eta)}+\sum_{h=0}^{\infty}\frac{(-1)^{h+\eta-1}\Gamma(h+\eta)}{2^{h+\eta-1}\left(\frac{r_1}{\theta}-\frac{1}{2}\right)^{h+\eta-1}}\right\}\times \\
&\left\{2\left(\frac{\xi_1}{(s+\xi_2)}\right)^{h-1/2}K_{h-1/2}\left(2\sqrt{(s+\xi_1)}\xi_1\right)-\left(\frac{1}{(s+\xi_2)^{h-1/2}}\right)\Gamma\left(h-\frac{1}{2},T_0,\xi_1(s+\xi_2)\right)\right\}+ \\
&J_2\left(\frac{\theta}{r_2}\right)\left\{exp\left(\frac{r_2\lambda}{\theta}\right)\sum_{h=0}^{\infty}\Gamma\frac{\left(h+\eta,\frac{\hat{\lambda}}{2}\right)}{\Gamma(h+\eta)}+\sum_{h=0}^{\infty}\frac{(-1)^{h+\eta-1}\Gamma(h+\eta)}{2^{h+\eta-1}\left(\frac{r_2}{\theta}-\frac{1}{2}\right)^{h+\eta-1}}\right\}\times \\
&\left\{\left(\frac{1}{(s+\xi_4)^{h-1/2}}\right)\Gamma\left(h-\frac{1}{2},y_0,\xi_3(s+\xi_4)\right)\right\}=\frac{\hat{\lambda}^{\eta-1}exp\left(-\frac{\hat{\lambda}}{2}\right)}{2^{\eta}\Gamma(\eta)}
\end{aligned} \tag{3.28}$$

Solving (3.28) numerically, we get the optimum value of $\hat{\lambda}$ and by using the optimum value of $\hat{\lambda}$, we can get optimum value of P_{MD}, P_{DT} and P_{TE}.

3.5 Results and Discussion

The inclusive study of the analytical expressions is derived and also offer exact numerical results and simulations for authentication purpose. The exact results are attained by replacing the PDF of the single integral (3.20) by (3.14) and then solving integral using MATLAB.

In Fig. 3.2, CROC curve is plotted under various shadowing environments such as light shadowing, moderate shadowing, and heavy shadowing and several values of received average SNR (dB). The plot also includes exact result and simulation for authentication purpose. Clearly, the analytical outcomes achieved by (3.22) are shown to coincide with that of exact and Monte Carlo Simulation. Moreover, as expected, the probability of miss detection is shown to be the lowest for light shadowing and maximum for heavy shadowing.

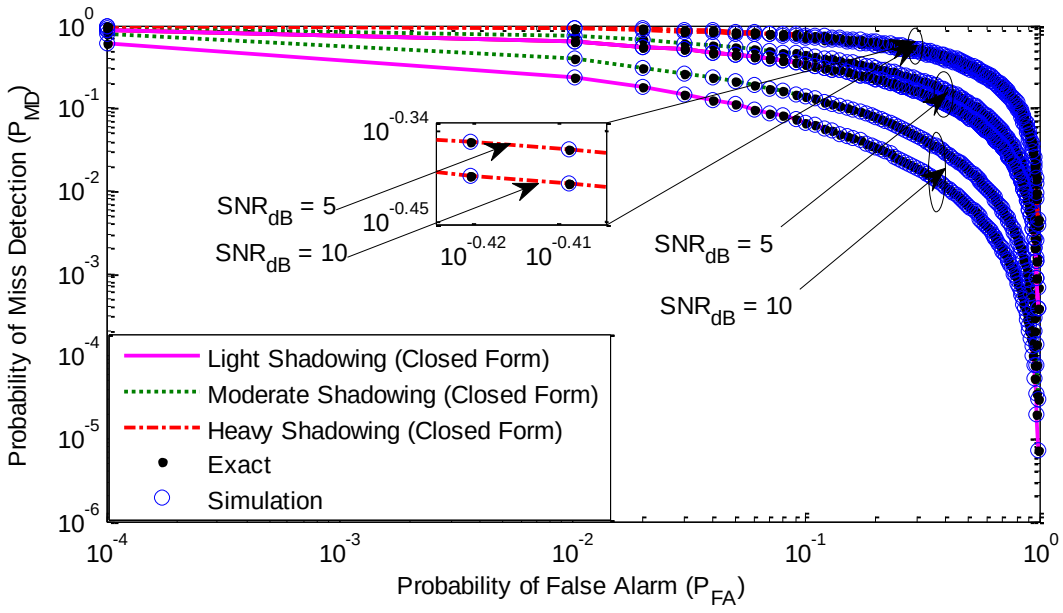

Fig. 3.2 CROC curves for SISO over IG for different shadowing at η=10

The optimization of the detection threshold parameter has been discussed in Fig. 3.3. The inverted bell-shaped plot has been obtained for several values of SNR (-10, 0-, 5, 10) in dB and different shadowing (σ (dB) = 2, 6) cases have been considered. It is witnessed from the Fig.

3.3 that the probability of error given by $P_{TE} = P(H_0)P_{FA} + P(H_1)P_{MD}$ has the global minimum with respect to the threshold ($\hat{\lambda}$).

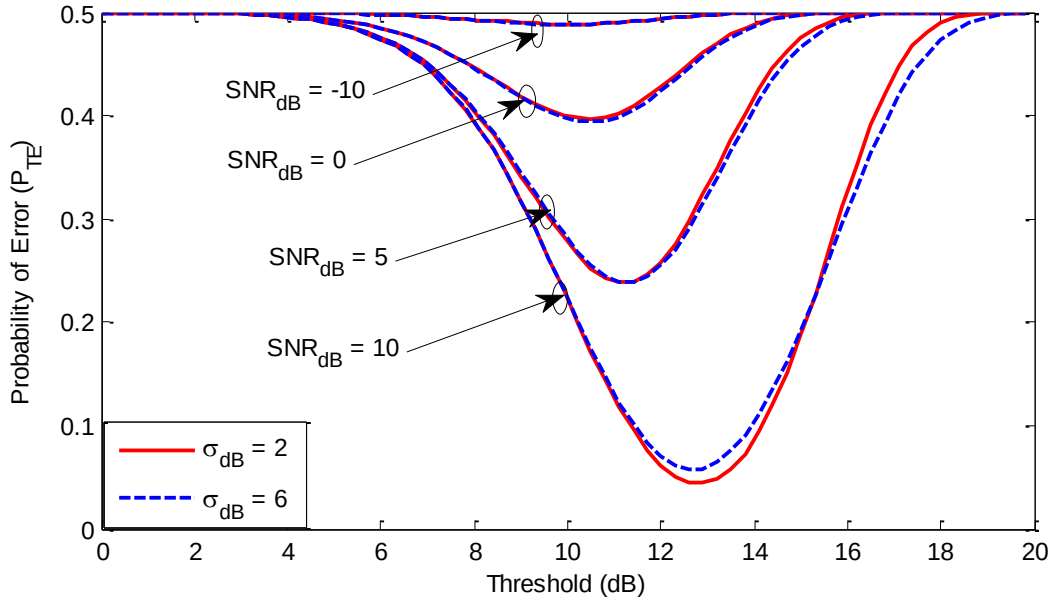

Fig. 3.3 P_{TE} curves vs. threshold $\hat{\lambda}$ (dB) at σ (dB) =2, 6 and SNR (dB) = -10, 0, 5, 10

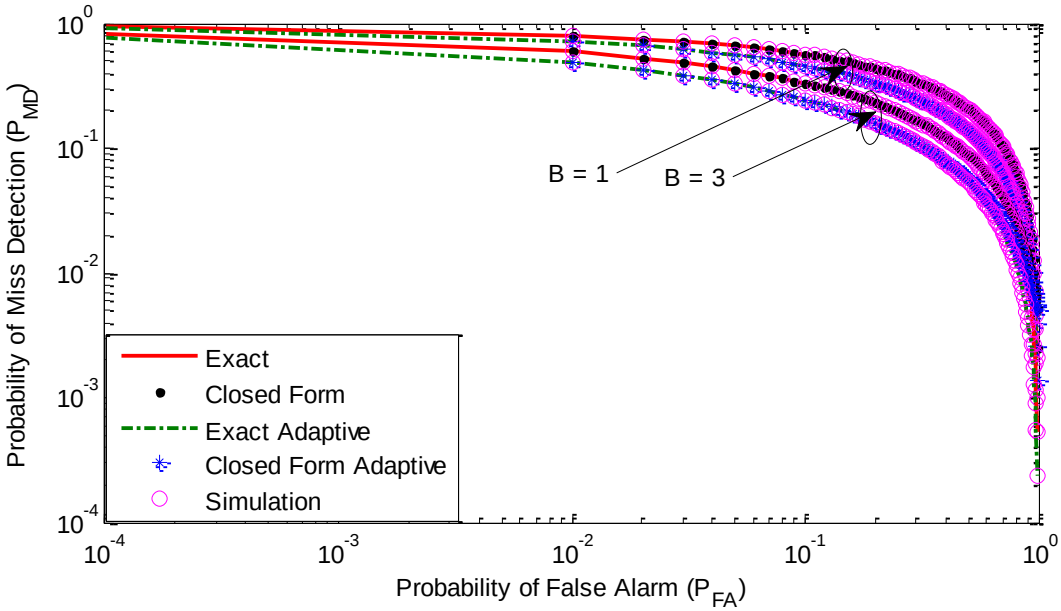

Fig. 3.4 CROC curves with $\sigma = 4\,dB$ and $\mu = 5\,dB$ with a fixed and adaptive threshold at *B*=1, 3

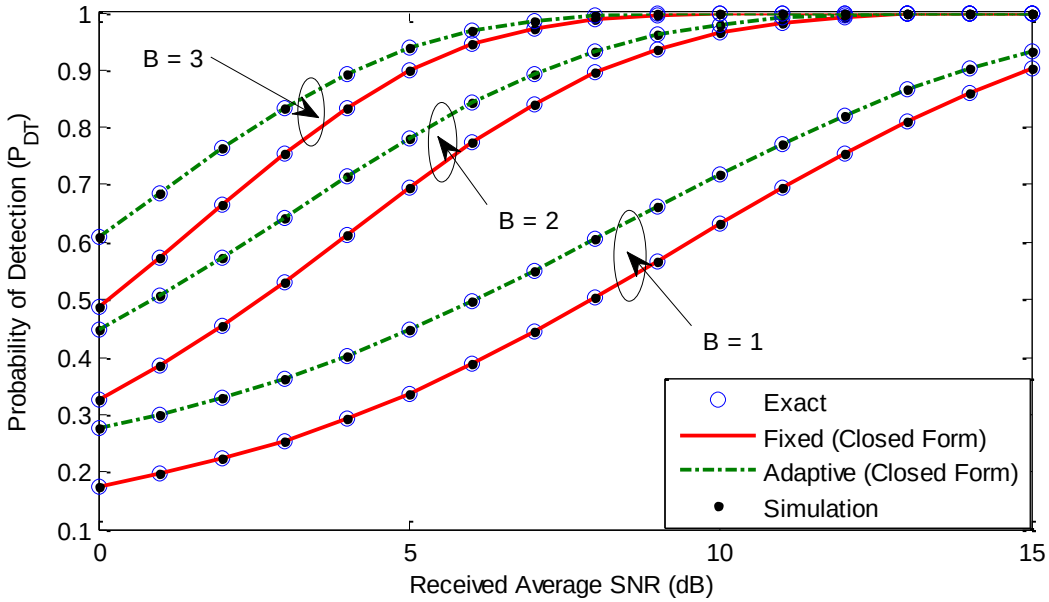

Fig. 3.5 Probability of detection as a function of received average SNR (dB) with a fixed and adaptive threshold at B=1, 2, 3

Fig. 3.4 shows the CROC curve under different SC branches (N=1 and 3) over IG channel for σ (dB) = 4 and μ (dB) = 5 with a fixed threshold and adaptive threshold (optimized threshold obtained from Fig. 3.3). The plot shows the analytical, exact and simulation results. Clearly, the adaptive threshold parameter results in less P_{MD} as compared to the non-adaptive threshold.

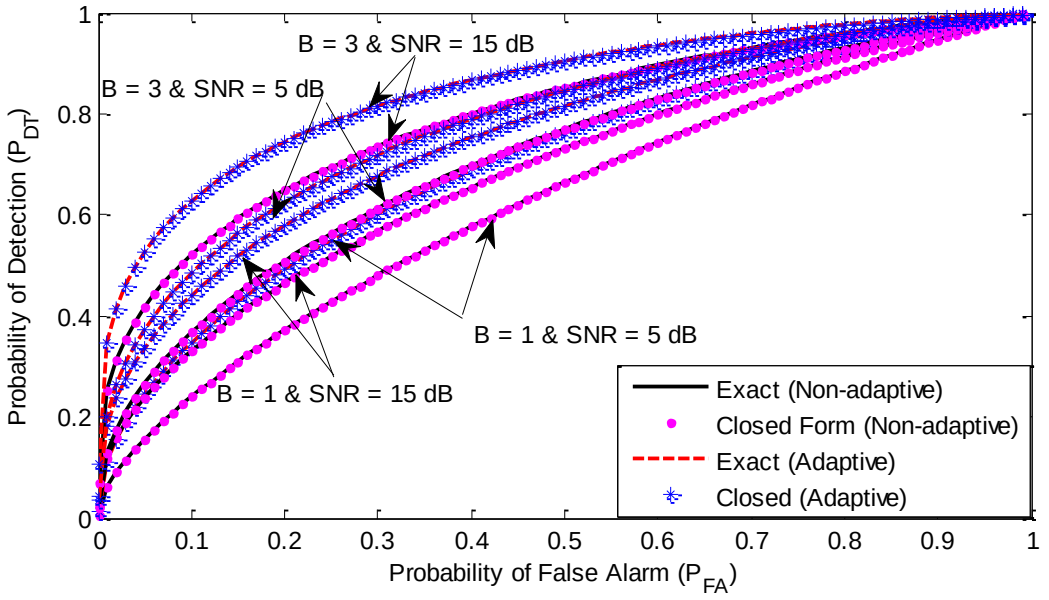

Fig. 3.6 ROC curves under different SC branches (N = 1 and 3) at SNR (dB) = 5, 10

ROC curve over IG channel is shown in Fig. 3.6 with different SC diversity branches (N= 1, 3) at different SNR (dB) = 5, 15. The plot also provides the comparison between ROCs using both fixed as well as an adaptive threshold. As estimated, the rise in diversity order and the optimizing threshold is revealed to advance the P_{DT} of the system.

3.6 Conclusion

In this chapter, an approximate closed-form expression of PDF of SC has been derived and, using this PDF, an analytical expression of the average probability of detection over IG channel using SC diversity technique is derived. Further, threshold parameter is optimized the by minimizing the probability of error. After applying the optimized threshold parameter, a significant improvement in the probability of detection has been demonstrated even at very low SNR. Hence, the performance of the optimized threshold is better than the fixed threshold.

Chapter 4

Performance Evaluation of Nakagami-m/Shadowed Channel with MRC Reception

In the previous chapter, we have discussed shadowed fading only but in this chapter combined effect of both fading i.e. composite multipath/shadowed fading on the channel with diversity technique is explained. Nakagami-m distribution is used to model small scale fading. The Nakagami-m distribution is a powerful statistical tool for modelling fading radio signals. It has the flexibility to describe a wide range of communication engineering problems and modelling reliability data as its hazard rate. The log-normal distribution is widely used in literature to model shadowing effects. The LN distribution is shown to characterize a number of wireless applications such as an outdoor scenario, indoor environments, radio channel affected by body body-worn device, ultra wideband indoor channel, and weak to moderate turbulence channels in free space optical channel. Small scale fading is mitigated through micro diversity while micro diversity is used to overcome the effect of large scale fading. Knowing the fact that maximum ratio combining gives the best performance of all the diversity, the Nakagami-m/Shadowed channel with MRC reception is investigated. The analytical expressions of the average probability of detection and average area under the receiver operating characteristic over Nakagami-*m*/log-normal with MRC are obtained using Gaussian-Hermite integration approximation. In addition, an optimized threshold has been incorporated to overcome the problem of spectrum sensing even at low signal-to-noise ratio.

4.1 Channel Model

The system model of the detection is already explained in the preceding chapter. The composite PDF of received SNR is achieved by averaging the conditional PDF of Nakagami-m

distribution over log-normal distribution. The conditional Nakagami-*m* distribution [50] is given by

$$p_{\gamma}\left(\gamma|v\right)=\frac{m^{m}\gamma^{m-1}}{\Gamma\left(m\right)v^{m}}exp\left(-\frac{m\gamma}{v}\right)\quad;\gamma\geq 0 \tag{4.1}$$

where, v is the average SNR at the receiver, m is the Nakagami-*m* fading parameter ($m\geq 1/2$). Short-term fading is mitigated through micro-diversity approaches using multiple antennas at the receiver [53]. When MRC diversity is incorporated, the overall SNR at the output of the receiver is the sum of SNR of all the individual branches multiplied by their proportional weights. The instantaneous SNR of MRC is given as

$$\gamma_{MRC}=\sum_{b=1}^{N}\gamma_{b} \tag{4.2}$$

where, N is the total number of branches used in the diversity combiner and γ_{b} is the instantaneous SNR of the b^{th} branch. All the branches are assumed to have identical fading statistics, then PDF of the output of MRC in [140] can be represented as

$$p_{\gamma_{MRC}}\left(\gamma|v\right)=\frac{m^{mN}\gamma^{mN-1}}{\Gamma\left(mN\right)v^{mN}}exp\left(-\frac{m\gamma}{v}\right)\quad;\gamma>0 \tag{4.3}$$

Shadowing is captured by log-normal distribution and its PDF is given by

$$p_{v}\left(v\right)=\frac{1}{\sigma v\sqrt{2\pi}}exp\left(-\frac{\left(lnv-\mu\right)^{2}}{2\sigma^{2}}\right) \tag{4.4}$$

where, μ, σ are mean and standard deviation of a random variable (RV) $\ln\left(v\right)$. In *dB*, they can be expressed as $\sigma_{dB}=\tau\sigma$ and $\mu_{dB}=\tau\mu$, where $\tau=10/ln\left(10\right)$ [92]. Averaging the conditional PDF of equation (4.3) w.r.t PDF of equation (4.4) as expressed in equation (4.5)

$$p_{\gamma_{MRC}}\left(\gamma\right)=\int_{0}^{\infty}p_{\gamma_{MRC}}\left(\gamma|v\right)p_{v}\left(v\right)dv \tag{4.5}$$

Substituting equations (4.3) and (4.4), into equation (4.5), we have

$$p_{\gamma_{MRC}}(\gamma)=\int_0^{\infty}\frac{m^{mB}\gamma^{mB-1}}{\Gamma(mB)v^{mB}}exp\left(-\frac{m\gamma}{v}\right)\frac{1}{\sigma v\sqrt{2\pi}}exp\left(-\frac{(lnv-\mu)^2}{2\sigma^2}\right)dv \tag{4.6}$$

It is mathematically intractable to get a closed-from expression of equation (4.6). Therefore, to obtained closed-form expression, approximate equation (4.6) by well know integration approximation called Gaussian-Hermite integration (G-HI). Applying G-HI [141], $\int_{-\infty}^{\infty}p(z)exp(-z^2)dz\approx\sum_{i=1}^{L}w_i p(z_i)$, where, w_i and z_i are weights and abscissas respectively. L is the number of sample points used in G-HI (it is observed that larger is the values of L, smaller is the truncation error). Assuming $z=\frac{(lnv-\mu)}{\sqrt{2}\sigma}$ in equation (4.6), we have

$$p_{\gamma_{MRC}}(\gamma)=\frac{m^{mN}\gamma^{mN-1}}{\Gamma(mN)\sqrt{\pi}}\int_{-\infty}^{\infty}exp\left(-m\left[N\left(\mu+\sqrt{2}\sigma z\right)+\gamma exp\left(-\left(\mu+\sqrt{2}\sigma z\right)\right)\right]\right)exp\left(-z^2\right)dz \tag{4.7}$$

Applying G-HI in equation (4.7); so, the PDF of composite NL fading with MRC diversity is written in equation (4.8) as

$$\begin{aligned}p_{\gamma_{MRC}}(\gamma)&\approx\frac{m^{mN}\gamma^{mN-1}}{\Gamma(mN)\sqrt{\pi}}\sum_{i=1}^{L}w_i\,exp\left(-m\left[N\left(\mu+\sqrt{2}\sigma z_i\right)+\gamma exp\left(-\left(\mu+\sqrt{2}\sigma z_i\right)\right)\right]\right)\\&=\frac{m^{mB}\gamma^{mB-1}}{\Gamma(mB)\sqrt{\pi}}\sum_{i=1}^{L}w_i a_i\,exp(-b_i\gamma)\end{aligned} \tag{4.8}$$

where, $a_i=exp\left(-mN\left(\mu+\sqrt{2}\sigma z_i\right)\right)$, $b_i=m\,exp\left(-\left(\mu+\sqrt{2}\sigma z_i\right)\right)$

Proof: See Appendix B

4.2 Average Probability of Detection

In a similar way, when experiencing a composite fading channel, P_{FA} in equation (3.8) will remain, be the same, since it does not dependent on the SNR. But, when g varies the $\overline{P_{DT}}$ can be easily evaluated by averaging P_{DT} in equation (3.9) over the SNR distribution as

$$\overline{P_{DT}} = \int_0^\infty P_{DT}(\gamma, \bar{\lambda}) p_{\gamma_{MRC}}(\gamma)\, d\gamma = \int_0^\infty Q_\eta\left(\sqrt{2\gamma}, \sqrt{\bar{\lambda}}\right) p_{\gamma_{MRC}}(\gamma)\, d\gamma \tag{4.9}$$

Putting values of equations (3.13) and (4.8) into equation (4.9), then the $\overline{P_{DT}}$ becomes as

$$\overline{P_{DT}} = \int_0^\infty \sum_{h=0}^{\infty} \frac{\gamma^h}{h!} \frac{\Gamma\left(h+\eta, \frac{\bar{\lambda}}{2}\right)}{\Gamma(h+\eta)} exp(-\gamma) \frac{m^{mN} \gamma^{mN-1}}{\Gamma(mN)\sqrt{\pi}} \sum_{i=1}^{L} w_i a_i exp(-b_i \gamma) d\gamma \tag{4.10}$$

$$\overline{P_{DT}} = \frac{m^{mN}}{\Gamma(mN)\sqrt{\pi}} \sum_{h=0}^{\infty} \frac{1}{h!} \sum_{i=1}^{L} w_i a_i \frac{\Gamma\left(h+\eta, \frac{\bar{\lambda}}{2}\right)}{\Gamma(h+\eta)} \int_0^\infty \gamma^h \gamma^{mN-1} exp(-b_i \gamma) exp(-\gamma)\, d\gamma \tag{4.11}$$

After some mathematical manipulation and used $\int_0^\infty z^q exp(-\beta z)\, dz = q! \beta^{-q-1}; \mathrm{Re}\,\beta > 0$ in equation (4.11), we have $\overline{P_{DT}}$ as shown in equation (4.12) as

$$\overline{P_{DT}} = \frac{m^{mN}}{\Gamma(mN)\sqrt{\pi}} \sum_{h=0}^{\infty} \sum_{i=1}^{L} \frac{\Gamma\left(h+\eta, \frac{\bar{\lambda}}{2}\right)}{h!\Gamma(h+\eta)} w_i a_i \left((h+mN-1)!\right)(1+b_i)^{-(h+mN)} \tag{4.12}$$

In equations (4.12), series truncation is essential to attain a certain numerical accuracy. In Table 4.1, the truncation error incurred in approximating the series of equation (4.12) to the term $h=2$ and $h=4$ for several SNR (dB) values has been calculated for all the three genuine scenarios such as light shadowing, average shadowing and heavy shadowing [138].

Table 4.1 Mean square error for convergence of the $\overline{P_{DT}}$ for various value of SNR (dB) and time-bandwidth product $\eta = 5$ for various realistic scenarios

SNR (dB)	Light shadowing		Average shadowing		Heavy shadowing	
	$h=2$	$h=4$	$h=2$	$h=4$	$h=2$	$h=4$
-10	7.241×10^{-9}	1.025×10^{-20}	8.422×10^{-7}	7.162×10^{-19}	4.024×10^{-8}	5.041×10^{-18}
-5	1.057×10^{-8}	5.071×10^{-16}	4.279×10^{-6}	4.264×10^{-17}	7.263×10^{-7}	7.152×10^{-16}

0	5.109×10^{-7}	7.891×10^{-14}	7.021×10^{-5}	4.291×10^{-15}	9.476×10^{-6}	8.102×10^{-14}
5	4.255×10^{-4}	9.472×10^{-12}	7.851×10^{-5}	4.054×10^{-13}	7.183×10^{-5}	7.185×10^{-11}
10	0.248×10^{-5}	4.820×10^{-10}	7.120×10^{-4}	4.254×10^{-11}	9.842×10^{-4}	7.831×10^{-9}

4.3 Average AUC

The AUC curve is a distinctive figure of merit that agreements better indulgences as to what characteristics mark the analysis of ED. The ROC curve is plotted between P_{FA} and P_{DT}, CROC curve is demonstrated between P_{FA} and P_{MD}. The average AUC is nothing but the area under the ROC curve. The signal detection capability of ED is quantified by AUC. Typically, as the λ in the ED lies between ∞ to 0. The P_{FA} and P_{DT} varies from 0 to 1 and accordingly, the AUC lies between 0.5 to 1. If the value of AUC is 0.5, the performance of ED decreases very badly just like tossing a coin and performance of ED increases when AUC value reaches to 1 as the threshold fluctuates from 0 to ∞. The $\overline{A}$ can be defined by [104, 142] as

$$\overline{A} = -\int_0^{\infty} \overline{P_{DT}} \frac{\partial P_{FA}(\lambda)}{\partial \lambda} d\lambda \tag{4.13}$$

where,

$$\frac{\partial P_{FA}(\lambda)}{\partial \lambda} = -\frac{\lambda^{\eta-1} e^{-\lambda/2}}{2^{\eta}\Gamma(\eta)} \tag{4.14}$$

Substituting (4.12) and (4.14) into (4.13), we have

$$\overline{A} = \begin{cases} \dfrac{m^{mN}}{\Gamma(mN)\sqrt{\pi}} \displaystyle\sum_{h=0}^{\infty}\sum_{i=1}^{L} \frac{w_i a_i \left((h+mN-1)!\right)\left(1+b_i\right)^{-(h+mN)}}{(h!)\Gamma(h+\eta)} \\ \times \dfrac{1}{2^{\eta}\Gamma(\eta)} \displaystyle\int_0^{\infty} \lambda^{\eta-1} e^{-\lambda/2}\, \Gamma(h+\eta, \lambda/2)\, d\lambda \end{cases} \tag{4.15}$$

Using [136] and [143] the final analytical expression of average AUC is obtained as

$$\overline{A}=\begin{cases}\dfrac{m^{mN}}{\Gamma(mN)\sqrt{\pi}}\displaystyle\sum_{h=0}^{\infty}\sum_{i=1}^{L}\dfrac{w_i a_i\left((h+mN-1)!\right)\left(1+b_i\right)^{-(h+mN)}}{(h!)\Gamma(h+\eta)} \\ \times\dfrac{\Gamma(2\eta+h)}{2^{2\eta+h}(\eta!)\Gamma}\,{}_2F_1\left(1,\,2\eta+h;\,\eta+1;\,1/2\right)\end{cases} \tag{4.16}$$

Where, ${}_aF_b(.)$ is the generalized hypergeometric function [136].

4.4 Optimization of Threshold

To enhanced spectrum utilization, the threshold should be optimized and that can be optimized if and only if by minimizing the P_{TE} . In convention threshold method, the threshold is static a specific point so when the received power of the signal swing SU. It is not possible to identify the signal along with it also does not work at very low SNR, adaptive or optimized threshold is wont to overwhelm the problem of low SNR. The threshold is varied by the variation of the received signal is called an optimized threshold. While comparing the fixed one with an optimized threshold, the optimized threshold provides better results. In the preceding chapter, the optimization of threshold is explained thoroughly. Hence, in similar fashion, the first term of equation (3.24) $\partial P_{FA}/\partial\lambda$ is obtained in equation (4.14) and the second term $\partial\overline{P_{MD}}/\partial\lambda=\partial\left(1-\overline{P_{DT}}\right)/\partial\lambda=-\partial\overline{P_{DT}}/\partial\lambda$ is obtained as

$$\frac{\partial\overline{P_{DT}}}{\partial\lambda}=\frac{m^{mN}}{\Gamma(mN)\sqrt{\pi}}\sum_{h=0}^{\infty}\sum_{i=1}^{L}\frac{w_i a_i}{h!}\left((h+mN-1)!\right)\left(1+b_i\right)^{-(h+mN)}\frac{\partial}{\partial\lambda}\left(\frac{\Gamma\left(h+\eta,\frac{\lambda}{2}\right)}{\Gamma(h+\eta)}\right) \tag{4.17}$$

Equation (4.17) can be written as

$$\frac{\partial\overline{P_{DT}}}{\partial\lambda}=-\frac{e^{-\lambda/2}m^{mN}}{\Gamma(mN)\sqrt{\pi}}\sum_{h=0}^{\infty}\sum_{i=1}^{L}\frac{w_i a_i\lambda^{h+\eta-1}}{h!2^{h+\eta}\Gamma(h+\eta)}\left((h+mN-1)!\right)\left(1+b_i\right)^{-(h+mN)} \tag{4.18}$$

After some mathematical calculation, we have $\partial\overline{P_{DT}}/\partial\lambda$. Now, adding equations (3.25) and (4.18) then (3.24) can be rewritten as

$$\frac{m^{mN}\Gamma(\eta)}{\Gamma(mN)\sqrt{\pi}}\sum_{h=0}^{\infty}\sum_{i=1}^{L}\frac{\lambda^{h}w_i a_i}{h!2^{h}\Gamma(h+\eta)}\left((h+mN-1)!\right)\left(1+b_i\right)^{-(h+mN)}=1 \tag{4.19}$$

The equation (4.19) can be easily executed through mathematical software such a MATHEMATICA or MATLAB because it is complex to derive the exact solution. Now, the P_{TE} given by equation (3.27) has a global minimum with respect to λ_{th} because the second derivative of P_{TE}, $\partial^2 P_{TE}/\delta\lambda_{th}^2 > 0$. So from equation (3.24), we get the optimum value of λ_{th} and by using the optimum value λ_{opt}, we can get the optimum value of P_{MD}, P_D and P_{TE}.

4.5 Results and Discussion

In this section, we present a comprehensive analysis of the analytical expressions derived in the preceding sections and provide exact numerical results and Monte Carlo simulations for validation purpose. We first generate 10^6 number of random samples from N-Nakagami-m/log-normal distributions. This particular random number of samples size pledges statistical convergence for values of average probability of detection of the order of 10^{-5}. In Fig. 4.1, CROC curves for dual branch diversity are plotted. To dodge curve mess, only two realistic shadowing scenario is taken into consideration, such as average shadowing and light shadowing. Three different values of *SNR*, such as 0 dB, 5 dB and 10 dB are assumed. The analytical expression achieved in equation (4.11) is presented to match with the exact and Monte Carlo simulation. At *SNR* = 10 dB, the probability of miss-detection is low for light shadowing and high for average shadowing. Similar condition is obtained for *SNR* = 0 dB and *SNR* = 5 dB. For a low value of *SNR*, the probability of miss-detection is more in comparison

to high *SNR*. Therefore, as the signal-to-noise ratio increases, the probability of detection increases and when the number of branches increases, quality of detection of signal improved.

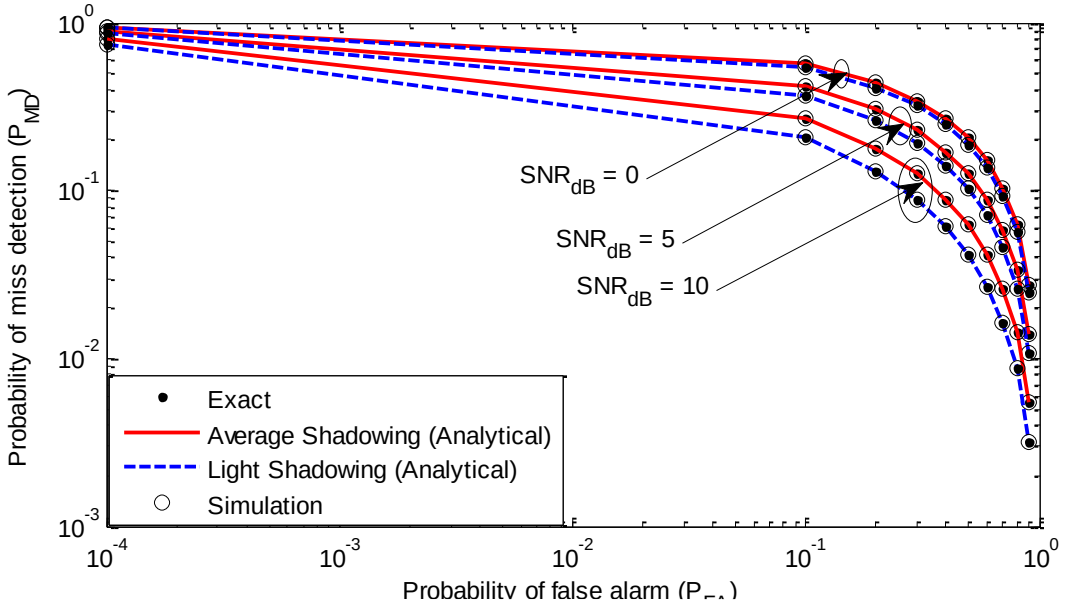

Fig. 4.1 CROC curves for light and average shadowing ($m=1, N=2, \eta=2$)

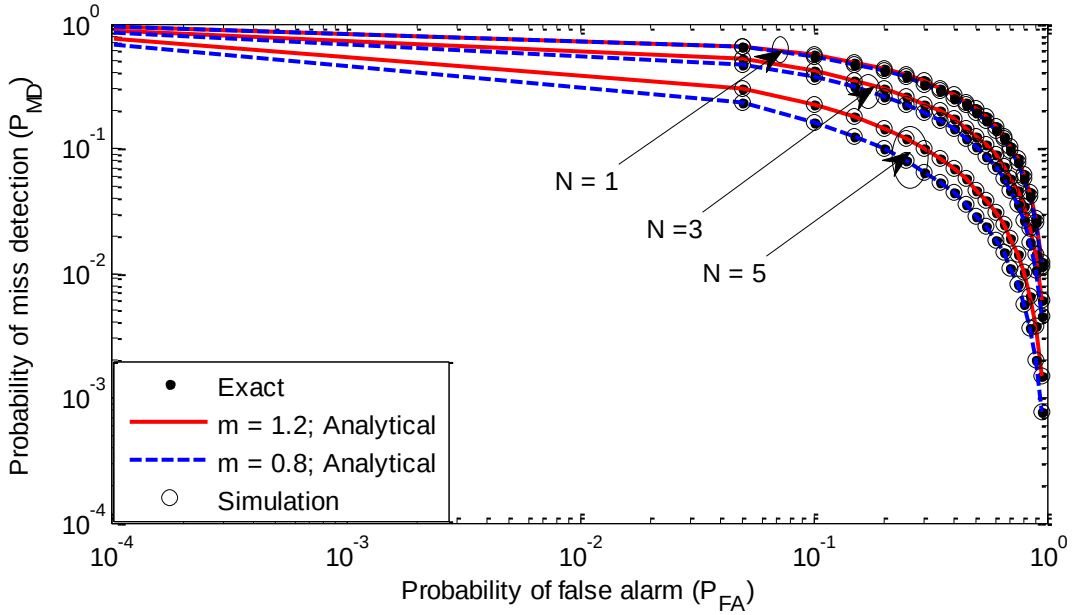

Fig. 4.2 CROC curves without and with diversity branches (η =4 and SNR = 5 dB)

As the number of diversity branches increases in MRC diversity scheme, the probability of miss detection is greatly reduced w.r.t. the probability of false alarm as shown in Fig. 4.2. When

no diversity case is applied, i.e. SISO then curves approximately overlapping to each other at different fading parameters (m = 0.8 and 1.2) but when the number of diversity branches increases ($N = 3,5$), the probability of detection is improved. At higher fading parameter, the probability of miss detection is more in comparison to the low fading parameter.

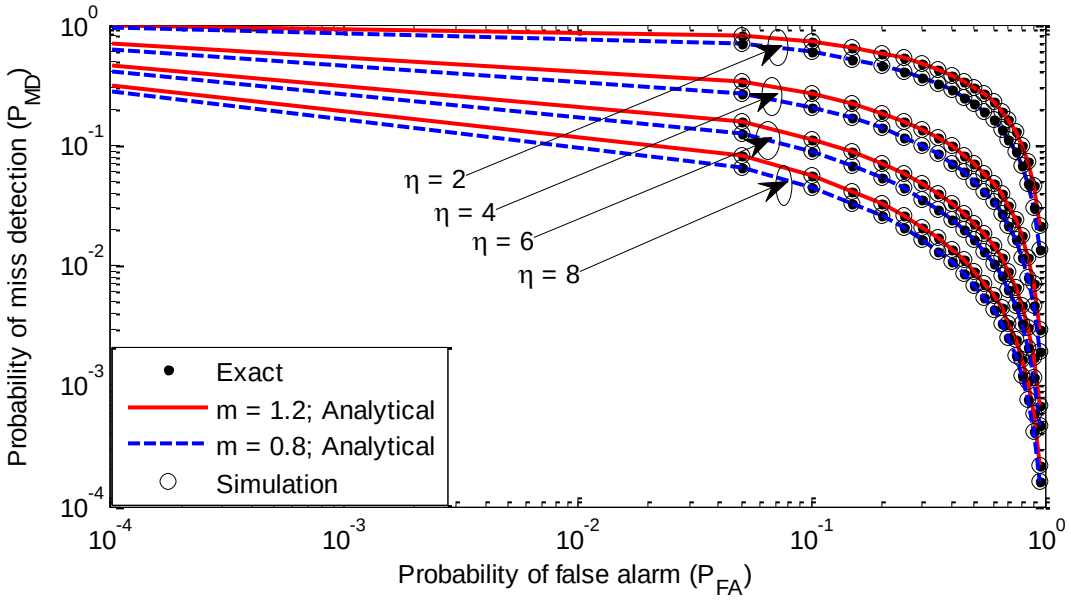

Fig. 4.3 CROC curves for different d with no diversity (m = 0.8, 1.2, SNR = 0 dB)

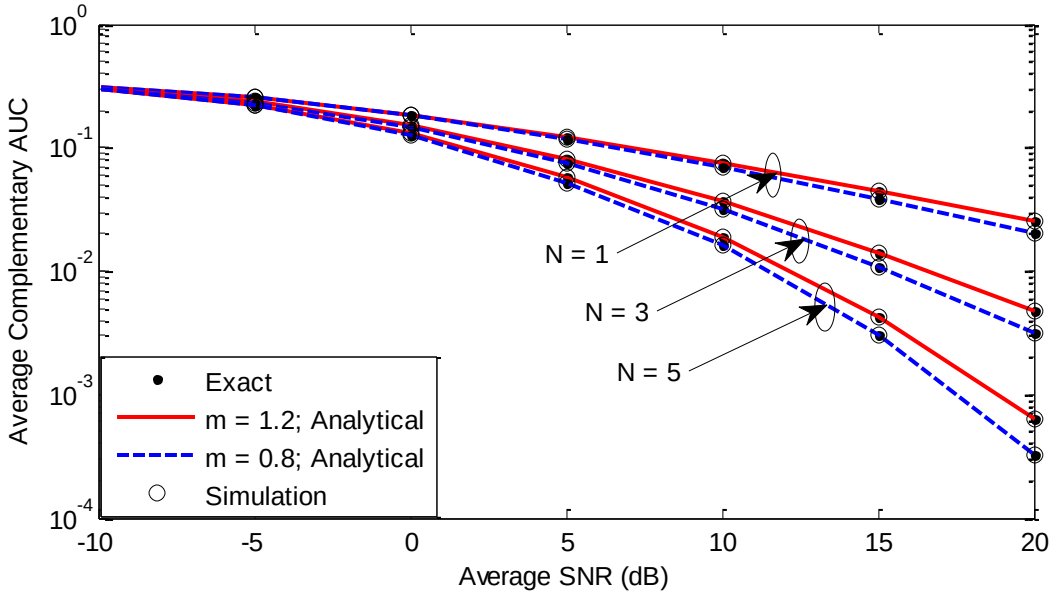

Fig. 4.4 CAUC curves w.r.t. average SNR without and with diversity reception at η =2

In Fig. 4.3, complementary ROC curve is plotted for different values of number of sample (η = 2, 4, 6 and 8) at different fading parameter (m = 0.8, 1.2) values. It is very much clear from the figure that as the number sample size increases, the probability of miss-detection reduces that shows the improvement in the detection of the unknown deterministic signal. For η = 8, the probability of detection increase at both the value of fading parameters but m = 1.2, the probability of miss-detection is more in comparison to the m = 1.2. This figure gives a very well match with exact, analytical and simulation results.

In Fig. 4.4, average complementary AUC (CAUC) curves versus average SNR for different values of fading parameters (m = 0.8, 1.2) under different diversity cases such as SISO and number of diversity branches. In SISO, detection capability is very poor because it gives a better response at a very high value of SNR but as the number of diversity branches increases, the performance of ED is improved. Hence, in low SNR and the higher number of diversity branches, the performance of detection of the signal is increased at both values of fading parameter with a slight deviation.

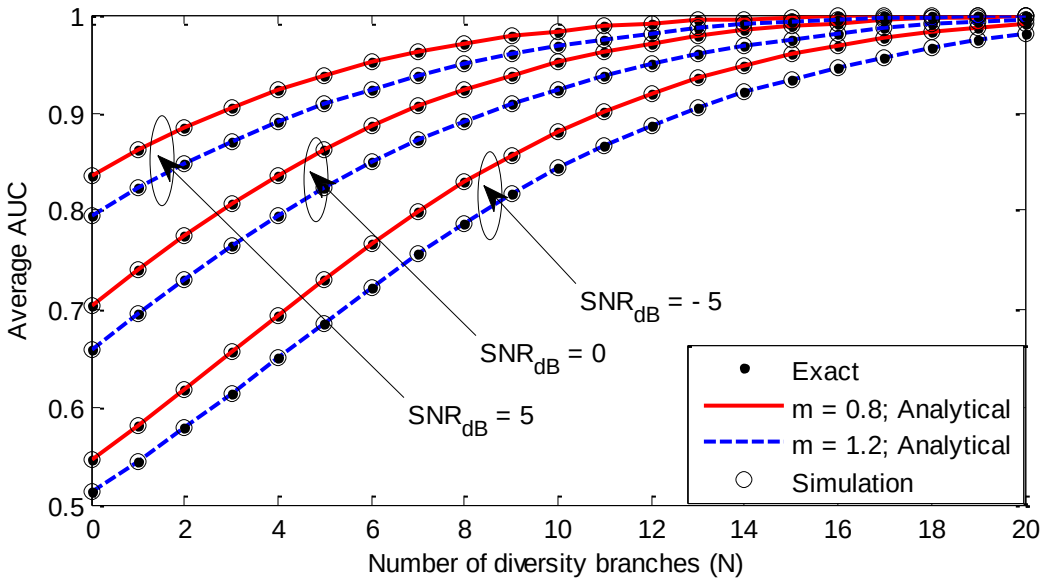

Fig. 4.5 Average AUC against diversity branches for different average SNR (η =3)

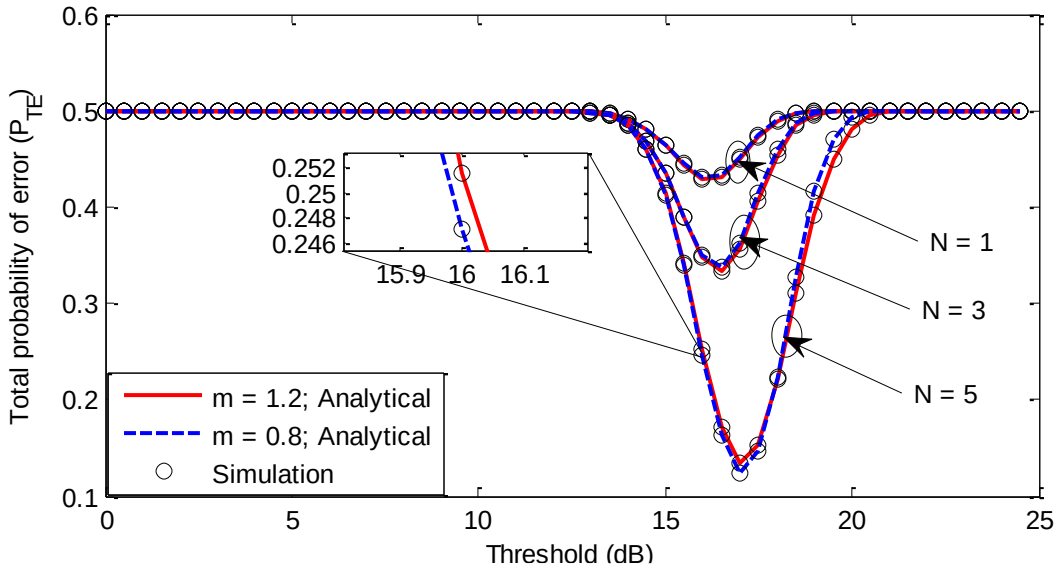

Fig. 4.6 P_{TE} versus threshold for the number of diversity branches (SNR_{dB} = 5 and η =2)

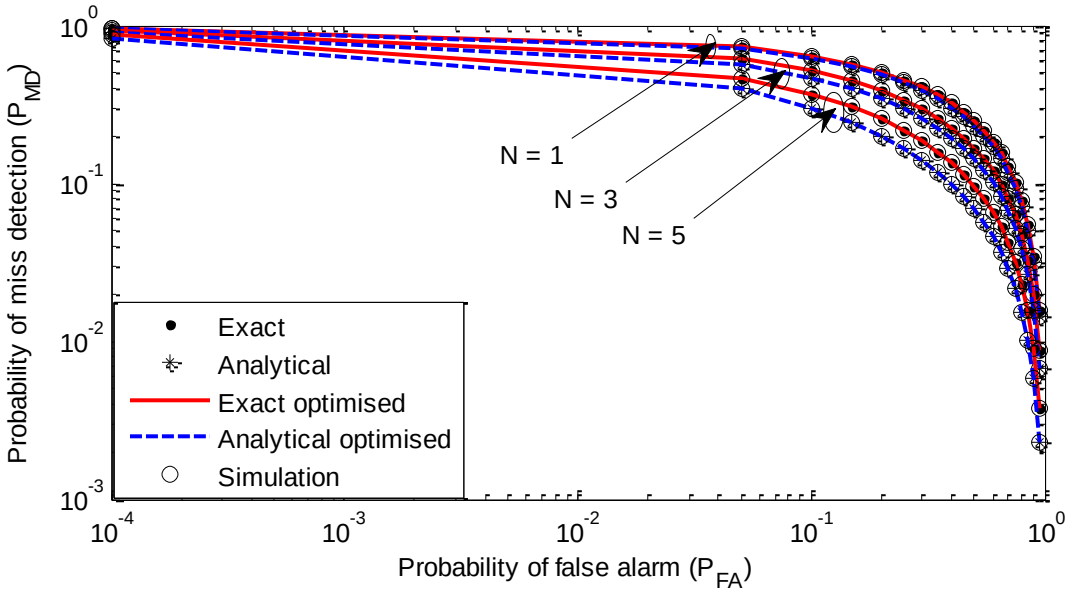

Fig. 4.7 CROC curves with a fixed and optimized threshold for different branches (m =0.8 and η = 2)

For MRC reception case, when a value of η is fixed at η =3 and considering different values of fading parameter as m = 0.8 and 1.2. Fig. 4.5 represents the fixed, analytical and simulation results for average AUC against the number of diversity branches (N) for several values of average SNR. It is a quite evident from the figure, as the number of branches increases, average

AUC curves converse to unity. For a particular value of SNR, say SNR = 5 dB, the MRC with 5 diversity branches average AUC is 0.93 at m = 1.2. Hence, average AUC converges to unity quickly when the average SNR increases.

The threshold optimization has been considered in Fig. 4.6. The inverted bell-shaped has been displayed at the different number of diversity branches (N =1, 3 and 5) with different fading parameter (m = 0.8 and 1.2) as obtained in equation (25) using equation (28). It is observed that the total probability of error (P_{TE}) has a global minima w.r.t threshold. The total probability of error decreases as the number of diversity branches increases but when no diversity case is considered, not enough improvement has been shown in the figure.

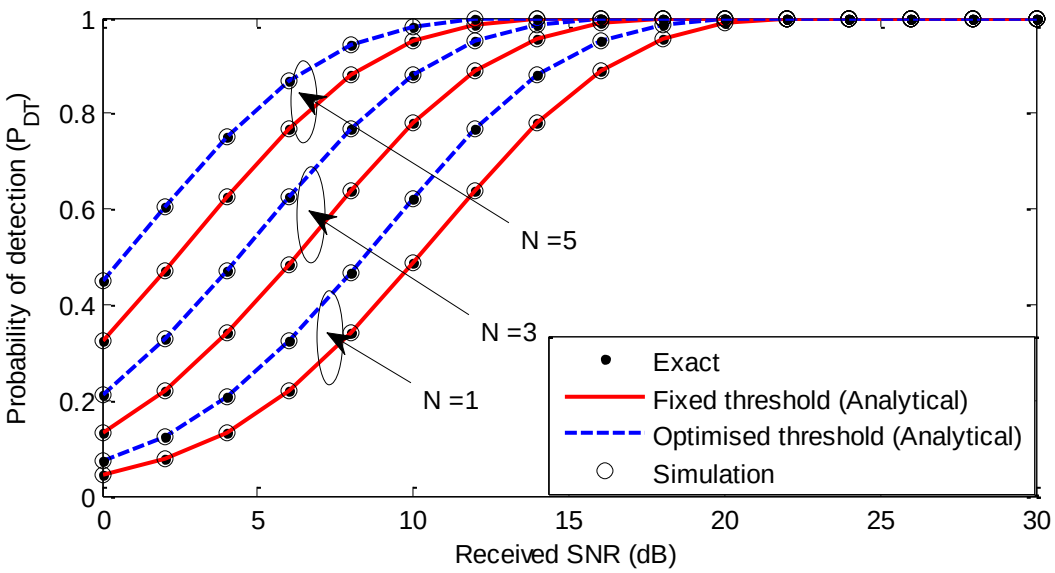

Fig. 4.8 Probability of detection against received *SNR* with a fixed and optimized threshold for diversity branches (m =0.8 and η = 2)

When the threshold optimization is considered, it gives better response in comparison to the fixed threshold because the probability of detection is possible even at very low SNR in case of the optimized threshold. Fig. 4.7 illustrate the best response in terms of threshold optimization because in this figure their comparison between the fixed threshold and the optimized threshold for the different number of diversity branches (N = 1, 3 and 5). When no

diversity case is considered, not enough deviation in CROC curve for fixed and threshold optimization but still there is a small change in optimized threshold. But when the number of diversity branches increases, a great improvement has been seen from the figure. The probability of detection increases, when the optimized threshold is applied in comparison to the fixed threshold as the number of diversity branches increases from $N = 3$ to $N = 5$.

In Fig. 4.8, the probability of detection is shown as a function of received SNR for the different number of diversity branches and with a fixed and optimized threshold. The fixed threshold ($\hat{\lambda}$) can be acquired for the specified P_{FA} and it is calculated from (3) and using that $\hat{\lambda}$ the probability of detection is achieved. The software package MATHEMATICA is used for computational. As the number of diversity branches and received SNR increases, the probability of detection converges towards unity. For no diversity case, the probability of detection is very small at lower values of SNR but in case of MRC diversity branches, the performance of detection shows great improvement as SNR increases.

4.6 Conclusion

An analytical expression of the average probability of detection with maximum ratio combining over composite NL fading channels by using Gaussian-Hermite integration approximation. Additionally, the optimized threshold can be achieved by minimizing the total probability of error. A major enhancement in the detection has been confirmed even at very low SNR when the optimized threshold is applied. Hence, the performance of the optimized threshold is better than the fixed threshold. The results, thus obtained, are estimated to simple, thus facilitating them to be used straightforward in some wireless applications such as cooperative and non-cooperative cognitive radio networks.

Chapter 5

Performance Evaluation of Weibull/Shadowed Channel with MRC Reception

In 5G wireless communication, SS is one of the practical technique to usage unused band of spectrum in the opportunistic ways. In this chapter, again we have considered composite fading channel as Weibull/log-normal, which is very close to a realistic scenario. The Weibull distribution is known to characterize the multipath fading of an indoor and outdoor channel which is based on its excellent matching with the measurement conducted in the appropriate environments. Beside characterize the wireless channel, Weibull distribution has an application in various fields such as radar cluster, failure data analysis, reliability engineering and mobile-to-mobile channels in a suburban area at 1.85 GHz with dense scattering environment. The LN distribution is used to characterize in several applications such as for multiple input multiple output indoor UWB channel, for medium scale fading, indoor and outdoor scenarios. To have the best possible detection of the signal, MRC reception is also incorporated. The analytical expressions of the average probability of detection and average AUC curves are mathematically achieved by means of Gaussian-Hermite integration. The influence of the system factors on the performance of energy detection is calculated in terms of complementary receiver operating characteristic curves and average area under the receiver operating characteristic curves. Furthermore, an optimized threshold has been applied. To authenticate the exactness of obtained analytical expressions have collaborated with simulations.

5.1 Channel Model

The Weibull channel shows an outstanding fit to multipath experimental fading channel measurements for indoor and outdoor environments and log-normal distribution is used to

represent shadowing. Composite fading situations are often met in real scenarios. Modelling of composite fading is significant in analysing the wireless communication system CR and MIMO network and in the modelling of interference in the cellular system. The conditional Weibull distribution [50, 144] is given as

$$p(\gamma|v)=\frac{c}{2}\left[\frac{\Gamma\left(1+\frac{2}{c}\right)}{v}\right]^{\frac{c}{2}}\gamma^{\frac{c}{2}-1}exp\left(-\left(\frac{\gamma}{v}\Gamma\left(1+\frac{2}{c}\right)\right)^{\frac{c}{2}}\right)\quad \gamma\geq 0 \tag{5.1}$$

where, c, v are the shape parameter and average SNR at receiver respectively. Shadowing is captured by log-normal distribution and it is given by (5.2) as

$$p(v)=\frac{1}{\sigma v\sqrt{2\pi}}exp\left(-\frac{(lnv-\mu)^2}{2\sigma^2}\right) \tag{5.2}$$

Averaging the conditional PDF (5.1) w.r.t. (5.2), composite PDF of Weibull/log-normal (WL) can be denoted as

$$p_\gamma(\gamma)=\int_0^\infty p(\gamma|v)p(v)dv \tag{5.3}$$

Substituting (5.1) and (5.2) into (5.3), assuming $z=(lnv-\mu)/\sqrt{2}\sigma$, we have

$$p_\gamma(\gamma)=\frac{\theta c\gamma^{\frac{c}{2}-1}}{2\sqrt{\pi}}\int_{-\infty}^{\infty}exp\left(-\frac{c}{2}\left(\mu+\sqrt{2}\sigma z\right)\right)exp\left(-\theta\gamma^{\frac{c}{2}}exp\left(-\frac{c}{2}\left(\mu+\sqrt{2}\sigma z\right)\right)\right)exp\left(-z^2\right)dz \tag{5.4}$$

where, $\theta=\left(\sqrt{1+2/c}\right)^{c/2}$

It is not easy to get closed-form expression straightforward by solving integration of (5.4). Applying G-HI in (5.4) becomes

$$p_{\gamma}(\gamma) \approx \frac{\theta c \gamma^{\frac{c}{2}-1}}{2\sqrt{\pi}} \sum_{j=1}^{J} w_j \, exp\left(-\frac{c}{2}\left(\mu + \sqrt{2}\sigma z_j\right)\right) exp\left(-\theta \gamma^{\frac{c}{2}} exp\left(-\frac{c}{2}\left(\mu + \sqrt{2}\sigma z_j\right)\right)\right) \quad (5.5)$$

Equation (5.5) can also be written as

$$P_{\gamma}(\gamma) = \frac{\theta c \gamma^{\frac{c}{2}-1}}{2\sqrt{\pi}} \sum_{j=1}^{J} w_j a_j exp\left(-\theta \gamma^{\frac{c}{2}} a_j\right) \quad (5.6)$$

where, $a_j = exp\left(-\frac{c}{2}\left(\mu + \sqrt{2}\sigma z_j\right)\right)$

The MRC diversity provides, the best performance among all others diversity methods. So, far i.i.d. channel environment, the output of SNR at the receiver is obtained as in (4.2). To overcome multipath fading effects, micro diversity using MRC is used at the receiver. Hence, the composite PDF of the output of MRC reception can be solved by applying [50] on [145], then substituting it in (5.6) and finally, we have composite PDF over N-Weibull/log-normal fading channel as

$$p_{\gamma_{MRC}}(\gamma) = \frac{\theta_{MRC}^{N} c \gamma^{\frac{Nc}{2}-1}}{2\sqrt{\pi}\left((N-1)!\right)} \sum_{j=1}^{J} w_j a_j^{N} exp\left(-\theta_{MRC} \gamma^{\frac{c}{2}} a_j\right) \quad (5.7)$$

where, $\theta_{MRC} = \left(\frac{\sqrt{N + (2/c)}}{N!}\right)^{\frac{c}{2}}$

5.2 Average Probability of Detection

Let the system, undergoing through the composite multipath/shadowing fading channel, in (3.8) will remain same since it does not depends on the SNR but when the channel gain varies the average probability of detection can easily be evaluated. So, Substituting (3.13) and (5.7) into (4.10), we have

$$\overline{P_{DT}} = \sum_{h=0}^{\infty}\sum_{j=1}^{J} \frac{\Gamma\left(h+\eta, \frac{\lambda}{2}\right)}{(h!)\Gamma(h+\eta)} \frac{\theta_{MRC}^{N} c w_j a_j^{N}}{2\sqrt{\pi}(N-1)!} \int_0^{\infty} \gamma^{h+\frac{Nc}{2}-1} exp(-\gamma) exp\left(-\theta_{MRC}\gamma^{-\frac{c}{2}} a_j\right) d\gamma \tag{5.8}$$

Using [143], Meijer G-function, (5.8) can be expressed as

$$\overline{P_{DT}} = \sum_{h=0}^{\infty}\sum_{j=1}^{J} \frac{\Gamma\left(h+\eta, \frac{\lambda}{2}\right)}{(h!)\Gamma(h+\eta)} \frac{\theta_{MRC}^{N} c w_j a_j^{N}}{2\sqrt{\pi}(N-1)!} H_{1\ 1}^{1\ 1}\left[\theta_{MRC} a_j \Big|_{(0,1)}^{\left(1-h-\left(\frac{Nc}{2}\right);\frac{c}{2}\right)}\right] \tag{5.9}$$

where, $H_{r\ s}^{p\ q}\left(.\Big|\begin{matrix}\cdot & \cdot \\ \cdot & \cdot\end{matrix}\right)$ is the Fox H-function.

Proof: See Appendix: C

5.3 Average AUC

The AUC is nothing but the area under the ROC curve. The signal detection capability of ED is also measured by AUC. Naturally, the threshold (λ) in the ED lies between ∞ to 0. The probability of false alarm and the probability of detection varies from 0 to 1 and accordingly, the AUC lies from 0.5 to 1. If the value of AUC is 0.5, the performance of ED decreases very badly just like tossing a coin and performance of ED increases when AUC value reaches to 1 as the threshold fluctuates from 0 to ∞. So, substituting (5.9) and (4.13) into (4.12), we have

$$\begin{aligned}\overline{A} = &\sum_{h=0}^{\infty}\sum_{j=1}^{J} \frac{\theta_{MRC}^{N} c w_j a_j^{N}}{2\sqrt{\pi}(N-1)!(h!)} \frac{1}{2^{\eta}\Gamma(\eta)\Gamma(h+\eta)} H_{1\ 1}^{1\ 1}\left[\theta_{MRC} a_j \Big|_{(0,1)}^{(1-h-(Nc/2);c/2)}\right] \\ &\times \int_0^{\infty} \lambda^{\eta-1} e^{-\lambda/2} \Gamma(h+\eta, \lambda/2) d\lambda\end{aligned} \tag{5.10}$$

Using [136], the average AUC can be written as

$$\begin{aligned}\overline{A} = &\frac{\theta_{MRC}^{N}(c/2)}{\sqrt{\pi}(N-1)!} \sum_{h=0}^{\infty}\sum_{j=1}^{J} \frac{w_j a_j^{N} \Gamma(2h+\eta)}{2^{2h+\eta}(h!)(\eta!)\Gamma(h+\eta)} H_{1\ 1}^{1\ 1}\left[\theta_{MRC} a_j \Big|_{(0,1)}^{(1-h-(Nc/2);c/2)}\right] \\ &\times_2 F^1(1, 2h+\eta; 1+\eta; 1/2)\end{aligned} \tag{5.11}$$

where, ${}_a F^b(x; y; z)$ is the confluent hypergeometric function.

5.4 Optimization of Threshold

In the preceding chapter, the optimization of the threshold is achieved by the P_{TE} . Hence, in the same way, the first term of equation (3.24) $\partial P_{FA} / \partial \lambda$ is obtained in equation (4.14) and the second term is obtained as

$$\frac{\partial \overline{P_{DT}}}{\partial \lambda} = -\frac{\theta_{MRC}^{N} \frac{c}{2}}{\sqrt{\pi}(N-1)!} \sum_{k=0}^{\infty} \sum_{j=1}^{J} \frac{w_j a_j^N \lambda^{d+k-1} e^{-\lambda/2}}{2^{d+k} k! \Gamma(d+k)} H_{1\ 1}^{1\ 1}\left[\theta_{MRC} a_j \Big|_{(0,1)}^{(1-k-(Nc/2);c/2)} \right] \tag{5.12}$$

Now, adding equations (3.25) and (5.12) then (3.24) can be rewritten as

$$\frac{\theta_{MRC}^{N}(c/2)}{\sqrt{\pi}(N-1)!} \sum_{k=0}^{\infty} \sum_{j=1}^{J} \frac{w_j a_j^N \lambda \Gamma(d)}{2^k (k!) \Gamma(d+k)} H_{1\ 1}^{1\ 1}\left[\theta_{MRC} a_j \Big|_{(0,1)}^{(1-k-(Nc/2);c/2)} \right] = 1 \tag{5.13}$$

The (5.13) can be easily executed through mathematical software packages such as MATHEMATICA or MATLAB. So from (3.24), we get the optimum value of λ and by using (5.13) optimized value of the detection threshold is obtained.

Table 5.1 Mean Square Error for convergence for several values of η and the number of diversity branches

Performance Parameters	$N = 1$		$N = 3$	
	$\eta = 2$	$\eta = 8$	$\eta = 2$	$\eta = 8$
$\overline{P_{DT}}$ (5.9)	1.9871×10^{-8}	6.1237×10^{-13}	7.0218×10^{-7}	2.0418×10^{-10}
$\overline{A}$ (5.11)	8.5462×10^{-7}	2.1278×10^{-12}	1.8531×10^{-6}	3.1482×10^{-10}
λ_{opt} (3.24)	2.0451×10^{-5}	1.1212×10^{-10}	3.5621×10^{-5}	1.9820×10^{-8}

In Table 5.1, mean square error (MSE) incurred in truncating the infinite series of equations (5.9), (5.11) and (3.24) respectively for several values of η and number of diversity branches (N) has been numerically estimated. From the table, it can be observed that MSE decreases with an increase in the number of samples and increases with an increase in N . The rate of the convergence of the infinite series has been witnessed to be fast and accurate.

5.5 Results and Discussion

We ratify the legitimacy of the analytical expressions obtained in the preceding sections. We have produced 10^6 number of random recognitions of shadowed N-Weibull fading RV for performance. The analytical outcomes are in completely match with the Monte Carlo simulations. In the statistical analysis, the correctness at 8^{th} place of decimal point has been retained by properly shortening the infinite series to a finite number of terms.

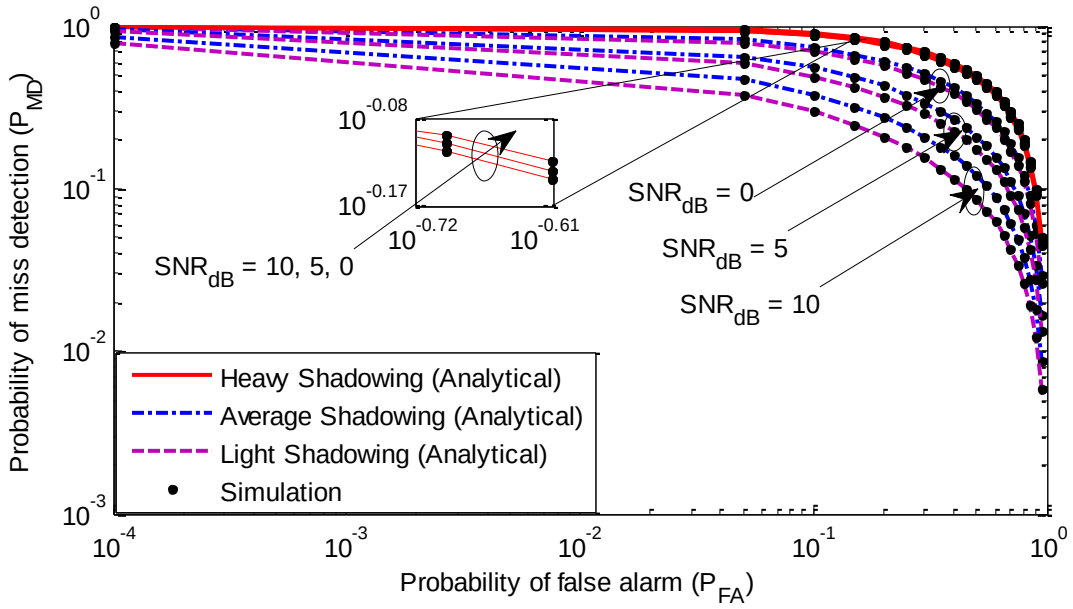

Fig. 5.1 CROC curves for heavy, average and light shadowing at $c = 2$, $\eta = 3$ and $N = 2$

In Fig. 5.1, $N = 2$, $c = 2$ and $\eta = 3$ has been considered for CROC curves and this figure is obtained from the analytical expression equation (5.9), which is perfectly matched with the simulations. All three realistic situation is taken into account, as light, average and heavy shadowing. CROC curves have been plotted for three points of SNR, as 10 dB, 5 dB, and 0 dB. As the value of SNR increases form 0 dB to 10 dB, P_{MD} decreases. For heavy shadowing, P_{MD} is approximately the same for all three values of SNR because it shows the deep fading, the signal is not detectable but when we consider the average and light shadowing, signal is detectable. If $SNR = 10\,dB$, the P_{FA} as well as the P_{MD} are very small for light and heavy

shadowing. Hence, the P_{DT} increases as the s SNR increases and quality of signal better when the number of diversity branch increases.

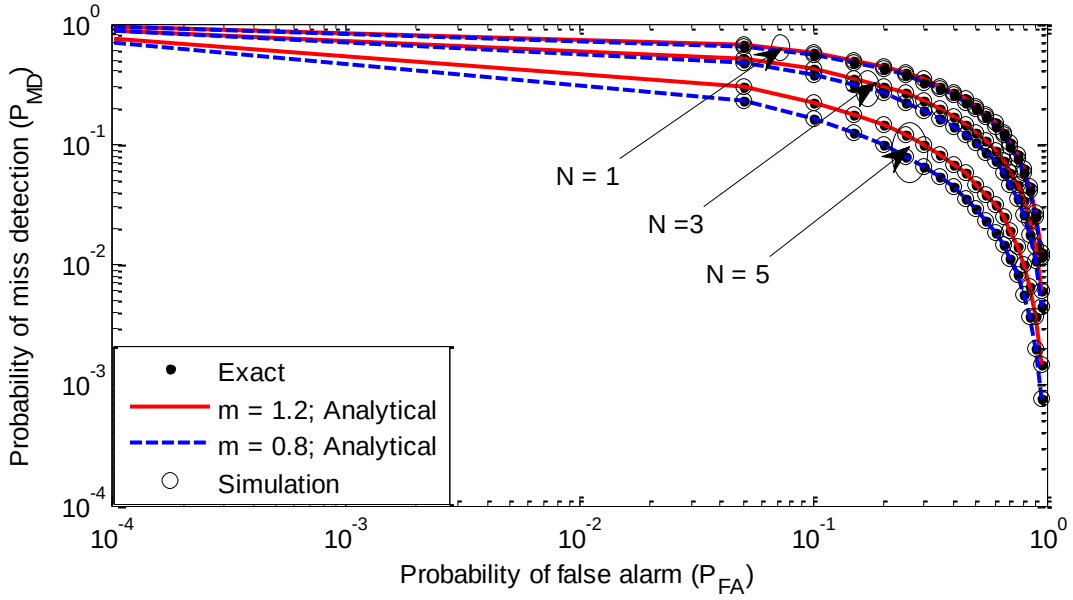

Fig. 5.2 CROC curves with SISO and MRC branches at $\eta = 3$ and SNR=5 dB

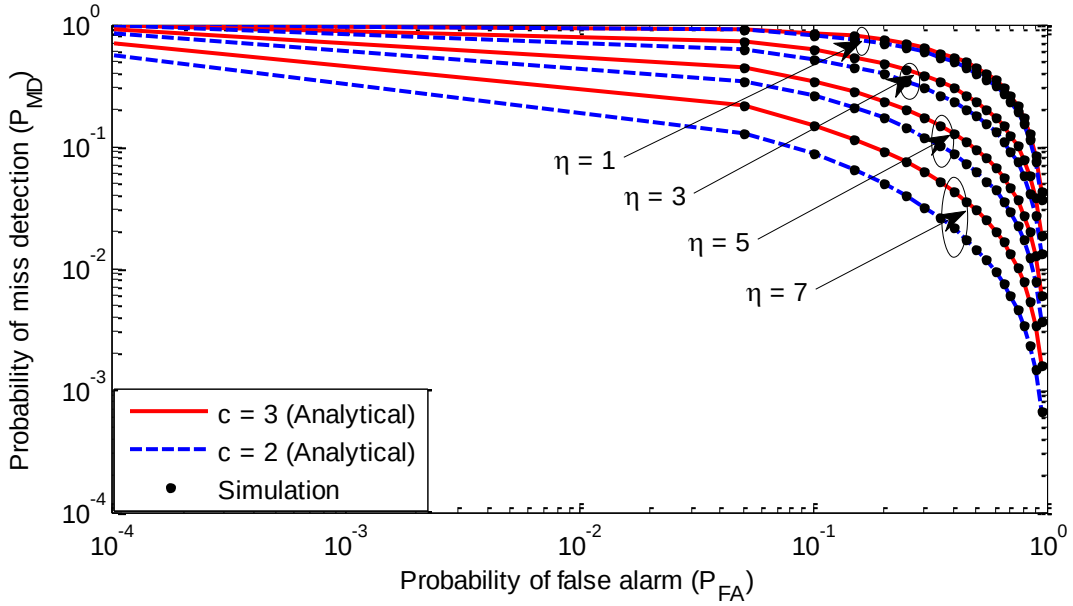

Fig. 5.3 CROC curves for different η at N = 2 and SNR = 5 dB

When the N increase from N = 1 to N = 5, then the P_{FA} and P_{MD} is reduced quickly as shown in Fig. 5.2. For the shape parameter $c = 2$, the probability of miss-detection is decreased if N

increases. In a similar way, if the shaping parameter is increased form c = 2 to c = 3, the P_{FA} also increases for a particular branch of diversity. So from this figure, it is quite obvious that the P_{DT} is gently enhanced by increasing the number of diversity branches.

At several values of η, CROC curves have been plotted at different shaping parameter as shown in Fig. 5.3. For this plot, the number of diversity branch, N = 2 and signal to noise ratio, SNR = 5 dB has been considered. If, we consider the number of samples i.e. $\eta = 1$, for both the shaping parameter ($c = 2,3$), both the CROC curves are approximately overlapping to each other and provide great agreement with analytical and simulation results. As the number of sample increases from 1 to 7, the P_{MD} decreases for both the shaping parameter but more for c = 2 and less for c = 3. When the shaping parameter increases, the P_{FA} decreases and hence, the P_{DT} increases.

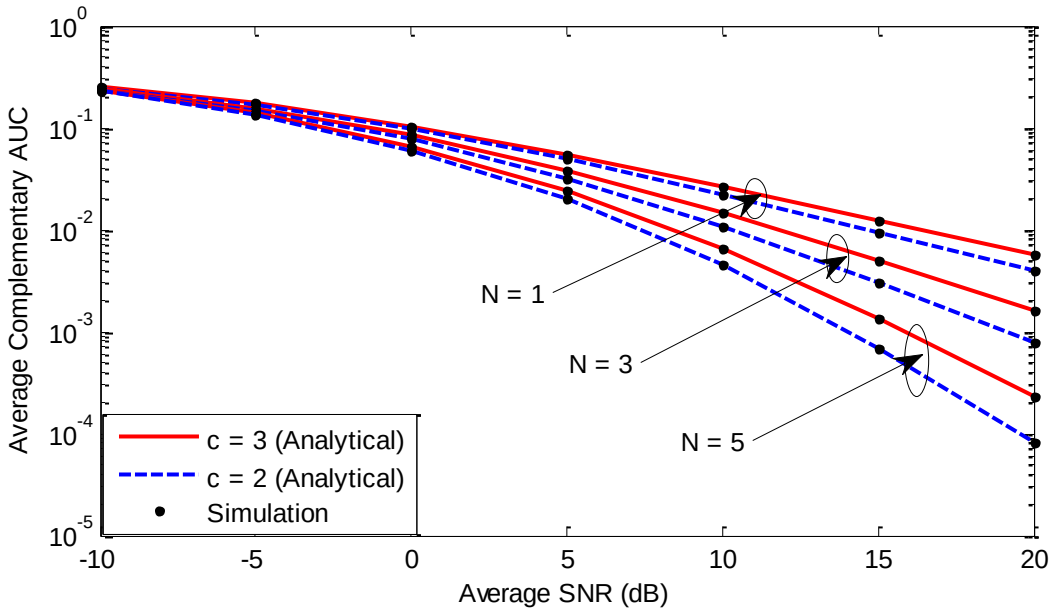

Fig. 5.4 Average CAUC curves versus average *SNR* with SISO and diversity at $\eta = 3$

Average complementary AUC (CAUC) curves with respect to average *SNR* has been plotted for the number of MRC branches (N = 1, 2, 3) and different shape parameter (c = 2, 3) at $\eta = 3$

as presented in Fig. 5.4. When the no diversity case is considered i.e. SISO, the probability of detection is not up to mark at low *SNR* values because it contributes improved result in high *SNR* values but the response of the detection in increased even at low *SNR*, as the *N* increases. Therefore, from the above discussion, we can conclude that performance of ED is improved at both values of shaping parameter with small deviation at low *SNR* and higher values of diversity branches. At *N* = 5 and *SNR* = 15 dB, the values of average CAUC curves decreases.

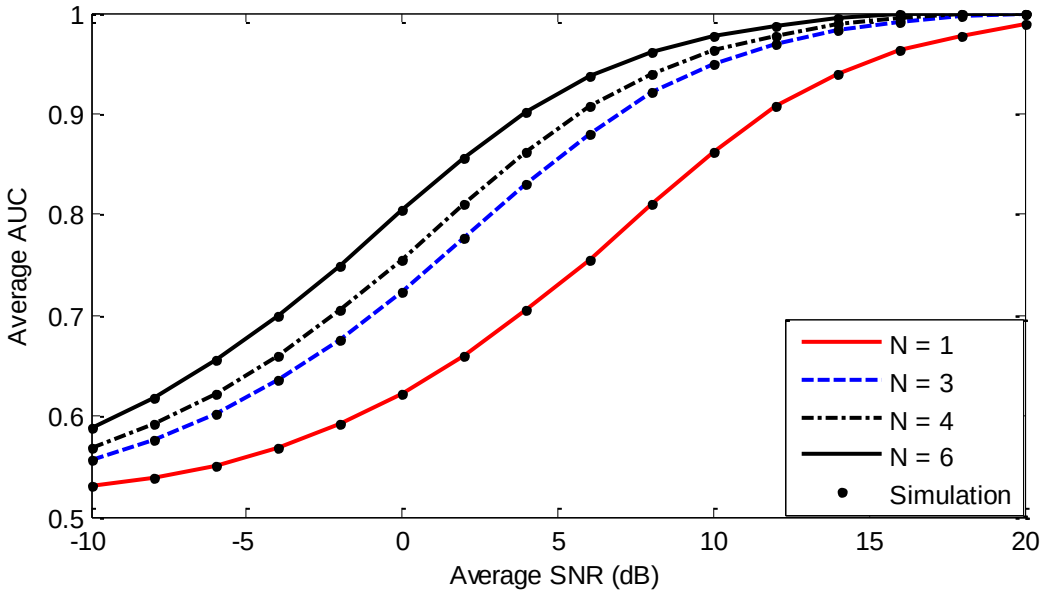

Fig. 5.5 $\overline{A}$ versus average SNR with SISO and diversity at c = 2, $\eta = 3$

For different values of diversity branch case, when shaping parameter is fixed at *c* = 2 and number of sample is fixed at $\eta = 3$, the average AUC versus average *SNR* has presented for analytical and simulation results for diversity branches (*N* = 1, 3, 4, 6) as shown in Fig. 5.5. The analytical result shows approximately close to the simulations result overall diversity cases. As the *N* increases from *N* = 1 to *N* = 6, the average AUC curves approach to unity very quickly that means the performance of energy detection increases. By considering a particular value of average AUC say, 0.85, the diversity scheme with the number of diversity branch three, the gain is about 6 dB in terms of average *SNR*. Hence, with no diversity scheme i.e.

SISO, the average AUC curves is not approaches to unity but the MRC is applied, curves is moved towards unity that proves the great performance of ED.

The analytical obtained in equation (5.11) and simulation for average AUC as a function of *N* for different points of average *SNR* and the different value of shaping parameter (*c* = 2, 4) but at fixed value of number of samples ($\eta = 4$) as shown in Fig. 5.6. The average AUC curves approach towards unity when the *N* increases as well as value of SNR, also increases. At a low value of SNR, -5 dB, the curve moving towards unity but not exactly unity that means the performance of ED degraded at low value of SNRs. For a particular value of SNR, 5 dB, the diversity branch (*N* = 6), the value of the average AUC is approximately 0.94. Hence, average AUC meets towards unity more rapidly, when the number of diversity branch increases.

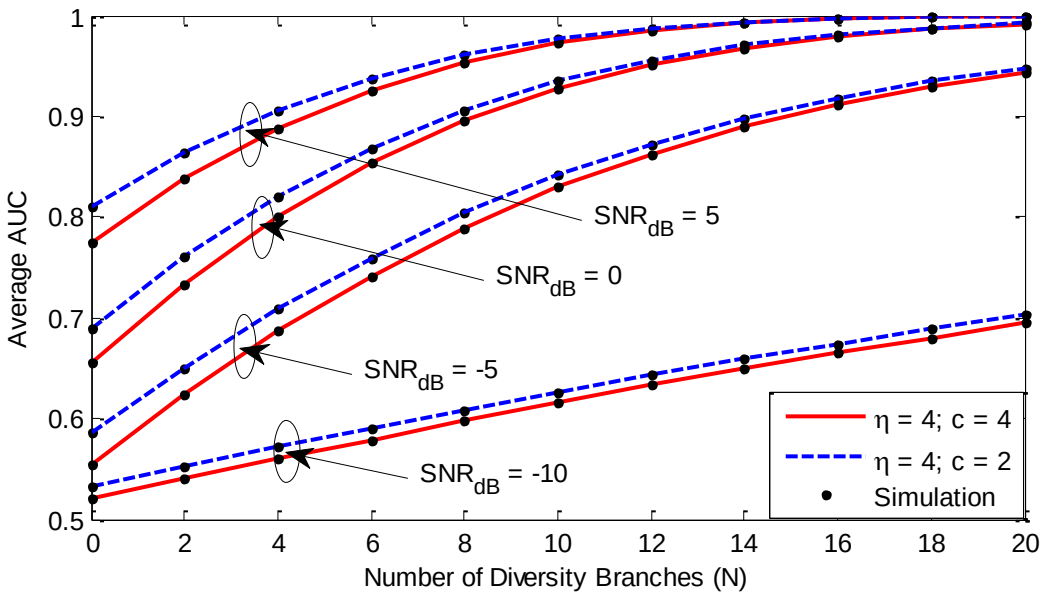

Fig. 5.6 $\overline{A}$ as a function of N for different SNR

The analytical obtained in equation (5.11) and simulation results for average AUC as a function of number of diversity branches (*N*) for different values of average *SNR* and different value of shaping parameter (*c* = 2, 4) but at fixed value of number of samples ($\eta = 4$) as shown in Fig. 5.6. The average AUC curves approaches towards unity, when the number of diversity

branches increases as well as value of SNR also increases. At low value of SNR, -5 dB, the curve moving towards unity but not exactly unity that means performance of ED degraded at low value of SNRs. For a particular value of SNR, 5 dB, the diversity branch (N = 6), the value of average AUC is approximately 0.94. Hence, average AUC meets towards unity more rapidly, when the number of diversity branch increases.

The effect of the different η on the average AUC is examined in Fig. 5.7 as a function of average *SNR*. When the η increases from 1 to 5, the average AUC decreases but at all the number of samples, the average AUC curves converges towards the unity as the average *SNR* increases. For the particular value of the number of samples, say $\eta = 3$ and at average *SNR* = 7 dB, the average AUC is 0.9, which depicts that performance of ED increases as curves tends towards unity. Similarly, in Fig. 5.8, the $\overline{A}$ as a function of average *SNR* is investigated for different values of shaping parameters with the dual number of diversity reception. The analytical and simulation results provide good agreement with each other. As the values of shaping parameter increase from c = 1 to c = 5, the average AUC curves touch the unity. Hence, detection capabilities are improved even both c and average SNR increases.

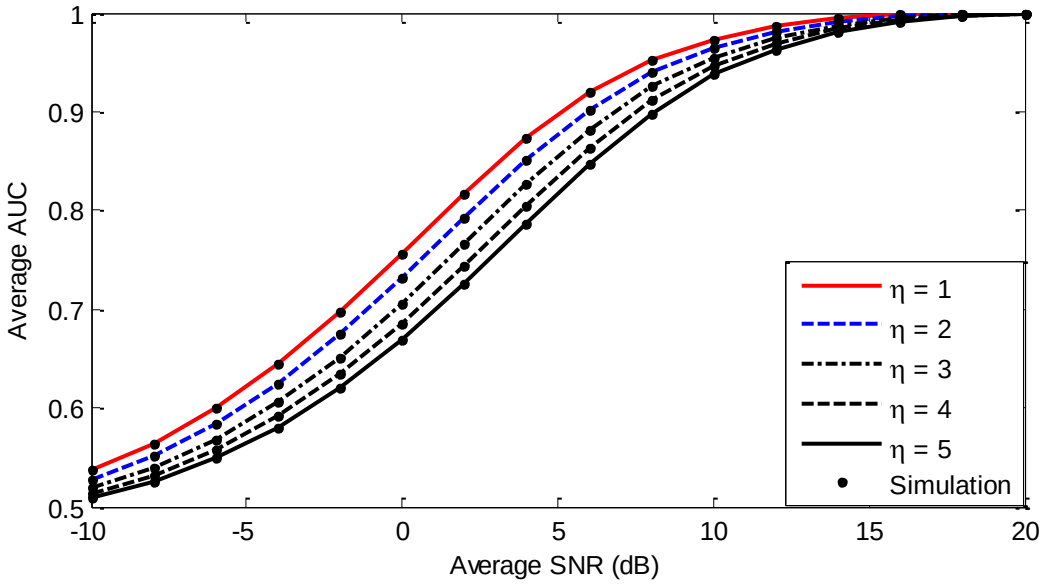

Fig. 5.7 $\overline{A}$ w.r.t average *SNR* with different η with no diversity at c = 3

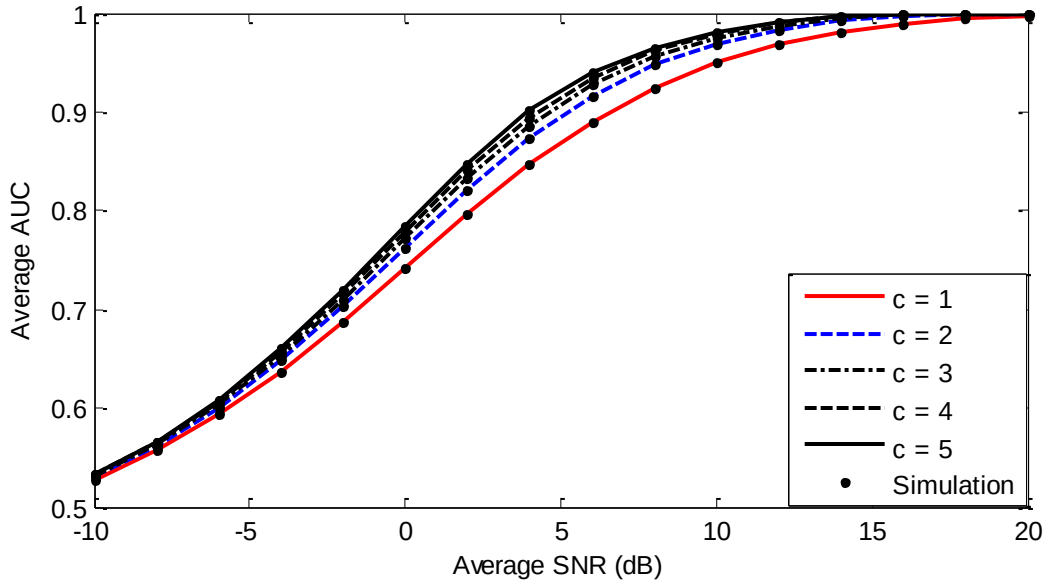

Fig. 5.8 $\overline{A}$ versus average SNR with different *c* and *N* = 2

For *N* = 1, 2, 3 and *c* = 2, 3, the optimization of threshold has been plotted between P_{TE} at fixed value of *SNR* = 4 dB and $\eta = 3$, the inverted bell-shaped is achieved using equation (3.12) as shown in Fig. 5.9. It is perceived that the P_{TE} has global minima with respect to λ. For both the shaping parameter, the P_{TE} is slightly different but as the *N* increases, the P_{TE} decreases but when SISO is considered, not enough enhancement has been shown. Hence, the performance of energy detection has improved, when threshold optimization is considered in contrast to the fixed threshold because the detection of the signal is probably even at low *SNR*.

The comparison between the fixed threshold and the optimized threshold has been in presented in Fig. 5.10. This figure shows that how the optimized threshold is better than the fixed threshold. For *N* = 1, 2, 3, the plot is achieved between P_{DT} and received *SNR* at fixed values of *c* = 2 and $\eta = 3$. When SISO is assumed, the curve has not shown enough deviation between the fixed and optimized threshold but still, there is a small deviation in optimized threshold in comparison to a fixed one but *N* increases from *N* = 2 to *N* = 3, the performance of probability

of detection has been seen from the curve. Hence, optimization of threshold provides better response in comparison to fixed threshold.

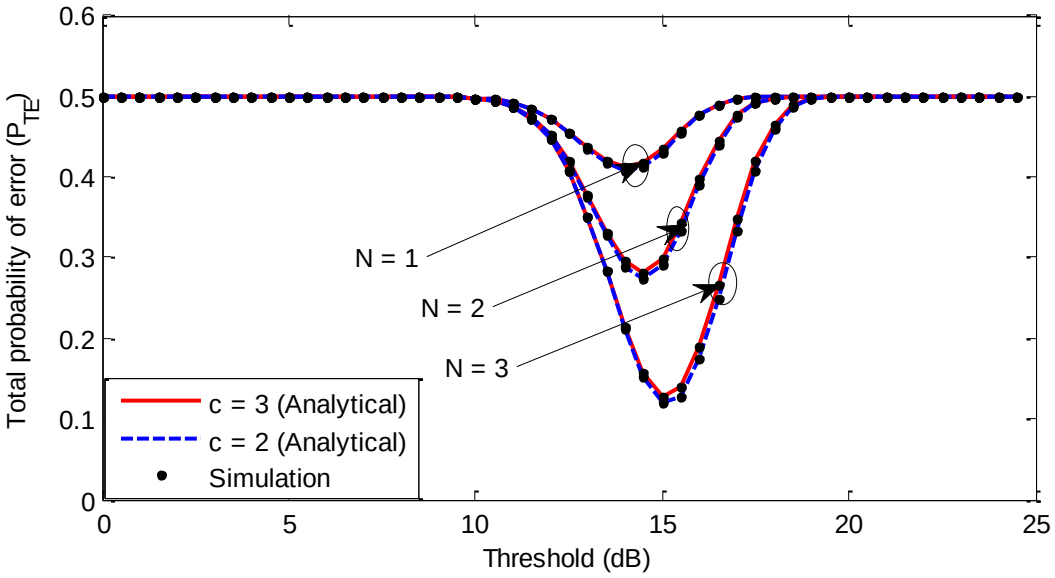

Fig. 5.9 P_{TE} as a function of threshold for different N at SNR = 4 dB, $\eta = 3$

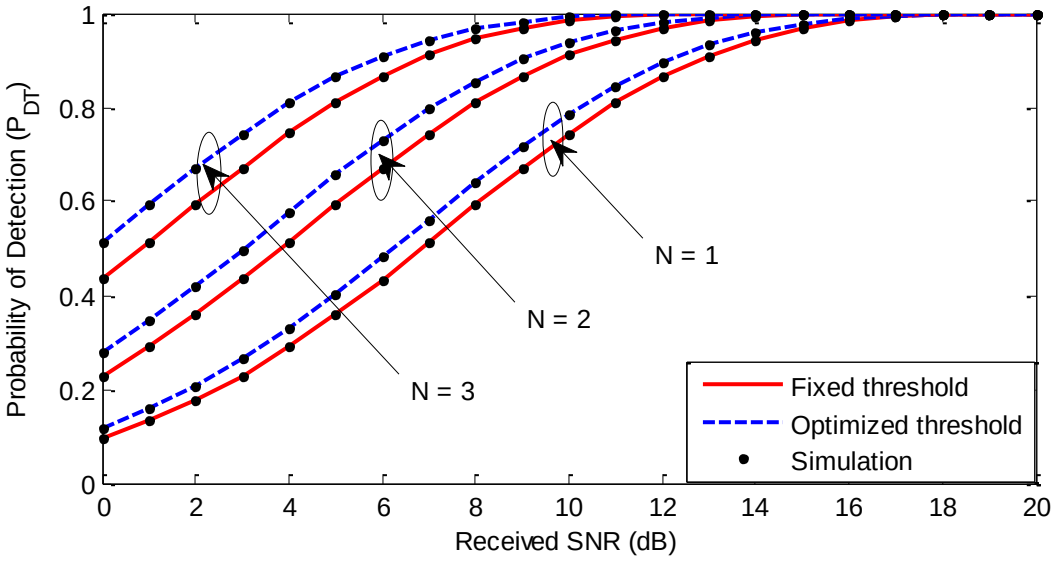

Fig. 5.10 P_{DT} versus received SNR at c = 2, $\eta = 3$

5.6 Conclusion

A simple analytical expression of the average probability of detection and average area under the operating characteristic curves with maximum ratio combining diversity scheme over

shadowed Weibull fading channels using an efficient mathematical approximation, Gaussian-Hermite integration is obtained. In addition, we have optimized the threshold by minimizing the total probability of error, global minima are obtained w.r.t threshold. When the optimized threshold is applied, a major improvement is validated in the probability of detection. The optimized threshold provides better detection capabilities in comparison to the fixed threshold. The derived analytical expressions results have been authenticated with the simulations.

Chapter 6

Performance Evaluation of Nakagami-m/log-normal Fading Channels

In this chapter, combined effect of small scale fading and large scale fading channel is considered. The small scale fading is modelled by Nakagami-m distribution and shadowed fading is modelled by a log-normal distribution. The Nakagami-m distribution is used to model densely scattered signals that reach at the receiver by multiple paths. The closed-form expressions of PDF and CDF is derived over composite Nakagami-m/log-normal (NL) fading channel by Holtzman approximation. The obtained PDF and CDF expressions are used to derive the important performance parameters of wireless communications systems. These performance matrices are the amount of fading (AF), outage probability (OP), average channel capacity (CC) and average symbol error probability (ASEP) of coherent modulation comprising binary orthogonal, antipodal, M-ary phase shift keying (M-PSK) and M-ary pulse amplitude modulation (M-PAM). Furthermore, energy detection is one of the ways to determine whether the signal is present or not. The performance of ED is studied in terms of CROC curves. To verify the correctness of our analysis, the derived closed-form expressions are corroborated via exact result and Monte Carlo simulations.

6.1 Channel Model

In this composite fading channel, the multipath effect is modelled by Nakagami-m distribution and shadowed effect is modelled by a log-normal distribution. The PDF of SNR of composite NL fading channel can be obtained by averaging the conditional PDF of Nakagami-*m* distribution over log-normal fading. Conditional distribution of Nakagami-*m* is expressed in equation (6.1) as

$$p(\gamma/v) = \frac{m^m \gamma^{m-1}}{\Gamma(m) v^m} exp\left(-\frac{m\gamma}{v}\right), \quad \gamma \geq 0 \tag{6.1}$$

If v is slow-varying, the conditional PDF in equation (6.1) converts statistical and its average must to be computed. The slow-varying signal is modelled by log-normal distribution with PDF as expressed as

$$p(v) = \frac{1}{\sigma v\sqrt{2\pi}} exp\left(-\frac{\left(\log_e v - \mu\right)^2}{2\sigma^2}\right) \tag{6.2}$$

Averaging the conditional PDF of equation (6.1) w.r.t PDF of equation (6.2) as expressed as

$$p(\gamma) = \int_0^\infty p(\gamma / v)\, p(v)\, dv \tag{6.3}$$

Substituting equations (6.1) and (6.2), into equation (6.3), we have

$$p(\gamma) = \int_0^\infty \frac{m^m \gamma^{m-1}}{\Gamma(m) v^m} exp\left(-\frac{m\gamma}{v}\right)\left\{\frac{1}{\sigma v\sqrt{2\pi}} exp\left(-\frac{\left(\log_e v - \mu\right)^2}{2\sigma^2}\right)\right\} dv \tag{6.4}$$

It is hard to get the closed-form expression of equation (6.4) directly and on the contrary to [138], log-normal has been estimated by IG distribution, here, we consider the efficient tool proposed by Holtzman [146] and by considering $\log_e v = x$ in equation (6.4) then equation (6.5) is obtained as

$$p(\gamma) = \int_0^\infty \psi(\gamma; x) \frac{1}{\sigma\sqrt{2\pi}} exp\left(-\frac{\left(x - \mu\right)^2}{2\sigma^2}\right) dx \tag{6.5}$$

Hence, the PDF of composite NL fading is obtained by equation (6.6) as

$$p(\gamma) = \frac{2}{3}\psi(\gamma; \mu) + \frac{1}{6}\psi\left(\gamma; \mu + \sqrt{3}\sigma\right) + \frac{1}{6}\psi\left(\gamma; \mu - \sqrt{3}\sigma\right) \tag{6.6}$$

where,

$$\psi(\gamma;x)=\frac{m^m\gamma^{m-1}}{\Gamma(m)exp(mx)}exp\left(-\frac{m\gamma}{exp(x)}\right) \tag{6.7}$$

The closed-form expression of CDF of composite NL fading channel is obtained in equation (6.8) by using equations (6.6) and (6.7) as

$$\begin{aligned}P(\gamma)&=\frac{1}{\Gamma(m)}\left\{\frac{2}{3}\Upsilon\left(m,\frac{m\gamma}{exp(\mu)}\right)+\frac{1}{6}\Upsilon\left(m,\frac{m\gamma}{exp\left(\mu+\sqrt{3}\sigma\right)}\right)+\frac{1}{6}\Upsilon\left(m,\frac{m\gamma}{exp\left(\mu-\sqrt{3}\sigma\right)}\right)\right\}\\&=\frac{1}{\Gamma(m)}\sum_{i=1}^{3}d_i\Upsilon\left(m,\frac{m\gamma_{th}}{exp(x_i)}\right)\end{aligned} \tag{6.8}$$

where, $\Upsilon(a,b)$, is the lower incomplete gamma function and $d_i\,(i=1,2,3)$ are 2/3, 1/6, 1/6 and $x_i\,(i=1,2,3)$ are $\mu,\mu+\sqrt{3}\sigma,\mu-\sqrt{3}\sigma$ respectively.

6.2 Performance Matrices

6.2.1 Amount of Fading

AF is the amount of severity of fading of the channel. In this section, AF of the composite NL fading channel is obtained [50]. The AF is expressed in equation (6.9) as

$$AF=\frac{E\left[\gamma^2\right]}{\left\{E[\gamma]\right\}^2}-1 \tag{6.9}$$

The closed-form expression obtained in equation (6.6) is nothing but the weighted sum of three terms of Nakagami-*m* and by assuming each term individually, so the k^{th} moment of γ is given in equation (6.10) as

$$E\left[\gamma^k\right]=\int_0^\infty\gamma^k\times\frac{m^m\gamma^{m-1}}{\Gamma(m)exp(mx)}exp\left(-\frac{m\gamma}{exp(x)}\right)d\gamma \tag{6.10}$$

After mathematical manipulation, equation (6.10) becomes

$$E\left[\gamma^k\right]=\left(\frac{exp(x)}{m}\right)^k\frac{\Gamma(m+k)}{\Gamma(m)} \tag{6.11}$$

Now, considering all the three terns of equation (6.6), k^{th} the moment of γ is given in equation (6.12) as

$$E\left[\gamma^k\right]=\frac{\Gamma(m+k)}{\Gamma(m)}\left\{\frac{2}{3}\left[\frac{exp(\mu)}{m}\right]^k+\frac{1}{6}\left[\frac{exp\left(\mu+\sqrt{3}\sigma\right)}{m}\right]^k+\frac{1}{6}\left[\frac{exp\left(\mu-\sqrt{3}\sigma\right)}{m}\right]^k\right\} \tag{6.12}$$

From equations (6.9) and (6.12), the AF of the composite NL fading channel is given in equation (6.13) as

$$AF=\left(\frac{m+1}{m}\right)\left[\frac{\left\{\frac{2}{3}+\frac{1}{6}exp\left(2\sqrt{3}\sigma\right)+\frac{1}{6}exp\left(-2\sqrt{3}\sigma\right)\right\}}{\left\{\frac{2}{3}+\frac{1}{6}exp\left(\sqrt{3}\sigma\right)+\frac{1}{6}exp\left(-\sqrt{3}\sigma\right)\right\}^2}-1\right] \tag{6.13}$$

6.2.2 Outage Probability

The OP is nothing but the typical performance measure of communication schemes operating over normal or composite fading channels and it is well-defined as the probability that the instantaneous error rate go beyond a quantified value, or equally, that γ drops below a pre-set threshold γ_{th} [50], which is expressed in equation (6.14) as

$$P_{out}\left(\gamma_{th}\right)=P\left[\gamma\le\gamma_{th}\right] \tag{6.14}$$

Equation (6.14) can be re-written by equation (6.15) as

$$P_{out}\left(\gamma_{th}\right)=\int_0^{\gamma_{th}}p(\gamma)\,d\gamma \tag{6.15}$$

Substitution of equation (6.7) into equation (6.15) yields the OP of composite NL fading in equation (6.16) as

$$P_{out}\left(\gamma_{th}\right)=\int_{0}^{\gamma_{th}}\frac{m^{m}\gamma^{m-1}}{\Gamma\left(m\right)exp\left(mx\right)}\exp\left(-\frac{m\gamma}{exp\left(x\right)}\right)d\gamma \tag{6.16}$$

After mathematical manipulation, equation (6.16) becomes

$$P_{out}\left(\gamma_{th}\right)=\frac{1}{\Gamma\left(m\right)}\Upsilon\left(m,\frac{m\gamma_{th}}{exp\left(x\right)}\right) \tag{6.17}$$

Now, considering all three terms of equation (6.6), OP of composite NL fading channel is given in equation (6.18) as

$$P_{out}\left(\gamma_{th}\right)=\frac{1}{\Gamma\left(m\right)}\sum_{i=1}^{3}d_{i}\Upsilon\left(m,\frac{m\gamma_{th}}{e^{x_{i}}}\right) \tag{6.18}$$

6.2.3 Average Channel Capacity

The closed-form expression of the average CC of the NL fading channel is derived [147-148]. The average CC is defined in equation (6.19) as

$$C=B\int_{0}^{\infty}\log_{2}\left(1+\gamma\right)p\left(\gamma\right)d\gamma \tag{6.19}$$

Substituting equation (6.6) into equation (6.19), the average CC of the composite NL fading is given in equation (6.20) as

$$\frac{C}{B}=\int_{0}^{\infty}\log_{2}\left(1+\gamma\right)\left(\frac{2}{3}\psi\left(\mu\right)+\frac{1}{6}\psi\left(\mu+\sqrt{3}\sigma\right)+\frac{1}{6}\psi\left(\mu-\sqrt{3}\sigma\right)\right)d\gamma \tag{6.20}$$

where, $\psi\left(x\right)$ is given in equation (6.7). Substituting $\psi\left(x\right)$ into equation (6.20) and after mathematical manipulation, equation (6.20) becomes

$$\frac{C}{B}=\frac{m^{m}}{\Gamma\left(m\right)ln\left(2\right)}\sum_{i=1}^{3}\frac{d_{i}}{exp\left(mx_{i}\right)}\int_{0}^{\infty}\gamma^{m-1}\log_{2}\left(1+\gamma\right)exp\left(-\frac{m\gamma}{exp\left(x\right)}\right)d\gamma \tag{6.21}$$

From [143], the following terms can be expressed in term of Meijer's-G function as

$$\ln\left(1+\gamma\right)=G_{2,2}^{1,2}\left[\gamma\left|\begin{matrix}1,1\\1,0\end{matrix}\right.\right] \tag{6.22}$$

$$exp\left(-\frac{m\gamma}{exp\left(x_i\right)}\right)=G_{0,1}^{1,0}\left[\frac{m}{exp\left(x_i\right)}\gamma\middle|0\right] \tag{6.23}$$

Substituting equations (6.22) and (6.23) into equation (6.21) as

$$\frac{C}{B}=\frac{m^m}{\Gamma\left(m\right)ln\left(2\right)}\sum_{i=1}^{3}\frac{d_i}{exp\left(mx_i\right)}\int_0^\infty \gamma^{m-1}G_{2,2}^{1,2}\left[\gamma\middle|\begin{matrix}1,1\\1,0\end{matrix}\right]G_{0,1}^{1,0}\left[\frac{m}{exp\left(x_i\right)}\gamma\middle|0\right]d\gamma \tag{6.24}$$

As per generalization of classical Meijer's integral from two Meijer G-functions [149], thus, the average CC of NL fading channel is given in equation (6.25) as

$$\frac{C}{B}=\frac{m^m}{\Gamma\left(m\right)ln\left(2\right)}\sum_{i=1}^{3}\frac{d_i}{exp\left(mx_i\right)}G_{2\ 3}^{3\ 1}\left[\frac{m}{exp\left(x_i\right)}\middle|\begin{matrix}-m,1-m\\0,-m,-m\end{matrix}\right] \tag{6.25}$$

6.2.4 Average Symbol Error Probability

ASEP is another important parameter to evaluate the performance of the composite NL fading channel. The instantaneous symbol error probability (SEP) obtained using maximum likelihood coherent detector in [50, 150] as

$$P_s\left(\gamma_r\right)=\sum_{l=1}^{L}\lambda_l Q^l\left(\sqrt{\lambda_0\gamma_r\omega_s}\right) \tag{6.26}$$

where, $Q\left(x\right)$ is Gaussian Q-function, λ_l and λ_0 are constants related to constellation type and size respectively. The statistical expectation of instantaneous SEP given by equation (6.26) w.r.t. the γ_r yields the ASEP expression in equation (6.27) as

$$\bar{P}_s=\int_0^\infty P_s\left(\gamma_r\right)p\left(\gamma_r\right)d\gamma_r \tag{6.27}$$

Substituting equations (6.24) and (6.6) into equation (6.27), shown in equation (6.28) as

$$\bar{P}_s=\begin{cases}\sum_{l=1}^{L}\lambda_l\int_0^\infty\left(\frac{c_1}{2}\exp\left(-\frac{t\lambda_0\gamma_r\omega_s}{2}\right)+\frac{c_2}{2}\exp\left(-t\lambda_0\gamma_r\omega_s\right)\right)^l\times\\ \sum_{i=1}^{3}\frac{d_i}{\exp\left(mx_i\right)}\frac{m^m{\gamma_r}^{m-1}}{\Gamma\left(m\right)}\times\exp\left(-\frac{m\gamma_r}{\exp\left(x_i\right)}\right)d\gamma_r\end{cases} \tag{6.28}$$

Now, equation (6.28) can be re-written for $l=1$ using Meijer-G function [149], ASEP becomes

$$\bar{P}_s = \lambda_l \sum_{i=1}^{3} \frac{d_i m^m}{\exp(m x_i)} \left(\frac{c_1}{2} \left(\frac{t\lambda_0 \omega_s}{2} + \frac{m}{\exp(x_i)} \right)^{-m} + \frac{c_2}{2} \left(t\lambda_0 \omega_s + \frac{m}{\exp(x_i)} \right)^{-m} \right) \tag{6.29}$$

where, $c_1 = 0.3070$, $c_2 = 0.4389$, and $t = 1.0510$.

Table 6.1 ASEP for different coherent modulation schemes

Modulation	BPSK: Binary antipodal	BPSK: Binary orthogonal	QPSK	M-PSK	M-PAM
L	1	1	1	1	1
λ_0	2	1	1	$2\sin^2(\pi/M)$	$6/(M^2-1)$

The instantaneous signal to noise ratio per symbol at the receiver is ω_s , where ω_s is a deterministic positive quantity representing received symbol SNR in AWGN and γ_r is a log-normally distributed non-negative random variable. ASEP for different coherent modulation schemes is presented in Table 6.1

6.3 Average Probability of Detection

In a similar way, when experiencing a composite fading channel, P_{FA} in equation (3.8) will remain, be the same, since it does not dependent on the SNR. But, when g varies the $\overline{P_{DT}}$ can be easily evaluated by averaging P_{DT} in equation (3.9) over the SNR distribution. Putting the value of (6.6) and (3.13) into (4.10), then the $\overline{P_{DT}}$ becomes as

$$\overline{P_{DT}} = \int_0^{\infty} \left(\sum_{h=0}^{\infty} \frac{\gamma^h}{h!} \frac{\Gamma\left(h+\eta, \frac{\hat{\lambda}}{2}\right)}{\Gamma(h+\eta)} exp(-\gamma) \right) \times \left(\frac{2}{3}\psi(\gamma;\mu) + \frac{1}{6}\psi\left(\gamma;\mu+\sqrt{3}\sigma\right) + \frac{1}{6}\psi\left(\gamma;\mu-\sqrt{3}\sigma\right) \right) d\gamma \tag{6.30}$$

After some mathematical manipulation [143], equation (6.30) can be approximated the average probability of detection as

$$\overline{P_{DT}} = \sum_{h=0}^{\infty} \sum_{i=1}^{3} \frac{\eta_i}{h!} \frac{\Gamma\left(h+\eta, \frac{\hat{\lambda}}{2}\right)}{\Gamma(h+\eta)} \frac{m^m}{\Gamma(m) exp(m x_i)} G_{1,1}^{1,1}\left[\frac{m}{exp(x_i)}\Big|_0^{1-k-m} \right] \tag{6.31}$$

In Table (5.2), the truncation error incurred in approximating the series of equation (6.31) to the term $h=2$ and $h=4$ for different values of SNR (dB) values has been analysed for all three realistic scenarios such as light and average shadowing.

Table 6.2 MSE for convergence of $\overline{P_{DT}}$ for various values of SNR (dB) and time-bandwidth product $\eta=12$ for various realistic scenarios

SNR (dB)	Light shadowing		Average shadowing	
	$h=2$	$h=4$	$h=2$	$h=4$
0	5.901×10^{-6}	5.482×10^{-26}	9.048×10^{-6}	8.041×10^{-23}
5	8.128×10^{-5}	5.122×10^{-23}	5.130×10^{-5}	5.180×10^{-21}
10	2.864×10^{-4}	4.271×10^{-20}	2.158×10^{-5}	3.492×10^{-18}

6.4 Results and Discussion

In this section, we present the graphical presentation of PDF, CDF, and various performance matrices as well as performance analysis of ED in terms of CROC. Fig. 6.1 illustrates the graphical outcome of the closed-form expression of PDF versus SNR (dB) for several values of m which signifies the amount of severity of multipath of composite NL fading channel. The plot also includes the exact result and Monte Carlo simulation for validation purpose. Clearly, the closed-form expression obtained in equation (6.6) is shown to coincide with that of exact

and very small variation in Monte Carlo simulation, when m increases. CDF is plotted w.r.t. threshold SNR for different values of average SNR as shown in Fig. 6.2. The plot shows the good agreement with the closed-form expression and simulations and the probability of accomplishing an assumed threshold SNR is decreased as average SNR increases.

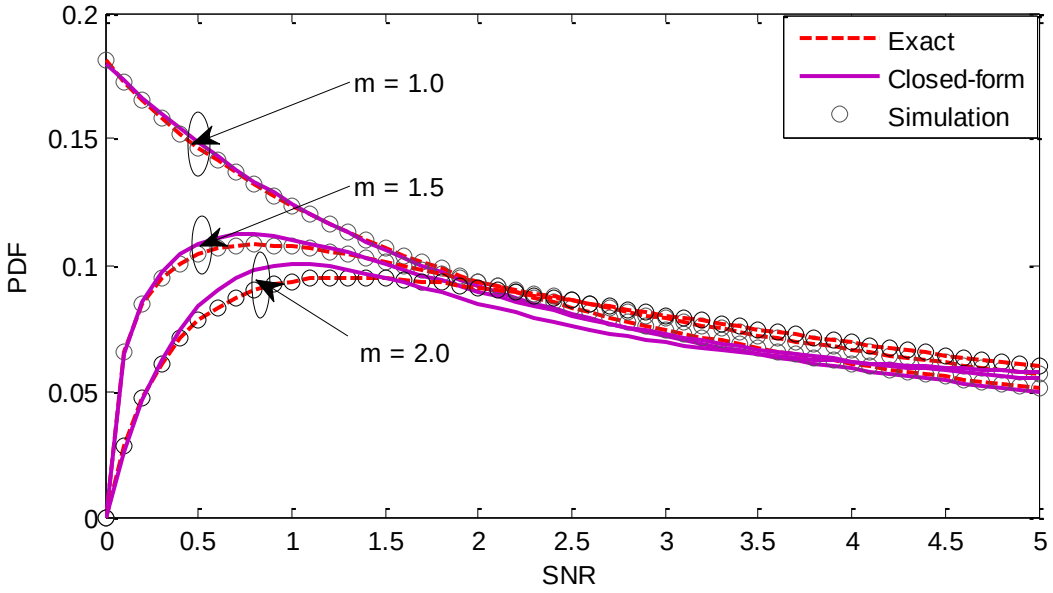

Fig. 6.1 PDF of composite NL fading channel at different fading parameter

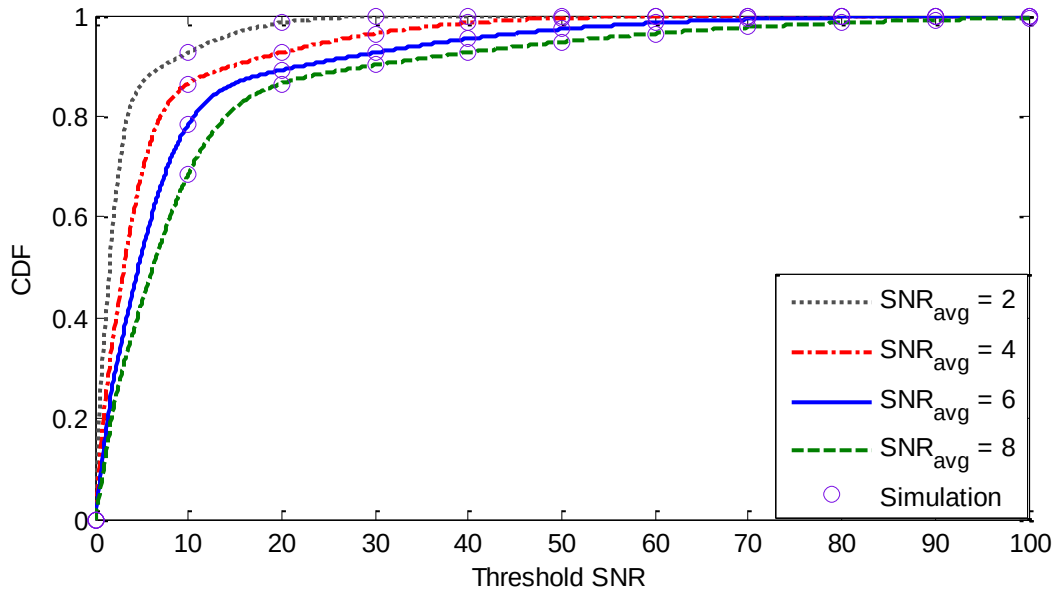

Fig. 6.2 CDF of composite NL fading against threshold SNR

Now, we can use the quantitative measure of AF to compare power fluctuation in the composite NL fading channels. Fig. 6.3 illustrates the AF against the multipath m for several σ using equation (6.13). The result points out that as the AF decreases with an increase in the m. As the severity of shadowing increases, the AF plots of composite fading moves upward indicate an increase in the randomness of channel deteriorating the performance of the receiver and provide good agreement with simulations.

In Fig. 6.4 and Fig. 6.5, we have analysed the performance parameter of the receiver in terms of OP, both figures are also simulated by Monte Carlo simulation using equation (6.18). Fig. 6.4 depicts the results of OP with respect to σ; it is clear from the plot that OP increases as σ increases, indicating the increase in the likelihood of the failure to achieve an assumed threshold SNR as a move from light shadowing to the scenario to average shadowing scenario.

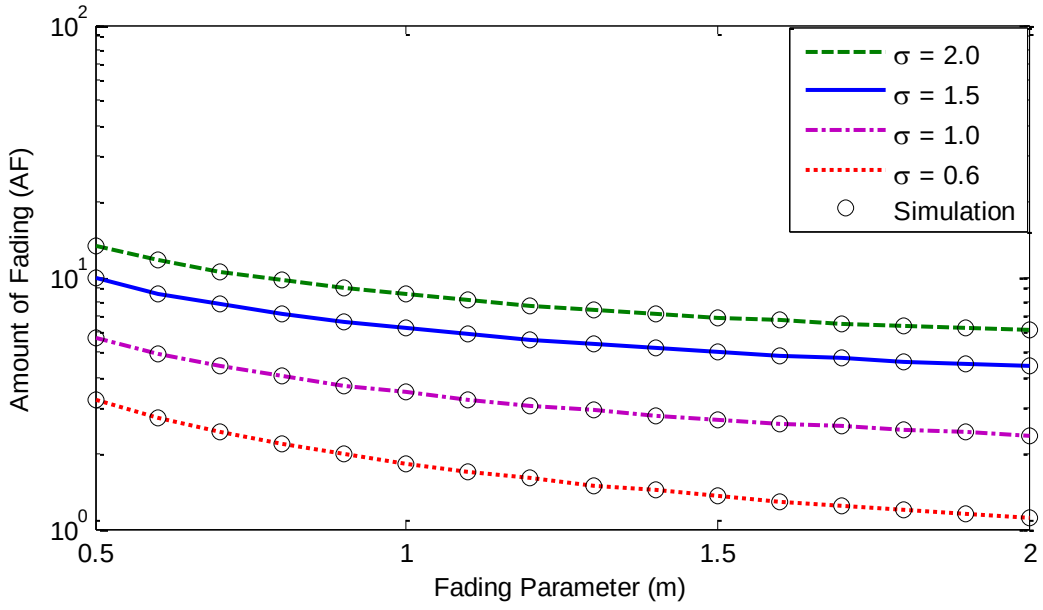

Fig. 6.3 AF against m for several values of σ

One can see the deleterious effect of σ deteriorating the receiver performance, thus, requiring the diversity combining to improve the performance. Fig. 6.5, the OP is obtained against multipath fading parameter (m) for several values of shadowing parameters (σ). OP is

witnessed to decreases as m increases, which is quite expected. Moreover, plots are shifted upwards for an increase in the shadowing.

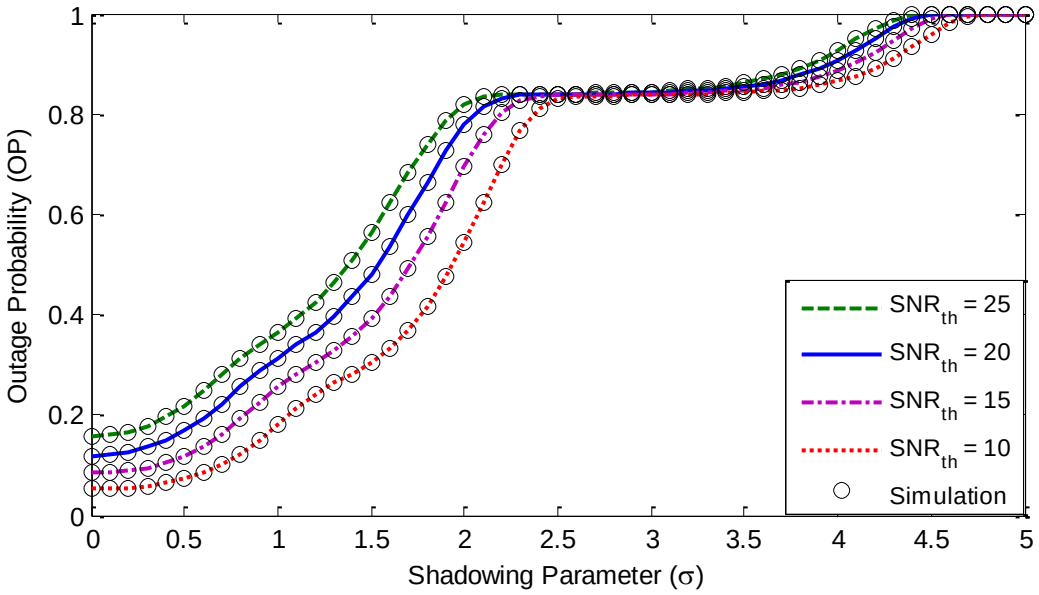

Fig. 6.4 OP as a function of σ at different SNR_{th}

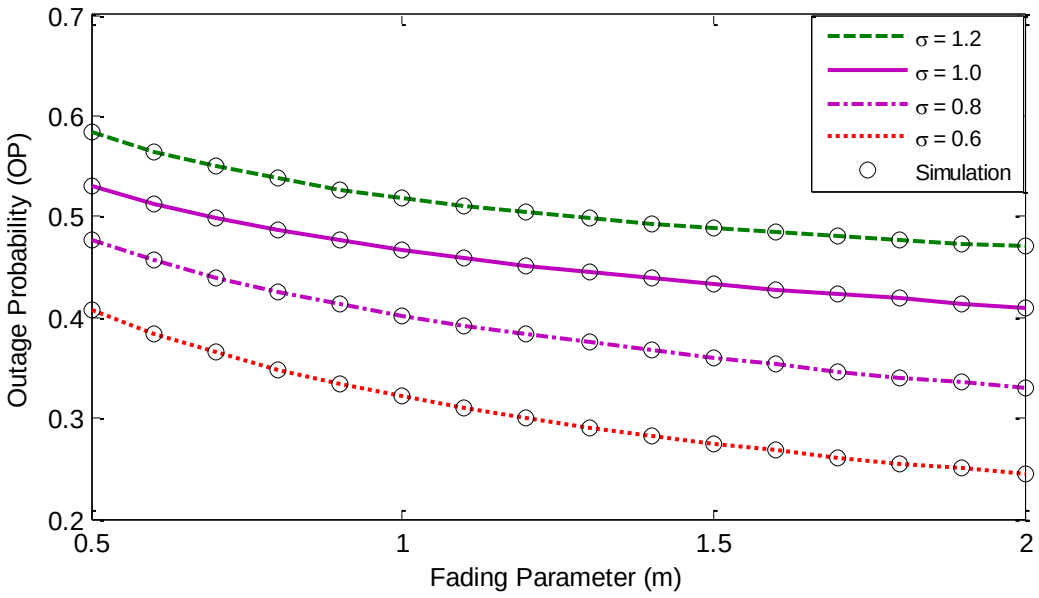

Fig. 6.5 OP verses m for different values of σ

In Fig. 6.6, average channel capacity is plotted against the average SNR with different values of m using equation (6.25). It is quite obvious that as average SNR increases channel capacity

also increases, which is as likely. Moreover, reduction in severity of multipath improves the channel capacity, thus, moving the plots upside and compared with simulation.

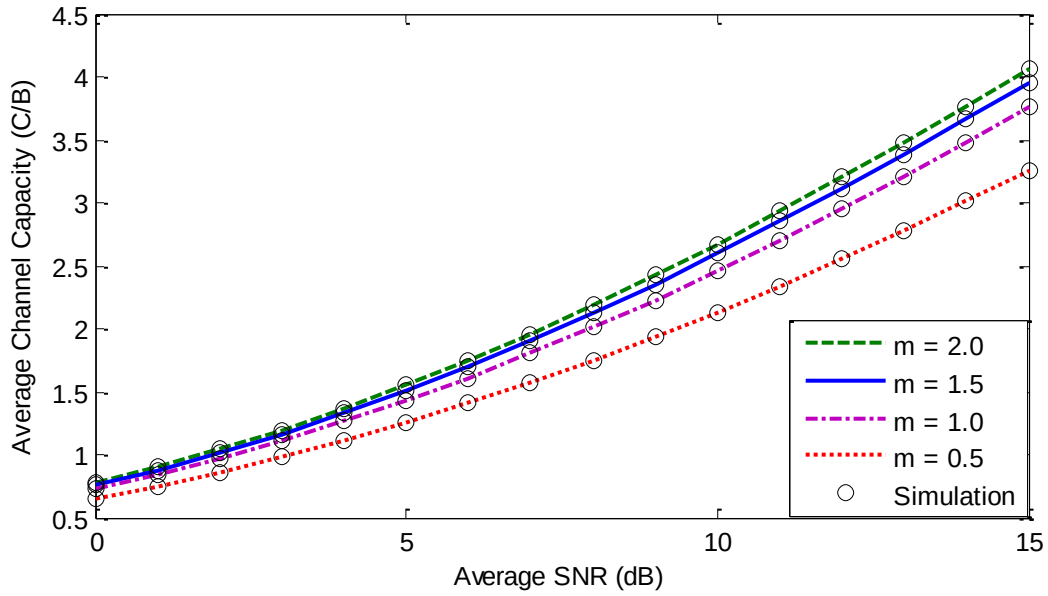

Fig. 6.6 Average channel capacity versus average SNR (dB) for different m

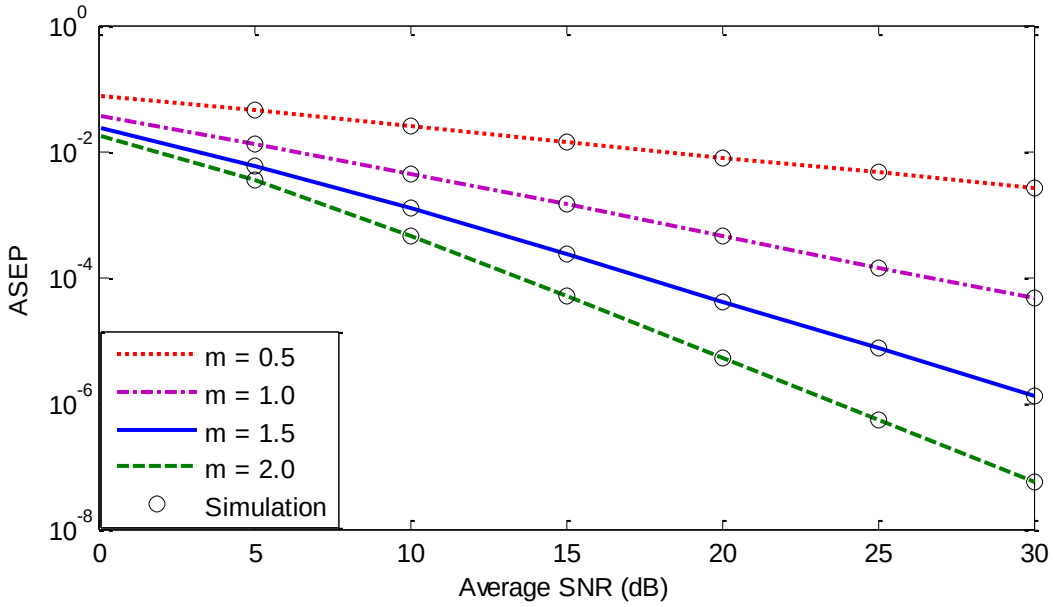

Fig. 6.7 ASEP verses average SNR (dB) of BPSK (antipodal) for different values of m

In Fig. 6.7 to 6.10, we have ASEP against average received SNR for different values of m as well as σ respectively and all the plots show the very tight bound of closed-form expression

with Monte Carlo simulations using equation (6.29). Various modulation formats have been considered such as BPSK, M-PSK, and M-PAM. Fig. 6.7 depicts that as average SNR increases, average symbol error rate decreases. The analogous tendency is witnessed in Figure 6.8 too, where the performance of system advances with channel situations shifting from average to light shadowed fading and in this plot comparison of BPSK is shown with QPSK.

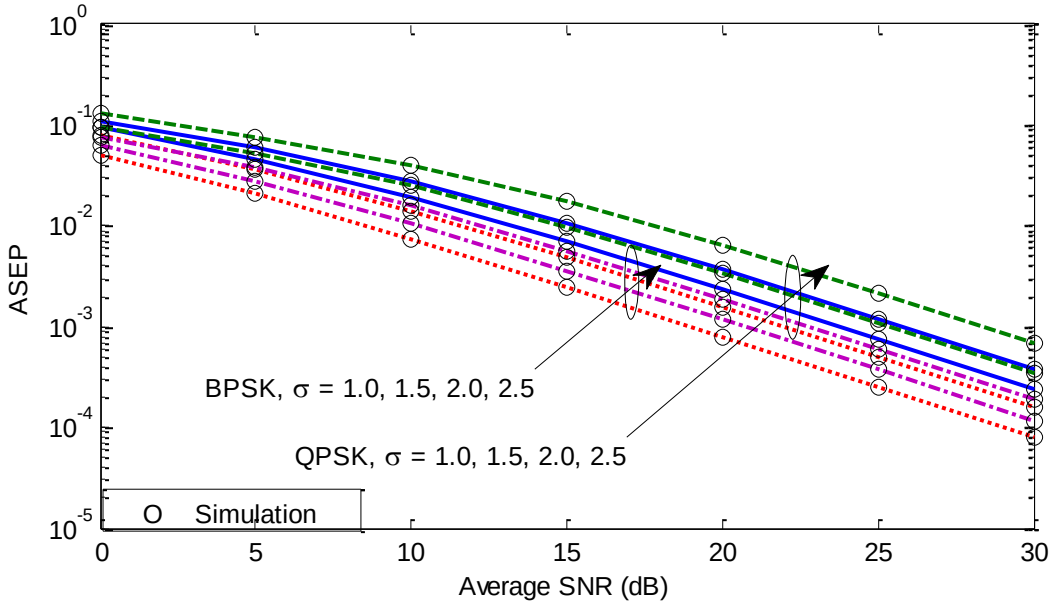

Fig. 6.8 ASEP verses average SNR (dB) of BPSK and QPSK for different values of σ

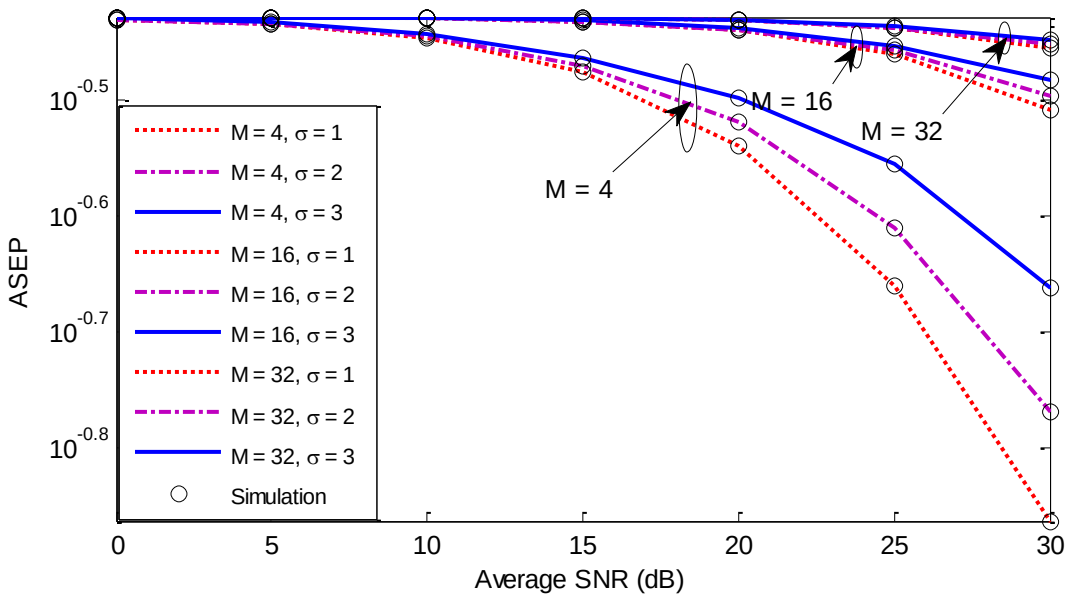

Fig. 6.9 ASEP against average SNR (dB) of M-PSK for different values of σ

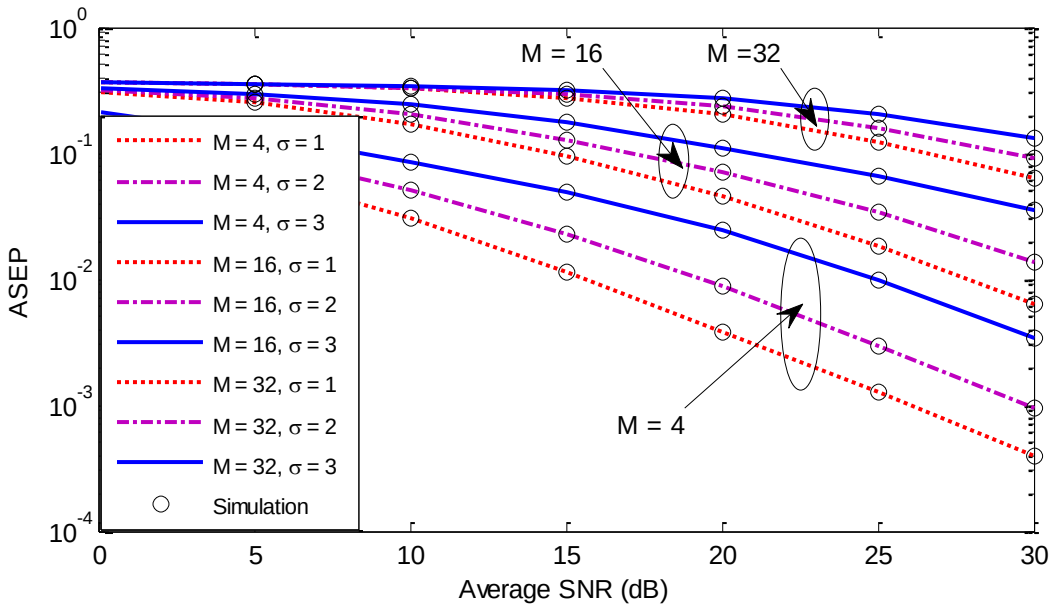

Fig. 6.10 ASEP verses average SNR (dB) of M-PAM for different values of σ

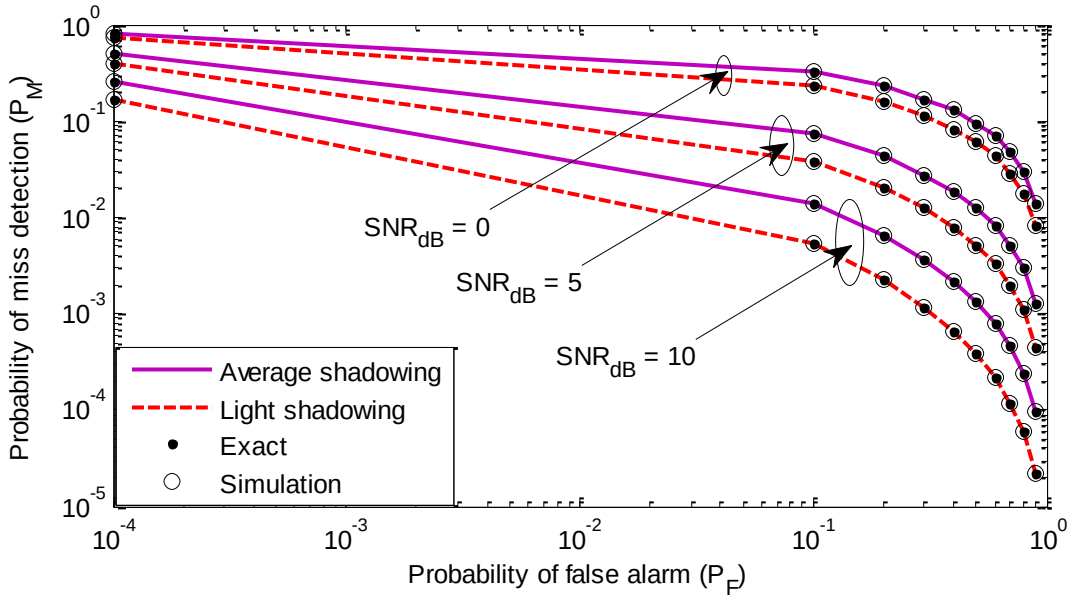

Fig. 6.11 CROC curve for light and average shadowing ($\eta = 12$)

In Fig. 6.9, ASEP is plotted against average SNR (dB) for M-PSK constellation. The plots are obtained for different values of $M = 4,16,32$ at fading parameter, $m = 1$ and shadowing parameter, $\sigma = 1,2,3$. It is evident from the plot that shadowing deteriorates the receiver performance. In Figure 6.10, the similar results are observed for M-PAM.

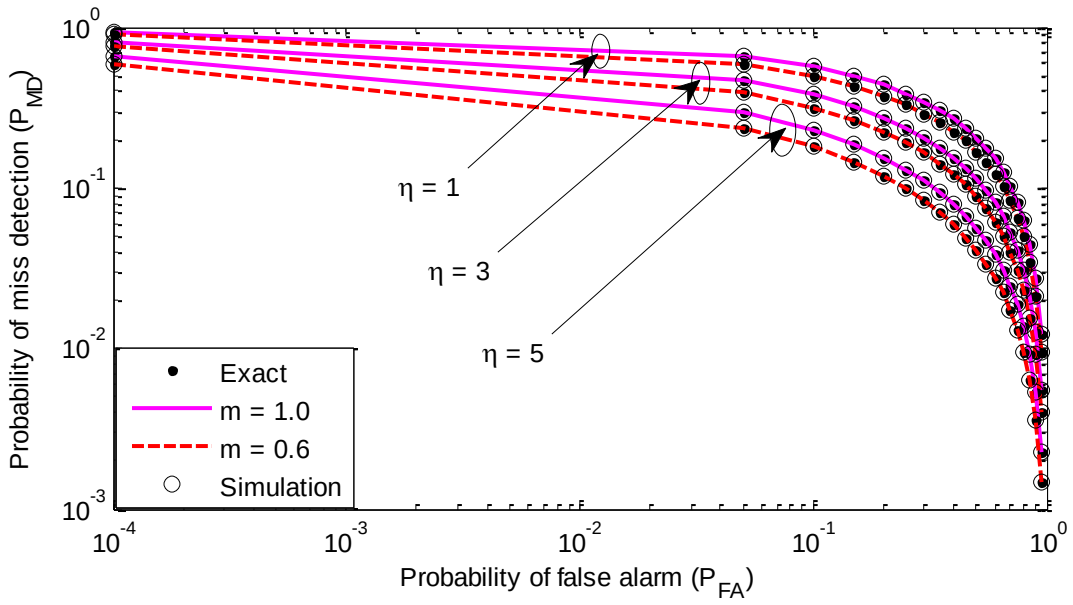

Fig. 6.12 CROC curves for different η with *m* 0.7 and 1.1 at SNR = 0 dB

In Fig. 6.11, CROC curve is plotted under shadowing conditions such as light and average shadowing for several values of received SNR (dB). The analytical result obtained in equation (6.31) is shown to coincide with that of exact result and Monte Carlo simulation. Moreover, as expected, the probability of miss detection is shown to be lowest for light shadowing and maximum for average shadowing. In Fig. 6.12, CROC curve is represented with different values of the number of samples such as 1, 3, 5 and 7 at dissimilar fading parameters 0.7 and 1.1. The probability of miss detection reduces as the number of the sample size increases that illustrations the perfection in the detection of the anonymous signal. For $d = 5$, detection probability increases at both the values of the fading parameters. This plot provides a very well match with exact, closed-form and simulation results.

6.5 Conclusion

In this chapter, we have formulated the closed-form result for PDF of instantaneous received SNR with the efficient approximation called Holtzman approximation of composite NL fading channel. The obtained result holds good for multipath fading and light, average shadowed

fading. Using closed-form expressions of PDF and CDF, we obtained closed-form expression of the amount of fading, outage probability, average channel capacity and average symbol error rate probability and their performance has been analysed. Exact results show good agreement with closed-form results along with Monte Carlo simulations. Another performance analysis of energy detector is observed in terms of complementary receiver operating characteristics.

Chapter 7

Conclusion and Future Scope

This chapter is divided into two parts: (i) conclusion of complete work, which has been included in the thesis; (ii) future scope of the given research work. This thesis mainly focuses on energy detection based spectrum sensing in cognitive radio for different wireless fading channels.

7.1 Conclusion

The main conclusions of this thesis are abridged as follows:

- Chapter 3 includes energy detection based spectrum sensing for inverse Gaussian fading channel with selection combining scheme. The performance analysis of energy detection has been investigated in terms of complementary receiver operating characteristic curves for the entire three realistic scenarios like light shadowing, moderate shadowing, and heavy shadowing for single input single output. Furthermore, the threshold is optimized by minimizing total probability of error and this optimized threshold provides better detection capability in comparison to a fixed threshold. For numbers of diversity branches, the probability of miss-detection decreases and optimized threshold gives better response in comparison to the fixed one in the CROC curves. The ROC curves also present the same behavior, i.e. probability of detection is high for an optimized threshold as well as the number of diversity branches. The exact result is also verified by the simulation results.
- Chapter 4 provides the performance analysis of energy detection based spectrum sensing over composite multipath/shadowed fading channel with maximum ratio combining scheme. In this chapter, the composite fading is considered as Nakagami-

m/log-normal fading channel. The average probability of detection and average AUC curves have been derived with MRC reception. The CROC curves have been presented for light shadowing and moderate shadowing at different values of SNR. The probability of miss-detection decreases as the number of sample value increases, which is presented in the CROC curves. The average CAUC curves have been plotted for different fading parameters and number of diversity branches. Further, threshold optimization has been considered, inverted bell-shaped has been displayed at different number of diversity branches. The optimized threshold presents the better probability of detection in comparison to the fixed threshold.

- Chapter 5 proposes the analytical expressions of the average probability of detection and average AUC curves over composite Weibull/shadowed fading channel with MRC reception by using Gaussian-Hermite integration approximation. The Weibull channel exhibits a perfect fit to multipath experimental fading channels for indoor and outdoor scenarios and log-normal is used to represent shadowing. The performance analysis is examined using CROC, ROC and average AUC curves for different parameters and number of diversity branches. Further, threshold is optimized by minimizing the total probability of error. The detection results show better in the optimized threshold.
- Chapter 6 derives the closed-form expressions of PDF, CDF, AF, OP, and ASEP over the composite Nakagami-*m*/log-normal fading channel by using Holtzman approximation. Another performance analysis of energy detection is observed in terms of CROC curves for light shadowing and average shadowing at different values of SNR. For different values of the number of samples and fading parameters, CROC curves has been presented, which shows that the probability of miss-detection becomes smaller when numbers of samples increases.

Hence, among all these presented fading channels, Weibull/log-normal fading channel is very close to real time or experimental environments, which provides better detection probability with maximum ratio combining scheme and in the optimized threshold.

7.2 Future Scope

In this thesis, concept related energy detection based spectrum sensing over different multipath and combination of both, multipath and shadowing fading channels with different diversity schemes have been addressed but there are still some fading channels need to be investigated in future work.

- **Performance of spectrum sensing in cognitive radio over fibre technology:** To get benefit from the performance of spectrum sensing with other technologies. The same methods can be used in cognitive radio over fibre technology (CRoF). The idea to explore some of the improvements that radio over fibre technology can bring to wireless networks when combined with CR techniques.
- **Spectrum sensing for UWB cognitive radio networks:** Implementation of spectrum sensing for cognitive UWB-OFDM systems and cooperative detection transmitter signal in UWB-CR systems.
- **Cooperative wideband spectrum sensing in cognitive radio networks:** Implementation of spectrum sensing over different fading channels. How the fusion center can collect the information of vacant spectrum from the cognitive radios.
- **Experimental study of spectrum sensing in cognitive radio networks:** Only mathematical analysis has been made till date over composite fading and generalized fading channel. So, all the above analysis can further be extended to measurement analysis by varying parameters of different fading channels.

- **Performance analysis of cognitive radio over generalized fading channels:** The behavior of energy detection over generalized composite fading with different diversity schemes can be considered. The average probability of detection and average AUC curves can be investigated over composite kappa-mu/shadowed, eta-mu/shadowed and alpha-mu/shadowed with MRC, EGC, and SC diversity schemes and threshold optimization can also be measured. The above-mentioned performance matrices can also be studied over generalized composite fading channels such as alpha-kappa-mu/shadowed and alpha-eta-mu/shadowed fading channels.
- **Time domain analysis over different fading channels:** It is not explained, how to incorporate spectrum sensing methods in the time domain and what will be the behavior of fading channels.
- **Spectrum sensing over other detection methods:** The proposed analysis over different fading channel can also be further extended to other spectrum sensing methods such as matched filter, cyclo-stationary feature detection, Eigen value-based detection, covariance-based detection.

References

1. Cisco Visual Networking Index: Global Mobile Data Traffic Forecast Update, Updated: March 28, 2017, 2016–2021 *White Paper*, Document ID: 1454457600805266.

2. S. K. Sharma, E. Lagunas, S. Chatzinotas, B. Ottersten, "Application of comprehensive sensing in cognitive radio communications: A Survey", *IEEE communications surveys & tutorials*, vol. 18, no. 3, pp. 1838-1860, 2016.

3. D. Cabric, S. M. Mishra, and R.W. Brodersen, "Implementation issues in spectrum sensing for cognitive radios", *Proc. 38th. Asilomar Conference on Signals, Systems, and Computers*, pp. 772–776, 2004.

4. V. Valenta, R. Marsalek, G. Baudoin, M. Villegas, M. Suarez, and F. Robert, "Survey on spectrum utilization in Europe: Measurements, analyses and observations," *in Proc. Fifth International Conference on Cognitive Radio Oriented Wireless Networks and Communications (CROWNCOM)*, pp. 1–5, June 2010.

5. FCC: Spectrum Policy Task Force Report. Nov 02, 2002: ET Docket No. 02-155.

6. S. Haykin, "Cognitive radio: Brain-empowered wireless communications, *IEEE Transactions on Information Theory*, vol. 23, no. 2, pp. 201–220, Feb 2005.

7. "Spectrum access and the promise of cognitive radio technology," Federal Communication Commision (FCC), *Cognitive Radio Technologies Proceeding (CRTP)*, ET Docket No. 03-108, May 2003.

8. C. Stevenson, G. Chouinard, Z. Lei, W. Hu, S. Shellhammer, and W. Caldwell, "IEEE 802.22: The first cognitive radio wireless regional area networks (WRANs) standards," *IEEE Communications Magazine*, vol. 47, no. 1, pp. 130–138, Jan. 2009.

9. J. Mitola, G.Q. Maguire, "Cognitive radios: making software radios more personal", *IEEE Pers. Communication*, vol. 6, no. 4, pp. 13–18, 1999.

10. T. Yucek and H. Arslan, "A Survey of Spectrum Sensing Algorithms for Cognitive Radio Applications", *IEEE Communications Surveys & Tutorials*, vol. 11, no. 1, pp. 116-130, 2009.

11. M. Sansoy, A.S. Buttar, "Spectrum sensing algorithms in Cognitive Radio: A survey", *International Conference on Electrical, Computer and Communication Technologies (ICECCT)*, pp. 1-5, 2015.

12. N. Muchandi, R. Khanai, "Cognitive Radio Spectrum Sensing : A Survey", *International Conference on Electrical, Electronics, and Optimization Techniques (ICEEOT)*, pp. 3233-3237, 2016.

13. I.F. Akyildiz, B.F. Lo, R.K. Balakrishnan, "Cooperative spectrum sensing in cognitive radio networks: A survey", *Physical Communication*, vol. 4, no. 1, pp. 40-62, 2011.

14. M. Subhedar, G. Birajdar, "Spectrum Sensing Techniques In Cognitive Radio Networks: A Survey", *International Journal of Next-Generation Networks (IJNGN)*, pp. 37-51, 2011.

15. G. Xiong, S. Kishore, A. Yener, "Spectrum sensing in cognitive radio networks: Performance evaluation and optimization", *Physical Communication*, vol. 9, pp. 171-183, 2013.

16. R. Umar, A.U.H. Sheikh, "A comparative study of spectrum awareness techniques for cognitive radio oriented wireless networks", *Physical Communication*, 2012.

17. Alexander M. Wyglinski, "*Cognitive Radio Communication and Networks*" Elsevier, 2010.

18. E. Hossin, V. Bhargva, "*Cognitive Wireless Communication Networks*", Springer, 2007.

19. Huseyin Arslan (Ed.), "*Cognitive radio, software defined radio, and adoptive wireless systems*," University of South Florida, Temp., FL, USA, spring 2007.

20. L. Bixio, M. Ottonello, M. Raffetto and C. Regazzani, "Comparison among cognitive radio architecture for spectrum sensing," *EURASIP Journal on Wireless Communication and Network*, vol. 2011, No. 749891, pp. 1018, Feb. 2011.

21. S.A. Mousavifar, C. Leung, "Energy Efficient Collaborative Spectrum Sensing Based on Trust Management in Cognitive Radio Networks", *IEEE Transactions on Wireless Communications*, vol. 14, no. 4, pp. 1921-1939, 2015.

22. A.A. Khan, M.H. Rehmani, M. Reisslein, "Cognitive Radio for Smart Grids: Survey of Architectures, Spectrum Sensing Mechanisms, and Networking Protocols", *IEEE Communications Surveys & Tutorials*, vol. 18, no. 1, pp. 860-898, 2016.

23. M.L. Benitez, F. Casadevall, "Signal Uncertainty in Spectrum Sensing for Cognitive Radio", *IEEE Transactions on Communications*, vol. 61, no. 4, pp. 1231-1241, 2013.

24. I.E. Atawi, O.S. Badameh, M.S. Aloqlah, R. Mehleh, "Energy-detection based spectrum-sensing in cognitive radio networks over multipath/shadowed fading channels", *Wireless Telecommunications Symposium (WTS)*, USA, pp. 1-6, 2015.

25. A. Ghasemi and E.S. Sousa, "Spectrum sensing in cognitive networks: requirements, challenges and decision trade-offs," *IEEE Communication Magazine*, vol. 446. No. 4, pp. 32-39, April 2008.

26. M. Yang, Y. Li, X. Liu, W. Tang, "Cyclostationary feature detection based spectrum sensing algorithm under complicated electromagnetic environment in cognitive radio networks", *China Communications*, vol. 12, no. 9, pp. 35-44, 2015.

27. A. Begwari, G.S. Tomar, "Comparison between Adaptive Double-Threshold Based Energy Detection and Cyclostationary Detection Technique for Cognitive Radio Networks", *5th International Conference and Computational Intelligence and Communication Network*s, pp. 182-185, 2013.

28. W.M. Jang, “Blind Cyclostationary Spectrum Sensing in Cognitive Radios”, *IEEE Communications Letters*, vol. 18, no. 3, pp. 393-396, 2014.

29. P.S. Yawada, A.J. Wei, “Cyclostationary Detection Based on Non-cooperative spectrum sensing in cognitive radio network”, *IEEE International Conference on Cyber Technology in Automation, Control, and Intelligent Systems (CYBER)*, pp. 184-187, 2016.

30. Y. ZhaoY. Wu, J. Wang, X. Zhong, L. Mei, “Wavelet transform for spectrum sensing in Cognitive Radio networks”, *International Conference on Audio, Language and Image Processing*, pp. 1-6, 2014.

31. S.V.R.K Rao, G. Singh, “Wavelet Based Spectrum Sensing Techniques in Cognitive Radio”, *Procedia Engineering*, vol. 38, pp. 880-888, 2012.

32. R. Verma, A. Mahapatro, “Cognitive Radio: Energy detection using wavelet packet transform for spectrum sensing”, *Third International Conference on Advances in Electrical, Electronics, Information, Communication and Bio-Informatics (AEEICB)*, pp. 1-5, 2017.

33. N.A. Hussien, M.A. Hafer, K. Shuaib, “Collaborative Wideband Spectrum Sensing for Cognitive Radio using Wavelet-based Detection”, *5th International Conference on Control, Decision and Information Technologies (CoDIT)*, pp. 492-497, 2018.

34. H. Tang, “Some physical layer issues of wide-band cognitive radio systems,” *in Proc. IEEE International Symposium on New Frontier in Dynamic Spectrum Access Networks*, Baltimore, Maryland, USA, Nov. 2005, pp. 151-159.

35. R. Tanda and A. Sahai, “Fundamental limits on detection in low SNR under noise uncertainty,” *in Proc. IEEE Int. Conf. Wireless Networks, Communication and Mobile Computing*, vol. 1, Maui, HI, June 2005, pp. 464-469.

36. D. Cabric, S. Mishra, and R. Brodersen, "Implementation issues in spectrum sensing for cognitive radios," *in Proc. Asilomar Conf. on Signals, System and Computers*, vol. 1, Pacific Gove, California, USA, Nov. 2004, pp. 772-776.

37. U. Gardner, WA, "Exploitation of spectrum redundancy in cyclostaionary signals," *IEEE Signal Processing Magazine*, vol. 8, No. 2, pp. 14-36, 1991.

38. D. Cabric, and R. Brodersen, "Physical layer design issues unique to cognitive radio systems," *in Proc. IEEE Int. Symposium on Personal, Indoor and Mobile Radio Communication*, vol. 2, Berlin, Germany, Sept. 2005, pp. 759-763.

39. F. Akyildiz and B. Lo, "Cooperative spectrum sensing in cognitive radio networks: A survey," *ELSEVIER Journal Computers and Electrical Engineering*, vol. 4, No. 1, pp. 40-62, Dec. 2010.

40. J. A. Bazerque, G.B. Giannkis, "Distributed spectrum sensing for cognitive radio networks by exploiting sparsity," *IEEE Transactions on Signal Processing*, vol. 58, No. 3. Pp. 1847-1862, March 2010.

41. O. Holland, H. Bogucka, A. Medeisis, "*Cooperative Sensing of Spectrum Opportunities*", Wiley Telecom, 1st Edition, 2015.

42. K.Q.T Zhang, "*Cognitive Radio*", Wiley Telecom, 1st Edition, 2015.

43. W. Na, J. Yoon, S. Cho, D. Griffith, N. Golmie, "Centralized Cooperative Directional Spectrum Sensing for Cognitive Radio Networks", *IEEE Transactions on Mobile Computing*, vol. 17, no. 6, pp. 1260-1274, 2018.

44. F. Chen, R. Qiu, "Centralized and Distributed Spectrum Sensing System Models Performance Analysis Based on Three Users", *6th International Conference on Wireless Communications Networking and Mobile Computing (WiCOM)*, China, pp. 1-4, 2010.

45. C.Y. Chen, Y.H. Chou, H.C. Chao, C.H. Lo, "Secure centralized spectrum sensing for cognitive radio networks", *Wireless Networks*, vol. 18, no. 8, pp. 667-677, 2012.

46. N. Noorshams, M. Malboubi, A. Bahai, "Centralized and decentralized cooperative spectrum sensing in cognitive radio networks: A novel approach", *EEE 11th International Workshop on Signal Processing Advances in Wireless Communications (SPAWC)*, Morocco, pp. 1-5, 2010.

47. T. Rappaport, "*Wireless Communication: Principles and Practice*", 2nd Edition, Pearson education, 2010.

48. A. Goldsmith, "*Wireless Communications*" Cambridge University Press, 2005.

49. V. Erceg, L. J. Greenstein, S. Y. Tjandra, S. R. Parkoff, A. Gupta, B. Kulic, A. A. Julius, and R. Bianchi, "An empirically based path loss model for wireless channels in suburban environments," *IEEE Journal on Selected Areas in Communications*, , vol. 17, no. 7, pp. 1205–1211, 1999.

50. M. K. Simon and M.-S. Alouini, "*Digital communication over fading channels*", Wiley-IEEE, 2005.

51. I. F. Akyildiz, B.F. Lo, R. Balakrishan, "Cooperative spectrum sensing in cognitive radio networks: A survey", *Physical Communication*, vol. 4, pp. 40-64, 2011.

52. A. Ali, W. Hamouda, "Advances on Spectrum Sensing for Cognitive Radio Networks: Theory and Applications", *IEEE Communications Surveys & Tutorials*, vol. 19, no. 2, pp. 1277-1304, 2017.

53. P.M. Shankar, "*Fading and Shadowing in Wireless Systems*", Springer, 2011.

54. S. Al-Ahmadi, H. Yanikomeroglu, "On the approximation of the generalized-K distribution by Gamma distribution for modeling composite fading channels", *IEEE Transactions on Wireless Communications*, vol. 9, pp. 706-713, 2010.

55. P.K. Verma, S.K. Soni, P. Jain, "Novel approximation of average symbol error rate probability of composite Nakagami-m/Log-normal fading channels", *1st IEEE*

International Conference on Power Electronics, Intelligent Control and Energy Systems, pp. 3196-3200, 2016.

56. H. Lei, I.S. Ansari, G. Pan, B. Alomair, M.S. Alouini, "Secrecy capacity analysis over alpha-mu fading channels", *IEEE Communications Letters*, vol. 21, no. 6, pp. 1445-1448, 2017.

57. S.P. Singh, M. Jadon, R. Kumar, S. Kumar, "BER analysis over alpha-mu fading channel using proposed novel MGF", *International Journal of Wireless and Mobile Computing*, vol. 10, no. 2, pp. 174-182, 2016.

58. C.B. Issaid, M.S. Alouini, R. Tempone, "On the fast and precise evaluation of the outage probability of diversity receivers over alpha-mu, kappa-mu, and eta-mu fading channels", *IEEE Transactions on Wireless Communications*, vol. 17, no. 2, pp. 1255-1268, 2018.

59. C.R.N. De-Silva, E.J. Leonardo, M.D. Yacoub, "Product of two envelops taken from alpha-mu, kappa-mu, and eta-mu distributions", *IEEE Transactions on Wireless Communications*, vol. 66, no. 3, pp. 1284-1295, 2018.

60. A.K. Papazafeiropoulos, S.A. Kotsopoulos, "The alpha-lambda-mu and alpha-eta-mu small scale general fading distributions: A unified approach", *Wireless Personal Communications*, vol. 57, no. 4, pp. 735-751, 2011.

61. O.S. Badarneh, M.S. Aloqlah, "Performance analysis of digital communication systems over alpha-eta-mu fading channels", *IEEE Transactions on Vehicular Technology*, vol. 65, no. 10, pp. 7972-7981, 2016.

62. T. Aldalgamouni, A.M. Magableh, S. Mater, O.S. Badarneh, "Capacity analysis of alpha-eta-mu channels over different adaptive transmission protocols", *IET Communications*, vol. 11, no. 7, pp. 1114-1122, 2017.

63. A. Bagheri, P.C. Sofotasios, T.A. Tsiftsis, K.H. Van, M.I. Loupis, S. Freear, M. Valkam, "Energy Detection Based Spectrum Sensing over Enriched Multipath Fading Channels",

IEEE Wireless Conference and Networking Conference (WCNC 2016) Track 1: PHY and Fundamentals, pp. 1-6, 2016.

64. H. Urkowitz, "Energy detection of Unknown deterministic Signals," *in Proc IEEE*, vol. 55, no. 4, pp. 523-531, 1967.

65. V.I. Kostylev, "Energy detection of a signal with random amplitude," *IEEE Int. Conf. ICC* 2002, vol. 3, pp. 1606 – 1610, 2002.

66. V. I. Kostylev, "Characteristics of Energy Detection of Quasi-deterministic Radio Signals," *Radio physics and Quantum Electronics*, vol. 43, pp. 833-839, October 2000.

67. F. F. Digham, M. S. Alouini, and M. K. Simon, "On the energy detection of unknown signals over fading channels", *IEEE Transaction Communication*, vol. 55, no. 1, pp. 21−24, 2007.

68. S. P. Herath and N. Rajatheva, "Analysis of equal gain combining in energy detection for cognitive radio over Nakagami channels", *in Proc. IEEE Globecom*, pp. 2972−2976, Dec. 2008.

69. A. Ghasemi and E.S. Sousa, "Collaborative spectrum sensing for opportunistic access in fading environments", *in Proc. DySpan*, pp.131−136, Nov. 2005.

70. A. Ghasemi and E.S. Sousa, "Impact of User Collaboration on the Performance of Sensing-Based Opportunistic Spectrum Access", *in Proc. IEEE Vehicular Tech. Conference*, pp. 1−6, Sep. 2006.

71. A. Ghasemi and E.S. Sousa, "Asymptotic Performance of collaborative spectrum sensing under correlated Log-normal shadowing", *IEEE Communication Letter*, vol. 11, no. 1, pp. 34−36, 2007.

72. S. Atapattu, C. Tellambura, and H. Jiang, "Relay based cooperative spectrum sensing in cognitive radio networks", *in Proc. IEEE Global Telecommunication Conference*, pp. 4310−4314, 2009.

73. S. Atapattu, C. Tellambura, and H. Jiang, "Energy detection based cooperative spectrum sensing in cognitive radio networks", *IEEE Transaction on Wireless Communication*, vol. 10, no. 4, pp. 1232−1241, Apr. 2011.

74. A. Shahini, A. Bagheri, and A. Shahzadi, "A unified approach to performance analysis of energy detection with diversity receivers over Nakagami-m fading channels", *in Proc. IEEE Int. Conf. on Connected Vehicles and Expo (ICCVE)*, pp. 707−712, Dec. 2013.

75. K. T. Hemachandra and N. C. Beaulieu, "Novel analysis for performance evaluation of energy detection of unknown deterministic signals using dual diversity", *in Proc. IEEE Vehicular Tech. Conference*, pp. 1−5, Sep. 2011.

76. S. P. Herath, N. Rajatheva, and C. Tellambura, "Energy detection of unknown signals in fading and diversity reception", *IEEE Transaction Communication*, vol. 59, no. 9, pp. 2443−2453, Sep. 2011.

77. A. Bagheri and A. Shahzadi, "Another look at performance analysis of energy detector with multichannel reception in Nakagami-m fading channels", *Wireless Personal Communication*, vol. 79, no. 1, pp. 527−544, 2014.

78. P. C. Sofotasios, M. K. Fikadu, K. Ho-Van, and M. Valkama, "Energy detection sensing of unknown signals over Weibull fading channels," *IEEE ATC*, pp. 414−419, Oct. 2013.

79. P. C. Sofotasios, L. Mohjazi, S. Muhaidat, M. Al-Qutayri, and G. K. Karagiannidis, "Energy detection of unknown signals over cascaded fading channels," *IEEE Antennas Wireless Propagation Letter*, vol. 15, pp. 135-138, 2015.

80. F.F. Digham, M.S. Alouini, M.K. Simon, "On the Energy Detection of Unknown Signals Over Fading Channels", *IEEE Transactions on Communications*, vol. 55, no. 1, pp. 21-24, January 2007.

81. Q. Wang, D.W. Yue, "A General Parameterization Quantifying Performance in Energy Detection", *IEEE Signal Processing Letters*, vol. 16, no. 8, pp. 699-702, 2009.

82. S. Nallagonda, S. Suraparaji, S.D. Roy, S. Kundu, "Performance of Energy Detection Based Spectrum Sensing in Fading Channels", *International Conference on Computer & Communication Technology (ICCCT)*, pp. 575-580, 2011.

83. S. Atapattu, C. Tellambura, and H. Jiang, "Energy Detection of Primary signals over η−μ fading channels", *in Proc. 4th Ind. Inf. Systems (ICIIS)*, pp. 1−5, Dec. 2009.

84. P. C. Sofotasios, E. Rebeiz, L. Zhang, T. A. Tsiftsis, D. Cabric, and S. Freear, "Energy Detection-Based Spectrum Sensing over κ−μ and κ−μ Extreme Fading Channels", *IEEE Trans. Veh. Techn.*, vol. 63, no 3, pp. 1031−1040, 2013.

85. A. Bagheri, P. C. Sofotasios, T. A. Tsiftsis, A. Shahzadi, S. Freear, and M. Valkama, "Area under ROC curve of energy detection over generalized fading channels," *IEEE 26th Annual International Symposium on Personal, Indoor, and Mobile Radio Communications (PIMRC)*, pp. 656-661, 2015.

86. Q. Shi, "A Unified MGF Based Approach to the Analysis of Area Under the ROC Curve of Energy Detection Over Generalized Fading Channels", *IEEE International Conference on Signal Processing, Communication and Computing (ICSPCC)*, pp. 1-4, 2013.

87. A. Annamalai, A. Olaluwe, "On the Energy Detection of Unknown Signals in κ-μ and η-μ Fading Channels with Diversity Receivers", *International Conference on Connected Vehicles and Expo (ICCVE)*, pp. 127-132, 2013.

88. E. Adebola, A. Annamalai, "Unified analysis of energy detectors with diversity reception in generalised fading channels", *IET Communications*, vol. 8, no. 17, pp. 3095-3104, 2014.

89. S.S. Yadav, S. Hariharan, P. Muthuchidambaranathan, "A PDF Based Approach for Average Detection Probability of Energy Detector over η − μ Faded Cooperative-MIMO Reporting Channel", *International Conference on Next Generation Intelligent Systems (ICNGIS)*, pp. 1-5, 2016.

90. H. Huang, C. Yuan, "Cooperative Spectrum Sensing over Generalized Fading Channels Based on Energy Detection", *China Communications*, pp. 128-137, 2018.

91. S. Kumar, "Performance of ED Based Spectrum Sensing Over alpha-eta-mu Fading Channel", *Wireless Personal Communication*, vol. 100, no. 4, pp. 1845-1857, 2018.

92. V. Khandelwal, Karmeshu, "A new approximation for average symbol error probability over log-normal channels", *IEEE Wireless Communication Letter*, vol. 3, no. 1, pp. 58-61, 2014.

93. H. Hashemi, "Impulse response modeling of indoor radio propagation channels", *IEEE J. Sel. Areas Communication*, vol. 11, pp. 967-978, 1993.

94. F. Hansen, F.I. Mano, "Mobile fading Rayleigh and log-normal superimposed", *IEEE Transactions on Vehicular Technology*, vol. 26, pp. 332-335, 1977.

95. P.S. Chauhan, "New analytical expressions for ASEP of modulation techniques with diversity over lognormal fading channels with application to interference-limited environment", *Wireless Personal Communications*, vol. 92, no. 2, pp. 695-716, 2018.

96. R. Singh, S.K. Soni, R.S. Raw, S. Kumar, "A new approximate closed-form distribution and performance analysis of a composite Weibull/lognormal fading channel", *Wireless Personal Communications*, vol. 93, no. 3, pp. 883-900, 2017.

97. S. Kumar, S.K. Soni, P. Jain, "Performance analysis of Hoyt-lognormal composite fading channel", *IEEE International Conference on Wireless Communications Signal Processing and Networking (WiSPNET)*, pp. 2503-2507 2017.

98. S. Kumar, S.K. Soni, P. Jain, "Micro-diversity analysis of error probability and channel capacity over Hoyt-Gamma fading", *Radioengineering*, vol. 26, no.4, pp. 1096-1103, 2017.

99. N.Y. Ermolova, "Capacity analysis of two wave diffused power fading channels using mixture Gamma distributions", *IEEE Communications Letters*, vol. 20, no. 11, pp. 2245-2248, 2016.

100. S. Kumar, "Energy Detection in Hoyt/Gamma Fading Channel with Micro-Diversity Reception", *Wireless Personal Communication*, vol. 101, no. 2, pp. 723-734, 2018.

101. S. Kumar, S.K. Soni, P. Jain, "Performance of MRC receiver over Hoyt-lognormal Composite Fading Channel", *International Journal of Electronics*, vol. 105, no. 9, pp. 1433-1450, 2018.

102. O. Olabiyi, S. Alam, A. Annamalai, "Further Results on the Energy Detection of Unknown Deterministic Signals over Generalized Fading Channel", *IEEE International Workshop on Recent Advances in Cognitive Communications and Networking*, pp. 908-912, 2011.

103. K. Ruttik, K. Koufos, R. Jantti, "Detection of Unknown Signals in a Fading Environment", *IEEE Communications Letters*, vol. 13, no. 7, pp. 498-500, 2009.

104. K.P. Peppas, G. Efthymoglou, V.A. Aalo, M. Alwakeel, S. Alwakeel, "Energy detection of unknown signals in Gamma-shadowed Rician fading environments with diversity reception", *IET Communications*, vol. 9, no. 2, pp. 196-210, 2015.

105. S. Atapattu, C. Tellambura, H. Jiang, "Performance of an Energy Detector over Channels with Both Multipath Fading and Shadowing", *IEEE Transactions on Wireless Communications*, vol. 9, no. 12, pp. 3662-3670, 2010.

106. J. Zhou, Y. Shen, Y. Tang, "Performance analysis of energy detection over composite Rayleigh and shadowed fading channels", *Electronics Letter*, vol. 48, no. 20, pp. 1-2, 2012.

107. H. Rasheed, N. Rajatheva, "Spectrum Sensing for Cognitive Vehicular Networks over Composite Fading", *International Journal of Vehicular Technology*, pp. 1-9, 2011.

108. K.P. Peppas, G. Efthymoglou, V.A. Aalo, M. Alwakeen, S. Alwakeen, "On the Performance Analysis of Energy Detection of Unknown Signals in Gamma Shadowed Ricean Fading Environments", *24th International Symposium on Personal, Indoor and Mobile Radio Communications*, pp. 756-760, 2013.

109. K.P. Peppas, G. Efthymoglou, V.A. Aalo, M. Alwakeen, S. Alwakeen, "Energy detection of unknown signals in Gamma-shadowed Rician fading environments with diversity reception", *IET Communications*, vol. 9, no. 2, pp. 196-210, 2015.

110. Q. Shi, "On the Performance of Energy Detection for Spectrum Sensing in Cognitive Radio Over Nakagami-Lognormal Composite Channels", *IEEE China Summit and International Conference on Signal and Information Processing*, China, pp. 1-4, 2013.

111. H.R. Alhennawi, M.H. Ismail, H.A.M. Mourad, "Performance evaluation of energy detection over extended generalized-K composite fading channels", *Electronics Letter*, vol. 50, no. 22, pp. 1643-1645.

112. O. Alhussein, A.A. Hammadi, P.C. Sofotasios, S. Muhaidat, J. Liang, M.A. Qutayri, G.K. Karagiannidis, "Performance Analysis of Energy Detection over Mixture Gamma based Fading Channels with Diversity Reception", *IEEE 11th International Conference on Wireless and Mobile Computing, Networking and Communications (WiMob)*, pp. 404-413, 2015.

113. W.D.A. Silva, K.M. Mota, U.S. Dias, "Spectrum Sensing over Nakagami-m/Gamma Composite Fading Channel with Noise Uncertainty", *RWS*, pp. 98-101, 2015.

114. S.K. Yoo, S.L. Cotton, P.C. Sofotasios, S. Muhaidat, O.S. Badarneh, G.K. Karagiannidis, "Entropy and Energy Detection-based Spectrum Sensing over F Composite Fading Channels", *submitted to IEEE Journal*, 2018.

115. S.K. Yoo, S.L. Cotton, P.C. Sofotasios, M. Matthaiou, M. Valkama, G.K. Karagiannidis, "The kappa-mu/Inverse Gamma Fading Model", *26th International Symposium on Personal, Indoor and Mobile Radio Communications*, pp. 949-953, 2015.

116. S. Alam, A. Annamalai, "Energy Detector's Performance Analysis over the Wireless Channels with Composite Multipath Fading and Shadowing Effects using the AVC Approach", *9th Annual IEEE Consumer Communications and Networking Conference - Wireless Consumer Communication and Networking*, pp. 771-775, 2012.

117. P.S. Chauhan, P. Negi, S.K. Soni, "A Unified Approach to Modelling of Probability of Detection over α-μ/IG, κ-μ/IG, and η-μ/IG Composite Fading Channels with Application to Co-operative System", *International Journal of Electronics and Communication*, vol. 87, pp. 33-42, 2018.

118. S. Kumar, M. Kaur, N.K. Singh, K. Singh, P.S. Chauhan, "Energy detection based spectrum sensing for gamma shadowed α–η–μ and α–κ–μ fading channels", *International Journal of Electronics and Communication*, vol. 93, pp. 26-31, 2018.

119. H. Al-Hmood, H.S. Al-Raweshidy, "Analysis of energy detection with diversity receivers over non-identically distributed κ − μ shadowed fading channels", *Electronics Letter*, vol. 53, no. 2, pp. 83-85, 2017.

120. H. Al-Hmood, H.S. Al-Raweshidy, "Unified Modeling of Composite κ − μ/Gamma, η − μ/Gamma, and α − μ/Gamma Fading Channels Using a Mixture Gamma Distribution With Applications to Energy Detection", *IEEE Antennas And Wireless Propagation Letters*, vol. 16, pp. 104-108, 2017.

121. P.C. Sofotasios, T.A. Tsiftsis, M. Ghogho, L.R. Wilhelmsson, M. Valkama, "The η−μ/IG Distribution: A Novel Physical Multipath/Shadowing Fading Model", *IEEE Wireless Communications Symposium*, pp. 5715-5719, 2013.

122. S. K. Yoo, S.L. Cotton, P.C. Sofotasios, M. Mattaiou, M. Valkama, G.K. Karagiannidis, "The kappu-mu / Inverse Gamma Fading Model", *IEEE 26th International Symposium on Personal, Indoor and Mobile Radio Communications - (PIMRC): Fundamentals and PHY*, pp. 949-953, 2015.

123. N. Wang, Y. Gao, X. Zhang, "Adaptive Spectrum Sensing Algorithm under Different Primary User Utilizations", *IEEE Communications Letters*, vol. 17, no. 9, pp. 1838-1841, 2013.

124. W. Zhang, R.K. Mallik, K.B. Letaief, "Optimization of Cooperative Spectrum Sensing with Energy Detection in Cognitive Radio Networks", *IEEE Transaction on Wireless Communication*, vol. 8, no. 12, pp. 5761-5766, 2009.

125. Chatziantoniou, E, Allen, B., Velisavljevic, V. (2015). Threshold Optimization for Energy Detection-Based Spectrum Sensing Over Hyper-Rayleigh Fading Channels. IEEE Communication Letters, 19 (6), 1077-1080, 2015.

126. Alam, S., Annamalai, A., Akujuobi, C.M. (2017). Optimizations of cooperative spectrum sensing with reporting errors over myriad fading channels. IEEE 7th Annual Computing and Communication Workshop and Conference (CCWC), 9-14, 2017.

127. Zhang, S., Bao, Z. (2011). An adaptive spectrum sensing algorithm under noise uncertainty. Proceedings of IEEE International Conference on Communication, pp. 1-5, 2011.

128. Kozal, A., Merabti, M., Bouhafs, F. (2012). An improved energy detection scheme for cognitive radio networks in low SNR region. Proc. IEEE International Symp. Comput. and Commun., pp. 684-689, 2012.

129. Bagwari, A., Tomar, G.S. (2013). Cooperative Spectrum Sensing with Adaptive Double-Threshold Based Energy Detector in Cognitive Radio networks. Wireless Personal Communication, vol. 73, pp. 1005-1019, 2013.

130. Singh, A., Bhatnagar, M.R., Mallik, R.K. (2012). Cooperative Spectrum Sensing in Multiple Antenna Based Cognitive Radio Network Using an Improved Energy Detector. IEEE Communication Letters, 16 (1), 64-67, 2012.

131. Singh, A., Bhatnagar, M.R., Mallik, R.K. (2011). Optimization of Cooperative Spectrum Sensing with an Improved Energy Detector over Imperfect Reporting Channels. In proceedings for IEEE Vehicular Technology Conference (VTC-Fall), San Francisco, pp. 1-5, 2011.

132. A.A. Hammadi, O. Alhussein, P.C. Sofotasios, S. Muhaidat, M. Al-Qutayri, S. Al-Araji, G.K. Karagiannidis, J. Liang, "Unified Analysis of Cooperative Spectrum Sensing Over Composite and Generalized Fading Channels", *IEEE Transactions on Vehicular Technology*, vol. 65, no. 9, pp. 6949-6961, 2016.

133. S. Kumar, P.K. Verma, M. Kaur, P. Jain, S.K. Soni, "On the spectrum sensing of gamma shadowed Hoyt fading channel with MRC reception", *Journal of Electromagnetic Waves And Applications*, pp. 1-10, 2018.

134. E. Chatziantoniou, B. Allen, V. Velisavljevic, "Threshold Optimization for Energy Detection-Based Spectrum Sensing Over Hyper-Rayleigh Fading Channels", *IEEE Communications Letters*, vol. 19, no. 6, pp. 1077-1080, 2015.

135. H. Sun, D.I. Laurenson, C.X. Wang, "Computationally Tractable Model of Energy Detection Performance over Slow Fading Channels", *IEEE Communication Letter*, vol. 10, pp. 924-926, 2010.

136. I.S. Gradshteyn, I.M. Ryzhik, "*Table of Integrals, Series, and Products*", 7th Edition, Academic Press, Elsevier, 2017.

137. P.M. Shankar, "Diversity in Cascaded N*Nakagami Channels", *Ann. of Telecommunication*, vol. 68, pp. 477-483, 2013.

138. A. Laourine, M.S. Alouini, "On the Performance Analysis of Composite Multipath/Shadowing Channels Using the G-Distribution", *IEEE Transaction on Communication*, vol. 57, no. 4, pp. 1162-1170, 2009.

139. S. Atapattu, C. Tellambura, H. Jiang, "Spectrum Sensing via Energy Detector in Low SNR", *IEEE ICC proceedings*, vol. 11, pp. 682-684, 2011.

140. A.V. Aalo, "Performance of maximum ratio diversity systems in a correlated Nakagami-fading environment", *IEEE Transactions in Communications*, vol. 43, no. 8, pp. 2360-2369, 1995.

141. M. Abramowitz, A.I. Stegun, "*Handbook of mathematical functions with formulas graphs, and mathematical tables*", Dover publications, Inc., New York 1972.

142. S. Attapattu, C. Tellambura, H. Jiang, "Analysis of area under the ROC curve of energy detection", *IEEE Trans. Wireless Communication*, vol. 9, no. 3, pp. 1216-1225, 2010.

143. The Wolfram function site [Internet]. [cited 2018 Jan 1]. Available from: http://functions.wolfram. com/PDF/MeijerG.pdf.

144. J. Lieblein, "On moments of order statistics from the Weibull distribution", *The Annals of Mathematical Statistics*, vol. 26, no. 2, pp. 330–333, 1955.

145. A. Bessate, F.El. Bouanani, "A Very Tight Approximate Results of MRC Receivers Over Independent Weibull Fading Channels", *Physical Communication*, vol. 21, pp. 30-40, 2016.

146. J.M. Holtzman, "A simple, accurate method to calculate spread multiple access error probabilities", *IEEE Trans. Communication*, vol. 40, pp. 461-464, 1992.

147. F.El. Bouanani, H. Ben-Azza, M. Belkasmi, "New results for the shannon channel capacity over generalized multipath fading channels for MRC diversity", *EURASIP Journal on Wireless Communications and Networking*, vol. 33, pp. 1-12, 2012.

148. Karmeshu, V. Khandelwal, "On the applicability of average channel capacity in log-normal fading environment", *Wireless Personal Communication*, vol. 68, pp. 1393-1402, 2013.

149. A.P. Prudnikov, Y.A. Brychkov, O.I. Marichev, "*Integrals and Series, Volume 3: More special functions*", New York, USA: Gordon and Breach Science Publishers, 1990.

150. S.L. Cotton, W.G. Scanlon, "Higher order statistics for log-normal small scale fading in mobile radio channels", *IEEE Antennas Wireless Propagation Letter*, vol. 6, pp. 540-543, 2007.

List of Research Papers in Journals and Conferences

International Journals:

1. **Pappu Kumar Verma**, Sanjay Soni, Priyanka Jain, "On the Performance of Energy Detection-based CR with SC Diversity over IG Channel", *International Journal of Electronics,* Taylor & Francis, vol. 104, no. 12, pp. 1945-1956, 2017.
   Indexing: SCI, SCIE; IF: 0.939; DOI: 10.1080/00207217.2017.1330425

2. **Pappu Kumar Verma**, Sanjay Soni, Priyanka Jain, "Performance Evolution of ED-based Spectrum Sensing in CR over Nakagami-m/Shadowed fading channel with MRC reception", *International Journal of Electronics and Communication (AEU),* Elsevier, vol. 83, pp. 512-518, 2018.
   Indexing: SCI, SCIE; IF: 2.115; DOI: 10.2016/j.aeue.2017.11.05

3. **Corrigendum** to **Pappu Kumar Verma**, Sanjay Soni, Priyanka Jain, "Performance evolution of ED-based spectrum sensing in CR over Nakagami-m/shadowed fading channel with MRC reception" *International Journal of Electronics and Communication (AEU),* Elsevier, vol. 95, pp. 355, 2018.
   Indexing: SCI, SCIE; IF: 2.115; DOI: 10.1016/j.aeue.2017.11.005

4. **Pappu Kumar Verma**, Sanjay Soni, Priyanka Jain, "Modelling and performance evaluation over Nakagami-m/log-normal fading environments", *International Journal of Communication Networks and Distributed Systems (IJSNDS),* Inderscience Publishers, 2018. (**In Production**)
   Indexing: ESCI, SCOPUS

5. Sandeep Kumar, **Pappu Kumar Verma**, M. Kaur, Priyanka Jain, Sanjay Kumar Soni, "On the spectrum sensing of gamma shadowed Hoyt fading channel with MRC reception", *Journal of Electromagnetic Waves And Applications*, Taylor & Francis, vol. 32, no. 16, pp. 2157-2166, 2018.
   Indexing: SCIE; IF: 0.864; DOI: 10.1080/09205071.2018.1493402

International Conferences:

6. **P. K. Verma**, S. K. Soni, Priyanka Jain, "Novel Approximation of Average Symbol Error Rate Probability of Composite Nakagami-m/Lognormal Fading Channel", *in Proceeding of the 1st **IEEE** International Conference on Power Electronics, Intelligent Control and Energy Systems (ICPEICES),* pp. 3196-3200, July 4-6, 2016.
   ISBN: 978-1-4673-8587-9/16

7. **P. K. Verma**, S. K. Soni, Priyanka Jain, "An Experimental Study of Wireless Transceiver of Modulation Schemes using Software Defined Radio", *in Proceeding of the 1st **IEEE** International Conference on Power Electronics, Intelligent Control and Energy Systems (ICPEICES),* pp. 3539-3544, July 4-6, 2016.
   ISBN: 978-1-4673-8587-9/16

8. **P. K. Verma**, Priyanka Jain, Sanjay Soni, R. S. Raw, "Channel Capacity of Different Adaptive Transmission Techniques over Log-normal Shadowed Fading Environments", in Proceeding of the 10th INDIACom-2016; 3rd IEEE International Conference on Computing for Sustainable Global Development, pp. 3455-3459, March 16-18, 2016.
   ISBN: 978-93-80544-21-2/16

9. Singh, S. K. Soni, **P. K. Verma**, Sandeep Kumar, "Performance Analysis of MRC Combiner Output Signal in Log-normal Shadowed Fading" in Proceeding of the IEEE International Conference on Computing, Communication and Automation (ICCCA), pp. 1116-1120, May 15-16, 2015.
   ISBN: 978-1-4799-8890-7/15

Author Biography

Pappu Kumar Verma born in Varanasi (Uttar Pradesh), India in 28th July 1987. He received his B. Tech. in Electronics & Communication Engineering from Gautam Buddha Technical University, Lucknow, Uttar Pradesh, India in 2010 and M. Tech. in Microwave & Optical Communication from Delhi Technological University, New Delhi, India in 2014. He joined for Ph.D. programm in the Department of Electronics and Communication Engineering form Delhi Technological University, New Delhi, India in July 2014. He has worked as a Lecturer in the Electronics and Communication Engineering Department at National Institute of Technology (NIT), Hamirpur, HP, India during January 2016 to December 2017. Currently, he is working as an Assistant Professor in the Electronics Engineering Department at Government Engineering College, Sonbhadra, Uttar Pradesh, India. He has authored or co-authored for more than 20 research papers in International Journals/National Journals/Conferences proceedings of repute. His research interests include wireless communications, cognitive radio networks and channel modelling.

APPENDIX A

Proof for chapter 3

Derivation of equation (3.18),

Considering SC diversity with each branch as i.i.d., the PDF of output SNR of SC [137] is defined as

$$p_{SC}(y) = B\left(P_{\Delta}(y)\right)^{B-1} \times p_{\Delta}(y) \tag{A.1}$$

The CDF and PDF for IG distribution [53] are given as

$$P_{\Delta}(y) = Q\left[\sqrt{\frac{\lambda}{y}}\left(\frac{1-y}{\theta}\right)\right] + exp\left(\frac{2\lambda}{\theta}\right)Q\left(\sqrt{\frac{\lambda}{y}}\left(\frac{1+y}{\theta}\right)\right) \tag{A.2}$$

$$p_{\Delta}(y) = y^{-3/2}\sqrt{\frac{\lambda}{2\pi}}exp\left(\frac{\lambda}{\theta}\right)exp\left(-\lambda\left(\frac{y}{2\theta^2}+\frac{1}{2y}\right)\right) \tag{A.3}$$

Substituting value of CDF in (A.1), we have

$$p_{SC}(y) = B\left(Q\left[\sqrt{\frac{\lambda}{y}}\left(\frac{1-y}{\theta}\right)\right] + exp\left(\frac{2\lambda}{\theta}\right)Q\left(\sqrt{\frac{\lambda}{y}}\left(\frac{1+y}{\theta}\right)\right)\right)^{B-1} \times p_{\Delta}(y) \tag{A.4}$$

Using $(a+x)^n = \sum_{k=0}^{N} {}^nC_k x^k a^{n-k}$ in (A.4),

$$p_{SC}(y) = B\left(\begin{array}{l}\sum_{k=0}^{B-1} {}^{B-1}C_k exp\left(\frac{2\lambda}{\theta}(B-k-1)\right)Q^k\left[\sqrt{\frac{\lambda}{y}}\left(\frac{1-y}{\theta}\right)\right] + \\ Q^{B-k-1}\left(\sqrt{\frac{\lambda}{y}}\left(\frac{1+y}{\theta}\right)\right)\end{array}\right)^{B-1} \times p_{\Delta}(y) \tag{A.5}$$

Now, $Q^k\left[\sqrt{\frac{\lambda}{y}}\left(\frac{1-y}{\theta}\right)\right]$; $say\sqrt{\frac{\lambda}{y}} = T$ then

$$Q^k\left[T\left(\frac{1-y}{\theta}\right)\right]=\left[\frac{a_1}{2}exp\left(-\frac{bT^2}{2}\left(\frac{1-y}{\theta}\right)^2\right)+\frac{a_2}{2}exp\left(-bT^2\left(\frac{1-y}{\theta}\right)^2\right)\right] \quad \text{(A.6)}$$

$$Q^k\left[T\left(\frac{1-y}{\theta}\right)\right]=\sum_{r=0}^{K}{}^kC_r\left(\frac{a_1}{2}\right)^{k-r}\left(\frac{a_2}{2}\right)^r exp\left(-bT^2\left(\frac{1-y}{\theta}\right)^2\left(\frac{k-r}{2}+r\right)\right) \quad \text{(A.7)}$$

Now, put $\sqrt{\frac{\lambda}{y}}=T$ in (A.7),

$$Q^k\left[T\left(\frac{1-y}{\theta}\right)\right]=\sum_{r=0}^{K}{}^kC_r\left(\frac{a_1}{2}\right)^{k-r}\left(\frac{a_2}{2}\right)^r exp\left(-b\frac{\lambda}{y}\left(\frac{1-y}{\theta}\right)^2\left(k+r\right)\right) \quad \text{(A.8)}$$

Similarly,

$$Q^{B-k-1}\left[T\left(\frac{1+y}{\theta}\right)\right]=\left\{\sum_{r_1=0}^{B-k-1}{}^{B-k-1}C_{r_1}\left(\frac{a_1}{2}\right)^{B-k-1-r_1}\left(\frac{a_2}{2}\right)^{r_1}\times exp\left(-\frac{b}{2}\frac{\lambda}{y}\left(\frac{1+y}{\theta}\right)^2\left(B-k-1+r_1\right)\right)\right. \quad \text{(A.9)}$$

Substituting (A.8) and (A.9) into (A.5), we have

$$p_{SC}\left(y\right)=B\left\{\left[\sum_{r=0}^{K}{}^kC_r\left(\frac{a_1}{2}\right)^{k-r}\left(\frac{a_2}{2}\right)^r exp\left(-b\frac{\lambda}{y}\left(\frac{1-y}{\theta}\right)^2\left(k+r\right)\right)\right]\times\left[\left\{\sum_{r_1=0}^{B-k-1}{}^{B-k-1}C_{r_1}\left(\frac{a_1}{2}\right)^{B-k-1-r_1}\left(\frac{a_2}{2}\right)^{r_1}\times exp\left(-\frac{b}{2}\frac{\lambda}{y}\left(\frac{1+y}{\theta}\right)^2\left(B-k-1+r_1\right)\right)\right\}\right]\times p_\Delta\left(y\right) \quad \text{(A.10)}$$

Now, substituting value of PDF in (A.10), we have

$$p_{SC}(y)=\begin{cases} B\sqrt{\frac{\lambda}{2\pi}}\sum_{k=0}^{B-1}\sum_{r=0}^{K}\sum_{r_1=0}^{B-k-1} {}^{B-1}C_k\,{}^{k}C_r\,{}^{B-k-1}C_{r_1} exp\left(\frac{2\lambda}{\theta}(B-k+r)\right)\times \\ \left(\frac{a_1}{2}\right)^{B-r-r_1-1}\left(\frac{a_2}{2}\right)^{r+r_1} exp\left(-\frac{b}{2}\frac{\lambda}{y}\left(\frac{1+y}{\theta}\right)^2(B-k-1+r_1)\right)\times \\ \left(\frac{1-y}{\theta}\right)^2(k+r)\,y^{-3/2} exp\left(\frac{\lambda}{\theta}\right) exp\left(-\lambda\left(\frac{y}{2\theta^2}+\frac{1}{2y}\right)\right) \end{cases} \tag{A.11}$$

Equation (A.11) can be re-written as,

$$p_{SC}(y)=\begin{cases} B\sqrt{\frac{\lambda}{2\pi}}\sum_{k=0}^{B-1}\sum_{r=0}^{K}\sum_{r_1=0}^{B-k-1} {}^{B-1}C_k\,{}^{k}C_r\,{}^{B-k-1}C_{r_1}\left(\frac{a_1}{2}\right)^{B-r-r_1-1}\left(\frac{a_2}{2}\right)^{r+r_1} y^{-3/2} \\ exp\left(\frac{\lambda}{\theta}\left(-b(B-2k+r_1-r-1)+2(B-K-1)+1\right)\right)\times \\ exp\left(-\frac{\lambda y}{2\theta^2}\left(b(B+r_1+r-1)+1\right)\right) exp\left(-\frac{\lambda}{2y}\left(b(B+r_1+r-1)+1\right)\right) \end{cases} \tag{A.12}$$

Above equation (A.12) is obtained for $\gamma<\theta$. Similarly, for $\gamma>\theta$ will be obtained. Hence, on combining equations for both the conditions and using the property of Q-function $Q(-x)=1-Q(x)$, we have

$$p_{SC}(\gamma)=\begin{cases} \sum_{k=0}^{B-1}\sum_{n=0}^{K}\sum_{j=0}^{M} B\sqrt{\frac{\lambda}{2\pi}}\left({}^{B-1}C_k\right)\left({}^{K}C_n\right)\left({}^{M}C_j\right)\left(\frac{a_1}{2}\right)^{B-n-j-1}\left(\frac{a_2}{2}\right)^{n+j}\times & \gamma<\theta \\ exp\left(\left(\frac{\lambda}{\theta}\right)\left\{-b(M+j-k-n)+2M+1\right\}\right)\left(\gamma^{-3/2}\right) exp\left(-\left\{\frac{\xi_1}{\gamma}+\xi_2\gamma\right\}\right) & \\ \sum_{k=0}^{L-1}\sum_{i=0}^{K}\sum_{n=0}^{I}\sum_{j=0}^{M} B\sqrt{\frac{\lambda}{2\pi}}\left({}^{B-1}C_k\right)\left({}^{K}C_i\right)\left({}^{I}C_n\right)\left({}^{M}C_j\right)\left(\frac{a_1}{2}\right)^{B-n-j-1}\left(\frac{a_2}{2}\right)^{n+j} & \gamma>\theta \\ \times exp\left(\left(\frac{\lambda}{\theta}\right)\left\{-b(M+j-i-n)+2M+1\right\}\right)\left(\gamma^{-3/2}\right) exp\left(-\left\{\frac{\xi_3}{\gamma}+\xi_4\gamma\right\}\right) & \end{cases} \tag{A.13}$$

where, $M=B-K-1$; $\xi_1=\frac{\lambda}{2}\left[b(B+n+j-1)+1\right]$; $\xi_2=\frac{\lambda}{2\theta^2}\left[b(B+n+j-1)+1\right]$

$$\xi_3=\frac{\lambda}{2}\left[b(B-K+n+i+j-1)+1\right];\quad \xi_4=\frac{\lambda}{2\theta^2}\left[b(B-K+n+i+j-1)+1\right]$$

$$J_1 = B\sqrt{\frac{\lambda}{2\pi}}\left({}^{N-1}C_k\right)\left({}^{K}C_n\right)\left({}^{M}C_j\right)\left(\frac{a_1}{2}\right)^{N-n-j-1}\left(\frac{a_2}{2}\right)^{n+j}$$

$$J_2 = B\sqrt{\frac{\lambda}{2\pi}}\left({}^{B-1}C_k\right)\left({}^{K}C_i\right)\left({}^{I}C_n\right)\left({}^{M}C_j\right)\left(\frac{a_1}{2}\right)^{B-n-j-1}\left(\frac{a_2}{2}\right)^{n+j}$$

$$x_1 = -b\left(M + j - k - n\right) + 2M + 1; \qquad x_2 = -b\left(M + j - i - n\right) + 2M + 1$$

$$\theta = \exp\left(\frac{\mu}{\xi} + \frac{\sigma^2}{2\xi^2}\right); \qquad \lambda = \frac{\theta}{\left(exp\left(\frac{\sigma^2}{\xi^2}\right) - 1\right)} \text{ and } \xi = \frac{10}{ln(10)}$$

Now, using the above notations, the equation (A.13) can concisely be expressed as

$$p_{SC}(\gamma) = \begin{cases} J_1\gamma^{-3/2} exp\left(\left(\frac{\lambda}{\theta}\right)r_1\right) exp\left(-\frac{\xi_1}{\gamma} - \xi_2\gamma\right) & \gamma < \theta \\ \\ J_2\gamma^{-3/2} exp\left(\left(\frac{\lambda}{\theta}\right)r_2\right) exp\left(-\frac{\xi_3}{\gamma} - \xi_4\gamma\right) & \gamma > \theta \end{cases} \tag{A.14}$$

APPENDIX B

Proof for chapter 4

Derivation of equation (4.8),

Assuming $z = \frac{(lnv - \mu)}{\sqrt{2}\sigma}$ in equation (4.6), we have

$$v = exp\left(\mu + \sqrt{2}\sigma z\right)$$

$dz = \frac{1}{\sigma\mu\sqrt{2}} dv$ and limits are as; when $v = 0$ then $z = -\infty$ and when $v = \infty$ then $z = \infty$

Now, the equation (4.6) can be written as,

$$p_{\gamma_{MRC}}(\gamma) = \frac{m^{mN}\gamma^{mN-1}}{\Gamma(mN)\sqrt{\pi}} \int_{-\infty}^{\infty} \begin{bmatrix} exp\left(-mN\left(\mu + \sqrt{2}\,\sigma z\right)\right)\times \\ exp\left((-m\gamma)\left(-\left(\mu + \sqrt{2}\,\sigma z\right)\right)\right) \end{bmatrix} exp\left(-z^2\right) dz \quad \text{(B.1)}$$

$$p_{\gamma_{MRC}}(\gamma) = \frac{m^{mN}\gamma^{mN-1}}{\Gamma(mN)\sqrt{\pi}} \int_{-\infty}^{\infty} exp\left(-m \begin{bmatrix} N\left(\mu + \sqrt{2}\,\sigma z\right) + \\ \gamma exp\left(-\left(\mu + \sqrt{2}\,\sigma z\right)\right) \end{bmatrix} \right) exp\left(-z^2\right) dz \quad \text{(B.2)}$$

Using Gaussian-Hermite Integration, $\int_{-\infty}^{\infty} p(z) exp\left(-z^2\right) dz \approx \sum_{i=1}^{L} w_i p(z_i)$, above equation can be written as,

$$p_{\gamma_{MRC}}(\gamma) \simeq \frac{m^{mN}\gamma^{mN-1}}{\Gamma(mN)\sqrt{\pi}} \sum_{i=1}^{N} W_i exp\left(-m\left[N\left(\mu + \sqrt{2}\,\sigma z\right) + \gamma exp\left(-\left(\mu + \sqrt{2}\,\sigma z\right)\right)\right]\right) \quad \text{(B.3)}$$

$$p_{\gamma_{MRC}}(\gamma) \simeq \frac{m^{mN}\gamma^{mN-1}}{\Gamma(mN)\sqrt{\pi}} \sum_{i=1}^{N} W_i a_i exp\left(-b_i\gamma\right) \quad \text{(B.4)}$$

where, $a_i = exp\left(-mN\left(\mu + \sqrt{2}\,\sigma z_i\right)\right)$, $b_i = m\,exp\left(-\left(\mu + \sqrt{2}\,\sigma z_i\right)\right)$

APPENDIX C

Proof for chapter 5

Derivation of equation (5.9),

Substituting (3.13) and (5.7) into (4.10), we have

$$\overline{P_{DT}} = \sum_{h=0}^{\infty}\sum_{j=1}^{J} \frac{\Gamma\left(h+\eta,\frac{\lambda}{2}\right)}{(h!)\Gamma(h+\eta)} \frac{\theta_{MRC}^{N} c w_j a_j^{N}}{2\sqrt{\pi}(N-1)!} \int_0^{\infty} \gamma^{h+\frac{Nc}{2}-1} exp(-\gamma) exp\left(-\theta_{MRC}\gamma^{-\frac{c}{2}} a_j\right) d\gamma \tag{C.1}$$

Using [143], Meijer G-function,

$$\overline{P_{DT}} = \sum_{h=0}^{\infty}\sum_{j=1}^{J} \frac{\Gamma\left(h+\eta,\frac{\lambda}{2}\right)}{(h!)\Gamma(h+\eta)} \frac{\theta_{MRC}^{N} c w_j a_j^{N}}{2\sqrt{\pi}(N-1)!} \int_0^{\infty} \gamma^{h+\frac{Nc}{2}-1} G_{0\ 1}^{1\ 0}\left[\gamma\middle|_0\right] G_{0\ 1}^{1\ 0}\left[\theta_{MRC} a_j \gamma^{c/2}\right] d\gamma \tag{C.2}$$

Multiplication of two Meijer G-functions can be written in Fox H-function as,

$$\int_0^{\infty} \gamma^{h+\frac{Nc}{2}-1} G_{0\ 1}^{1\ 0}\left[\gamma\middle|_0\right] G_{0\ 1}^{1\ 0}\left[\theta_{MRC} a_j \gamma^{c/2}\right] d\gamma = H_{1\ 1}^{1\ 1}\left[\theta_{MRC} a_j \middle|_{(0,1)}^{\left(1-h-\left(\frac{Nc}{2}\right);\frac{c}{2}\right)}\right] \tag{C.3}$$

From equations (C.2) and (C.3), we have

$$\overline{P_{DT}} = \sum_{h=0}^{\infty}\sum_{j=1}^{J} \frac{\Gamma\left(h+\eta,\frac{\lambda}{2}\right)}{(h!)\Gamma(h+\eta)} \frac{\theta_{MRC}^{N} c w_j a_j^{N}}{2\sqrt{\pi}(N-1)!} H_{1\ 1}^{1\ 1}\left[\theta_{MRC} a_j \middle|_{(0,1)}^{\left(1-h-\left(\frac{Nc}{2}\right);\frac{c}{2}\right)}\right] \tag{C.4}$$